NASA TECHNICAL NOTE

NASA TN D-5759

FLUTTER, VIBRATION, AND BUCKLING OF TRUNCATED ORTHOTROPIC CONICAL SHELLS WITH GENERALIZED ELASTIC EDGE RESTRAINT

by Sidney C. Dixon and M. Latrelle Hudson

Langley Research Center
Hampton, Va. 23365

NATIONAL AERONAUTICS AND SPACE ADMINISTRATION • WASHINGTON, D. C. • JULY 1970

1. Report No. NASA TN D-5759	2. Government Accession No.	3. Recipient s catalog No.
4. Title and Subtitle FLUTTER, VIBRATION, AND BUCKLING OF TRUNCATED ORTHOTROPIC CONICAL SHELLS WITH GENERALIZED ELASTIC EDGE RESTRAINT		5. Report Date July 1970
		6. Performing Organization Code
7. Author(s) Sidney C. Dixon and M. Latrelle Hudson		8. Performing Organization Report No. L-6663
		10. Work Unit No. 124-08-20-04
9. Performing Organization Name and Address NASA Langley Research Center Hampton, Va. 23365		11. Contract or Grant No.
		13. Type of Report and Period Covered Technical Note
12. Sponsoring Agency Name and Address National Aeronautics and Space Administration Washington, D.C. 20546		14. Sponsoring Agency Code

15. Supplementary Notes

Part of the information presented herein was included in a thesis submitted by Sidney C. Dixon in partial fulfillment of the requirements for the Degree of Doctor of Philosopy in Engineering Mechanics, Virginia Polytechnic Institute, Blacksburg, Virginia, March 1967.

16. Abstract

A theoretical investigation has been made of the flutter, vibration, and buckling of truncated conical shells with generalized elastic edge restraint. The shell analysis is of the classical Donnell type, in-plane inertias and structural damping are neglected, and the aerodynamic loading is represented by the inviscid two-dimensional quasi-steady approximation. An approximate solution is obtained by the generalized Galerkin method. The accuracy and limitations of the analysis are illustrated by comparing numerical results for buckling and vibration with results of other investigations for various boundary conditions, applied loads, and shell geometries and stiffnesses. Sufficient numerical results are presented to permit the determination of the flutter condition for simply supported isotropic conical shells for a wide range of cone angle, length-radius ratio, and radius-thickness ratio. Results are also presented to indicate some effects of variations in edge restraint, applied loads, and ring or stringer stiffening.

17. Key Words (Suggested by Author(s)) Flutter Vibration Buckling Truncated orthotropic conical shells Elastic edge restraint	18. Distribution Statement Unclassified — Unlimited		
19. Security Classif. (of this report) Unclassified	20. Security Classif. (of this page) Unclassified	21. No. of Pages 79	22. Price* $3.00

*For sale by the Clearinghouse for Federal Scientific and Technical Information
Springfield, Virginia 22151

CONTENTS

FLUTTER, VIBRATION, AND BUCKLING
OF TRUNCATED ORTHOTROPIC CONICAL SHELLS WITH
GENERALIZED ELASTIC EDGE RESTRAINT[*]

By Sidney C. Dixon and M. Latrelle Hudson
Langley Research Center

SUMMARY

A theoretical investigation has been made of the flutter, vibration, and buckling characteristics of orthotropic truncated conical shells with generalized elastic edge restraint. The problem is simplified by making certain assumptions which are considered justified by the results for cylinders; the shell analysis is of the classical Donnell type, in-plane inertias and structural damping are neglected, and the aerodynamic loading is represented by the inviscid two-dimensional quasi-steady approximation (modified piston theory). The principle of virtual work is utilized to formulate the problem. An approximate solution is obtained by the generalized Galerkin method in terms of assumed displacement functions that must satisfy only geometric constraints. A stress function is introduced so that only the normal displacement need be assumed. The equation for the stress function is solved exactly in terms of the arbitrary coefficients in the assumed displacement.

The accuracy and limitations of the present analysis are illustrated by comparing numerical results for buckling and vibration with results of other investigations for various boundary conditions, applied loads, and shell geometries and stiffnesses. Numerical results for flutter of conical shells reveal that trends established for buckling and vibration do not necessarily hold for flutter. Increasing cone semivertex angle (up to about 15°) for length-radius ratios greater than about 1 increases the resistance to flutter even though the buckling load and natural frequencies decrease. Also, increasing the axial edge restraint can decrease the resistance to flutter even though both the buckling load and natural frequencies are increased. These phenomena are attributed to the fact that flutter depends on frequency spectrum as well as magnitude. Sufficient numerical results are presented to permit the determination of the flutter condition for simply supported isotropic conical shells for a wide range of cone angle, length-radius ratio, and radius-thickness ratio. Results are also presented to indicate some effects of variations in axial, radial, circumferential, and rotational edge restraint, applied load, and ring or stringer stiffeners.

INTRODUCTION

Prior to about 1950 there was a paucity of theoretical and experimental information on the static and dynamic behavior of truncated conical shells primarily because of the mathematical difficulties encountered in theoretical analyses and because thin conical shells had limited application as structural components. However, more recently thin conical shells have been used as load-carrying structural components in adapter sections of multistage rockets and in proposed truncated-cone nose-cap configurations for planetary entry vehicles; therefore, a thorough knowledge of the static and dynamic characteristics of such configurations is required. This need and the availability of digital computers to aid in circumventing the mathematical difficulties encountered in cone analyses have resulted in considerable research effort on the buckling characteristics of cones (for example, refs. 1 to 4) and on the vibrational characteristics of cones (for example, refs. 5 to 7); however, only limited results are available for the effects of various classical boundary conditions or elastic edge support, which have been shown to be important for cylindrical shells (for example, refs. 8 to 13). Also, there is still an almost complete dearth of theoretical and experimental information on flutter of conical shells (ref. 14).

The present investigation considers the flutter, vibration, and buckling of a truncated orthotropic conical shell with generalized elastic edge restraint. The problem is simplified by making certain assumptions which are considered justified by the results for flutter of cylinders. The principle of virtual work is utilized to formulate the governing equations of the problem. An approximate solution is obtained by the generalized Galerkin method (refs. 15 and 16); that is, a procedure in which the displacement functions must satisfy only geometric constraints. A stress function is introduced so that only the normal displacement need be assumed. The equation for the stress function is solved exactly in terms of the arbitrary coefficients in the assumed displacement.

The accuracy and limitations of the present analysis are illustrated in the appendixes by comparing numerical results for buckling and vibration with results of other investigations for various boundary conditions, applied loads, and shell geometries and stiffnesses. Flutter results are presented to indicate the effects of conicity and shell geometry on the flutter characteristics of simply supported isotropic conical shells. Sufficient numerical results are presented in the form of general flutter boundaries to permit the determination of the flutter condition for wide ranges of cone semivertex angle, length-radius ratio, and radius-thickness ratio. Results are presented to indicate the effects of applied loads, ring and stringer stiffeners, and finite elastic edge restraint provided by massless uncoupled springs; the limiting cases of free and clamped edges are also considered.

Certain lengthy expressions developed in this analysis are required for complete documentation. Since they are of limited interest, these expressions are included in a "Supplement to NASA TN D-5759," which is available upon request. A request form is included at the back of this paper.

SYMBOLS

The units for the physical quantities defined in this paper are given both in the U.S. Customary Units and in the International System of Units, SI. Appendix A presents factors relating these two systems of units.

A   cross-sectional area of stiffener

$a_o, \bar{a}_o, a_m$ coefficients in assumed normal deflection function

B   extensional stiffness, $\dfrac{Eh}{1 - \mu^2}$

B_y, B_θ extensional stiffness in y- and θ-direction, respectively

$B_{y\theta}$ in-plane shear stiffness

$C_P = \dfrac{R_1 P}{D_y}$

$C_p = \dfrac{R_1^3 p}{D_y}$

$C_\omega = \left(\dfrac{\omega}{\omega_r}\right)^2 - ig_a\left(\dfrac{\omega}{\omega_r}\right)$

c_{air} speed of sound in air

c_m speed of sound in cone material

D   bending stiffness, $\dfrac{Eh^3}{12\left(1 - \mu^2\right)}$

D_y, D_θ bending stiffness in y- and θ-direction, respectively

$D_{y\theta}$ in-plane twisting stiffness

d   stiffener spacing

E   Young's modulus

F   stress function

F_u, F_v, F_w forces in direction of u, v, and w applied to cone edge by elastic medium

$f = e^{-x}F$

G   shear modulus

G_{ij} inertia coefficients

g_a aerodynamic damping coefficient, $\dfrac{\rho c_{air}}{\gamma \omega_r}$

H,V   radial and axial components of force resultants

h   thickness of isotropic cone

I   moment of inertia of stiffener about its centroid

i,j   integers

J   torsional constant for stiffener

K_{ij} stiffness coefficient representing restraint of elastic medium at cone edges

k_1, k_2, k_3, k_4 stiffness of springs resisting axial, circumferential, and radial edge displacements, and edge rotation, respectively

$\bar{k}_1, \bar{k}_3$ stiffness of springs resisting meridional and normal edge displacement, respectively

L   height of conical frustum

$L_1( ), L_2( ), L_3( )$ operators defined by equations (B15), (B33), and (B59)

l slant length of conical frustum

M   maximum number of terms in sine series

4

M_l local Mach number

M_∞ free-stream Mach number

$M_y, M_\theta, M_{y\theta}$ moment resultants

$\overline{M}_y, \overline{M}_{y\theta}$ externally applied moment resultants

M_w moment applied to shell edge by elastic medium

m, p integers

$N_y, N_\theta, N_{y\theta}$ force resultants

$\overline{N}_y, \overline{N}_{y\theta}$ externally applied force resultants

$n = \dfrac{\eta}{\sin \alpha}$

P applied axial load, positive for compression

P_1, P_2 constants defined by equation (B53)

p lateral pressure load on shell (positive for external pressure)

p_s surface loading induced by shell vibration or flutter

p_t total surface load acting on shell, $p + p_s$

Q_y, Q_θ transverse shear force resultants

$\overline{Q}_y$ externally applied transverse shear force resultant

q local dynamic pressure of airflow

R radius of conical frustum normal to axis of revolution

r radius of cross section of circular end ring

$S_{ij} = \left(\dfrac{R_1}{\cos \alpha}\right)^3 \dfrac{K_{ij}}{D_y}$ $(i,j = 1,2,3)$

$$S_{4j} = \left(\frac{R_1}{\cos \alpha}\right)^2 \frac{K_{4j}}{D_y} \qquad \left(S_{4j} = S_{j4}, \quad j = 1,2,3\right)$$

$$S_{44} = \frac{R_1}{\cos \alpha} \frac{K_{44}}{D_y}$$

t	time
U_s	strain energy of shell
u,v,w	displacements of middle surface of conical frustum (see fig. 1)
u_H, u_V	radial and axial components of displacements
x	transformed coordinate, $\quad x = \ln \dfrac{y}{y_2}$

$$x_1 = \ln \frac{y_1}{y_2}$$

y,z	orthogonal coordinates (see fig. 1)
$\bar{z}$	distance from centroid of stiffener to middle surface of conical shell, $z_c + z_s$
z_c	distance from neutral axis of sheet-stiffener combination to middle surface of conical shell
z_s	distance from neutral axis of sheet-stiffener combination to centroid of stiffener
α	semivertex angle of cone

$$\beta = \sqrt{M_l^2 - 1}$$

γ	shell mass per unit area
Δ	frequency spectrum parameter, $\quad \dfrac{\omega_2^2 - \omega_1^2}{\omega_r^2}$
$\delta\Omega_e$	virtual work done by generalized elastic edge restraint
$\delta\Omega_f$	virtual work of boundary forces

$\delta\Omega_p$ virtual work of total surface pressure p_t

$\delta\Omega_t$ total virtual work of all external forces

$\epsilon_\theta, \epsilon_y, \epsilon_{y\theta}$ strains at middle surface

η number of circumferential waves

θ circumferential coordinate (see fig. 1)

λ flutter parameter, $\dfrac{2qR_1^3}{D_y\beta}$

$$\bar{\lambda} = \frac{\lambda}{\left(1 - \mu^2\right)\left(R_1/h\right)^x} \quad \text{where} \quad x = \tanh\left(0.5\,\frac{L}{R_1}\right)$$

$$\lambda_0 = \sqrt{B_\theta/B_y}$$

λ_1, λ_2 constants defined by equations (B55)

μ Poisson's ratio for isotropic cone

μ_θ, μ_y Poisson's ratio for bending in θ- and y-direction, respectively

μ_θ', μ_y' Poisson's ratio for extension in θ- and y-direction, respectively

ρ local density of air

τ thickness of end ring

$\phi = \theta \sin \alpha$

$\chi_\theta, \chi_y, \chi_{y\theta}$ curvatures at middle surface

ω circular frequency

$$\omega_r = \left(\frac{D_y}{\gamma R_1^4}\right)^{1/2}$$

ω_1 first natural frequency for given value of n

ω_2 second natural frequency for given value of   n

Superscript:

*   indicates variable is function of   x   only

Subscripts:

A   conditions existing prior to buckling, vibration, or flutter

B   conditions existing at buckling, vibration, or flutter

cr   critical value required for buckling

cyl   equivalent cylinder

o   conditions at $\eta = 0$

Im   imaginary part

Re   real part

R   ring

S   stringer

1   small end of cone

2   large end of cone

A subscript preceded by a comma indicates partial differentiation with respect to that subscript.

ANALYSIS

Statement of Problem

The flutter, vibration, and buckling characteristics of orthotropic truncated conical shells with generalized elastic edge restraint are investigated. The configuration and the notation for coordinates and displacements, force and moment resultants, and loads

are shown in figure 1. The cone is subjected to uniform supersonic airflow over its external surface at a local Mach number M_l, dynamic pressure q, and density ρ. Also, the cone is subjected to either internal or external lateral (normal) pressure loading p and an applied axial load P. The pressure is uniform and acts in a constant direction. The movement of the cone edges is resisted by a general elastic medium that can be represented by a 4 by 4 matrix of stiffness coefficients K_{ij} (ref. 17). The mass effects of the edge support are represented by a 4 by 4 matrix of inertia coefficients G_{ij}. The off-diagonal terms in these boundary-condition matrices account for the coupling that can exist between the various displacements due to the interaction of the shell and the elastic medium. This coupling must be considered if the edge restraint is provided by a ring (ref. 18).

The shell is stiffened in such a manner that the cone material has orthotropic stiffness properties in two orthogonal directions. The principal axes of orthotropy are alined with the shell coordinate axes (θ,y). The five extensional stiffness properties B_y, B_θ, $B_{y\theta}$, μ'_y, and μ'_θ and the five bending stiffness properties D_y, D_θ, $D_{y\theta}$, μ_y, and μ_θ are needed to describe the material properties. From the reciprocal theorem (for example, ref. 19), the following relations must hold:

$$\left.\begin{aligned} B_y\mu'_\theta &= B_\theta\mu'_y \\[2mm] D_y\mu_\theta &= D_\theta\mu_y \end{aligned}\right\} \tag{1}$$

Thus, there are eight independent elastic constants.

The flutter, vibration, and buckling characteristics are determined for various combinations of cone geometry, stiffness properties, elastic edge restraint, and loadings p and P.

<div align="center">Assumptions</div>

The stability characteristics of truncated conical shells should be basically similar to the stability characteristics of cylindrical shells. Therefore, the wealth of information on cylinder buckling and flutter should be a useful guide as to what simplifying assumptions can be made without seriously affecting the accuracy of the theoretical results.

Only flutter resulting from coalescence of the first two longitudinal modes of vibration (ω_1,ω_2) is considered since it has been shown theoretically (ref. 20) and experimentally (ref. 21) that this type of flutter represents the critical stability boundary for cylinders. This type of flutter is usually associated with a mode shape having many circumferential waves and has been referred to as plate-type flutter (ref. 20). The plate-type flutter is affected little theoretically by in-plane inertias and structural damping

(ref. 20). Thus a Donnell type theory, which should be sufficiently accurate for moderate to large values of η (ref. 22), is used and in-plane inertias and structural damping are neglected.

Recent investigations have revealed that the aerodynamic boundary layer does not play an important role in shell flutter with many circumferential waves (ref. 21); thus, inviscid theory is used. Furthermore, it has been shown (ref. 21) that piston theory aerodynamics provides a convenient and useful tool for cylinder flutter and hence is used herein.

A recent nonlinear analysis (ref. 23) indicates that cylindrical shell flutter can occur at aerodynamic pressures below the stability boundary for infinitesimal disturbances. However, to make the present overall investigation tractable the small displacement infinitesimal linear flutter theory is employed. The stresses resulting from the loads p and P are obtained from the linear membrane solution, because stress distributions from the more accurate solutions have been shown to have only a slight effect for a wide class of buckling problems. (See, for example, ref. 24.) Furthermore, the effects of displacements which occur prior to flutter, vibration, or buckling are neglected herein since they do not significantly influence cone buckling induced by lateral pressure (ref. 25) or the flutter characteristics of cylinders (ref. 26).

Rings and/or stringers are assumed to be closely spaced so that their effect may be smeared out by use of equivalent orthotropic stiffness properties. Stiffness properties were calculated from the formulas given in table I. The approach used herein neglects the effects of stiffener eccentricity.

Governing Equations

The principle of virtual work is used to derive the general nonlinear equilibrium equations and the linearized stability equations. A stress function is introduced so that the number of unknowns is reduced from three displacements to the stress function and the normal displacement. The introduction of the stress function necessitates the use of a compatibility equation.

The equations are solved by an assumed displacement method. The normal displacement is assumed, the compatibility equation is solved exactly in terms of the arbitrary coefficients in the assumed displacement, and then the equation for the displacement is solved by the generalized Galerkin method (refs. 15 and 16). Details of the derivation and solution of the governing equations are given in appendix B. These governing equations are as follows:

$$\left(y N_{yB}\right)_{,y} + N_{y\theta B,\phi} - N_{\theta B} = 0 \tag{2a}$$

$$N_{\theta B,\phi} + \left(y N_{y\theta B}\right)_{,y} + N_{y\theta B} = 0 \tag{2b}$$

$$D_y L_1(w_B) - N_{\theta B} \cot \alpha - y N_{yA} w_{B,yy} - N_{\theta A}\left(\frac{1}{y} w_{B,\phi\phi} + w_{B,y}\right) - y p_s = 0 \tag{2c}$$

where $L_1(\ )$ is an operator defined by equation (B15).

The boundary conditions on an edge $y = $ Constant are to prescribe

$$N_{yB} - F_{uB} = 0 \qquad \text{or} \qquad u_B \tag{3a}$$

$$N_{y\theta B} - F_{vB} = 0 \qquad \text{or} \qquad v_B \tag{3b}$$

$$Q_{yB} - F_{wB} = 0 \qquad \text{or} \qquad w_B \tag{3c}$$

$$M_{yB} - M_{wB} = 0 \qquad \text{or} \qquad w_{B,y} \tag{3d}$$

Equations (2a) and (2b) are identically satisfied if the stress function F is introduced (refs. 27 and 28) so that, for $\eta > 0$,

$$N_{\theta B} = F_{,yy} \tag{4a}$$

$$N_{yB} = \frac{1}{y} F_{,y} + \frac{1}{y^2} F_{,\phi\phi} \tag{4b}$$

$$N_{y\theta B} = \frac{1}{y^2} F_{,\phi} - \frac{1}{y} F_{,y\phi} \tag{4c}$$

or, for $\eta = 0$,

$$N_{\theta B} = F_{o,y} \tag{4d}$$

$$N_{yB} = \frac{1}{y} F_o \tag{4e}$$

$$N_{y\theta B} = 0 \tag{4f}$$

The stress functions are obtained from the compatibility equations (eqs. (B31) and (B34)). In terms of F, the compatibility equation is

$$L_2(F) = -B_\theta\left(1 - \mu'_\theta \mu'_y\right) w_{B,yy} \cot \alpha \tag{5a}$$

where $L_2(\ )$ is an operator defined by equation (B33). For $\eta = 0$ the equation for the stress function is

$$F_{o,yy} + \frac{1}{y} F_{o,y} - \frac{B_\theta}{B_y}\frac{F_o}{y^2} = -\frac{1}{y} B_\theta\left(1 - \mu'_\theta \mu'_y\right) w_{B,y} \cot \alpha \tag{5b}$$

The boundary conditions for the stress function are the boundary conditions for u_B and v_B, that is, equations (3a) and (3b).

11

To investigate flutter it is necessary that the surface loading p_s represent the inertial and aerodynamic loading acting on the shell. If the piston theory aerodynamic approximation is used to represent the aerodynamic forces (for example, ref. 29), p_s can be expressed as

$$p_s = -\gamma w_{B,tt} - \frac{2q}{\beta} w_{B,y} - \rho c_{air} w_{B,t} \tag{6}$$

where in the denominator of the second term on the right the Mach number M_l has been replaced by $\beta = \sqrt{M_l^2 - 1}$. Preference for the compressibility factor β is based on its demonstrated usefulness for the flutter of flat plates.

With the use of equations (4a) and (6), the governing equation for the normal displacement w_B (eq. (2c)), becomes

$$D_y L_1(w_B) - y N_{yA} w_{B,yy} - N_{\theta A}\left(\frac{1}{y} w_{B,\phi\phi} + w_{B,y}\right) - \cot \alpha \, F_{,yy}$$

$$+ y\left(\gamma w_{B,tt} + \frac{2q}{\beta} w_{B,y} + \rho c_{air} w_{B,t}\right) = 0 \tag{7}$$

For $\eta = 0$, the term $F_{,yy}$ is replaced by $F_{0,y}$.

The flutter, vibration, and buckling characteristics of a truncated orthotropic conical shell are now completely described by the equations for F (eqs. (5)) and the equation for w_B (eq. (7)) with the appropriate boundary conditions (eqs. (3)). If the orthotropic character of the shell can be described by only distinguishing between Young's modulus and Poisson's ratio in the y- and θ-directions, equations (5a) and (7) reduce to those obtained by Singer (ref. 30) for $p_s = 0$. If the shell is isotropic, the equations reduce to those obtained by Seide (refs. 27 and 28) for $p_s = 0$.

The governing equations are solved in appendix B. The normal displacement w_B is assumed, and the equations for the stress function are solved exactly in terms of the arbitrary coefficients in the assumed displacement. The membrane stresses $N_{\theta A}$ and N_{yA} are related to the loadings p and P by the linear membrane expressions (eqs. (B36)), and the forces and moments applied to the shell edge by the elastic medium are expressed in terms of generalized stiffness and mass coefficients and shell displacements (eq. (B46)). The governing equation for w_B is then solved by the generalized Galerkin method (refs. 15 and 16), which yields

$$\left[\left[b_{ij}\right] + \frac{C_P}{2\pi \sin^2\alpha \cos\alpha}\left[c_{ij}\right] + \frac{C_p}{\sin^2\alpha \cos\alpha}\left[d_{ij}\right] - \frac{C_\omega}{\sin^4\alpha}\left[e_{ij}\right] + \frac{\lambda}{\sin^3\alpha}\left[f_{ij}\right]\right]\left\{\begin{array}{c} a_0 \\ \bar{a}_0 \\ a_1 \\ \cdot \\ \cdot \\ \cdot \\ a_M \end{array}\right\} = 0$$

(8)

where a_0, $\bar{a}_0$, and a_m are the coefficients of the assumed normal displacement w_B, and

$$\left.\begin{array}{c} C_P = \dfrac{R_1 P}{D_y} \\[2mm] C_p = \dfrac{R_1^3 p}{D_y} \\[2mm] C_\omega = \left(\dfrac{\omega}{\omega_r}\right)^2 - ig_a\left(\dfrac{\omega}{\omega_r}\right) \\[2mm] g_a = \dfrac{\rho c_{air}}{\gamma \omega_r} \\[2mm] \lambda = \dfrac{2qR_1^3}{\beta D_y} \\[2mm] \omega_r^2 = \dfrac{D_y}{\gamma R_1^4} \end{array}\right\}$$

(9)

The matrix elements b_{ij}, c_{ij}, d_{ij}, e_{ij}, and f_{ij} are given in the supplement to NASA TN D-5759.

For buckling, the parameters C_ω and λ are zero, either C_p or C_P is specified, and the remaining parameter becomes the eigenvalue. For free vibrations, $C_{\dot{p}}$ and C_P are specified, λ is zero, and C_ω is the eigenvalue. For flutter, C_ω is again the eigenvalue but in addition to specifying C_p and C_P, λ and g_a must also be specified. For $g_a > 0$ it is necessary to specify the cone material, altitude (ρ and c_{air}), and Mach number. For buckling and flutter, the circumferential wave number η must be varied to determine the stability boundary.

For flutter, solution of equation (8) requires the extraction of complex eigenvalues for C_ω which occur as conjugate pairs. Thus,

$$\omega = \omega_{Re} + i\omega_{Im} \tag{10}$$

and

$$C_\omega = C_{\omega Re} + iC_{\omega Im} \tag{11}$$

The complex eigenvalues were found with the QR transform of Francis (ref. 31). As previously stated in the section "Assumptions," only the two lowest natural frequencies were examined to determine flutter. For $g_a = 0$, flutter is defined as the lowest value of λ for which C_ω becomes complex and the first two natural frequencies coalesce. For $g_a > 0$, the aerodynamic damping coefficient g_a is related to $C_{\omega Im}$ and $C_{\omega Re}$ by (see, for example, ref. 32)

$$g_a = \frac{|C_{\omega Im}|}{\sqrt{C_{\omega Re}}} \tag{12}$$

Further, g_a can be related to λ from the defining relationships given in equations (9); for isotropic shells the relation is

$$g_a = \frac{0.662}{\left(1 - \mu^2\right)^{1/6}} \left(\frac{\rho}{\gamma/h} \frac{c_m}{c_{air}} \frac{M_l^2 - 1}{M_l^4}\right)^{1/3} \lambda^{2/3} \tag{13}$$

Thus, for $g_a > 0$ flutter is defined as the value of λ for which equations (12) and (13) give identical values of g_a.

RESULTS AND DISCUSSION

Results are presented to indicate the flutter characteristics of simply supported isotropic conical shells. Sufficient numerical results are presented in the form of general flutter boundaries to permit the determination of the flutter condition for a wide range of cone angle, length-radius ratio, and radius-thickness ratio. In addition, results are presented to indicate the trends of the effects of hydrostatic pressure, axial load, and ring and stringer stiffeners. Finally, results are presented to indicate the trends of the effects of finite elastic edge restraint provided by massless uncoupled springs; the limiting cases of free and clamped edges are also considered. Springs resisting only the meridional displacement u_B and the normal displacement w_B (or the axial and radial displacements u_{VB} and u_{HB}), the circumferential displacement v_B, and the rotation $w_{B,y}$ are considered herein. In this investigation "conical" simple support is defined by $N_{yB} = v_B = w_B = M_{yB} = 0$ and "cylindrical" simple support is defined by $V_B = v_B = u_{HB} = M_{yB} = 0$; clamped support is defined by $u_B = v_B = w_B = w_{B,y} = 0$.

14

Buckling and vibration results are presented in appendixes C and D. These results are compared with results of other investigations to indicate the accuracy and limitations of the present analysis. In addition, the trends of the effects of conicity, elastic edge restraint, applied loads, and ring and stringer stiffeners are indicated. Up to 40 terms were used in the computations to insure converged results. Results were assumed to be converged when the results (eigenvalues) for $I + 4$ terms differed by less than 1 percent from the results for I terms.

Simply Supported Shells

Effects of aerodynamic damping.- The variation of the flutter parameter λ with wave number η for an isotropic conical shell with cylindrical simple support is shown in figure 2 along with the shell properties. The solid curve is for $g_a = 0$; typical stabilizing effects of aerodynamic damping are indicated by the dashed curve. The minimum point of the flutter boundary was increased by about 8 percent for g_a based on aluminum at sea level at $M_l = 3$. For denser materials or higher altitudes the effect would be even less. Calculations for cylinders based on the present theory (ref. 33) indicate the effects of aerodynamic damping on flutter increase with L/R and R/h. The magnitude of the effect was of the order of 20 percent for very large values of L/R and R/h but for practical values of these ratios is generally less than 10 percent. The effects of aerodynamic damping are not considered in the remaining calculations.

Effects of conicity.- Some effects of conicity on the flutter of isotropic conical shells with cylindrical simple support are shown in figure 3. Figure 3(a) shows the variation of λ with cone angle α for two values of the ratio of length to radius at the small end of the cone L/R_1. The dashed portion of the curves represent extrapolation to $\alpha = 0^O$. The extrapolated result for $L/R_1 = 6$ is in good agreement with the result of a corresponding cylinder presented in reference 34. For small values of α ($\alpha < 15^O$), λ increases with increasing α. The phenomenon of increase in flutter resistance with increasing α has been obtained previously for three layered conical frustums (ref. 35). This trend is in marked contrast to the trends for buckling and vibration (appendixes C and D); the buckling load and natural frequencies always decreased with increasing α. However, the variation of λ with L/R_1 (fig. 3(b)) is similar to the trends for buckling and vibration.

The increase in λ with α is attributed to the fact that the shell flutter characteristics depend on the natural frequency spectrum as well as the magnitude of the frequencies. For example, a two-mode analysis of cylinder flutter (ref. 20) reveals that the critical value of the flutter parameter is proportional to Δ, the normalized difference in the square of the first two in vaccuo natural frequencies for a given value of η. Figure 4 gives the variation of Δ with α for $L/R_1 = 6$ for $\eta = 6$ to 9. For $\alpha = 0^O$

the value of η for which Δ is a minimum ($\eta = 8$) coincides with the value of η for which λ is a minimum (table 5.2 of ref. 34). For $\alpha > 0^O$ the values of η for which Δ and λ were minimums differed only slightly; the difference tended to increase with increasing α. Thus, Δ may be useful for predicting the critical value of wave number for flutter of both cylindrical and conical shells. For small values of α ($\alpha < 15^O$), the effect of increases in frequency spacing with α is apparently greater than the effect of decreases in frequency magnitude and Δ increases as does the flutter resistance. However, for large values of α ($\alpha > 15^O$), increases in α affect the frequency spacing and magnitudes in such a manner that Δ decreases, as does the flutter resistance.

The variation with L/R_1 of the ratio of the maximum value of q/β to the value for $\alpha = 0^O$ is indicated in figure 5. As can be seen the variation of $\dfrac{(q/\beta)_{max}}{(q/\beta)_{\alpha=0}}$ with L/R_1 is essentially linear and depends on the value of R_1/h. For $R_1/h = 200$, $(q/\beta)_{max}$ occurs at $\alpha = 0^O$ for $L/R_1 \leqq 1$.

For a cylinder, λ is based on free-stream conditions, which are the same as local conditions, whereas for a cone, λ is based on local conditions behind the cone bow shock. In order to determine the trends for λ based on free-stream conditions, the results for $L/R_1 = 6$ were converted to free-stream conditions by use of reference 36. The free-stream Mach number M_∞ was taken to be 3.0. The results for both local and free-stream conditions are shown in figure 6 in terms of λ and α. Comparison of these results reveals that use of free-stream conditions can significantly reduce the magnitude of λ for $\alpha > 5^O$ but does not alter the overall trends.

Comparison with previous investigation.- Shulman (ref. 34) presents flutter results for a simply supported conical shell with $L/R_1 = 8.13$, $R_1/h = 148$, and $\alpha = 5^O$. These proportions are such that $l/R_{av} = 6$ and $R_{av}/h = 200$. In the reference, results for the cone were compared with results for a cylinder with $L/R = 6$ and $R/h = 200$ to indicate the effects of conicity on flutter. The flutter analysis was formulated on the basis of Donnell shell theory and piston theory aerodynamics. The stress function was eliminated from the governing equation for the displacement w, and the resulting eighth-order equation was solved by the Galerkin method. It should be noted that not all boundary conditions were satisfied by the assumed displacement for the cone.

The results of reference 34 for eight and four terms are shown in the following tables in terms of the parameter of the present investigation along with the results from the present investigation for the same two shells; for both investigations, $g_a = 0$. The results for the cylinder from the present investigation were obtained by extrapolation. For $L/R_{av} = 6$ and $R_{av}/h = 200$ and for $\alpha = 0^O$,

η	λ for —	
	Present investigation	Reference 34
	8 terms	8 terms
6	605	605
7	410	412
8	355	352
9	370	360
10	425	427

and for $\alpha = 5^O$

η	λ for —				
	Present investigation				Reference 34
	4 terms	6 terms	8 terms	12 terms	4 terms
4	812	1037	1056	1074	1251
5	492	577	588	590	688
6	622	582	604	607	669
7	1042	627	643	652	714

Examination of these tables reveals that the results of the present investigation are in excellent agreement with the results of reference 34 for the cylinder. The results of reference 34 for the 5° cone indicate that conicity has a large stabilizing effect, the critical value of λ being increased by nearly a factor of 2. The results of the present investigation also indicate a similar stabilizing effect of conicity but slightly less than the increase given by the results of reference 34. In the flutter parameter used in reference 34, there appears a quantity defined by equation (3-31e) of reference 34 to be

$$f(\delta) = \ln \delta_* = \frac{1}{\delta} \tanh^{-1} \delta$$

where

$$\delta_* = \frac{R_2}{R_1} = \frac{1 + \delta}{1 - \delta}$$

There appears to be a typographical error in the first definition and it should read

$$f(\delta) = \frac{\ln \delta_*}{2\delta} = \frac{1}{\delta} \tanh^{-1} \delta$$

The reasons for the larger difference in flutter results for the 5° cone as compared with the flutter results for the cylinder are attributed in part to the use in reference 34 of

17

the Galerkin method in conjunction with the uncoupled eighth-order shell equation and an assumed displacement that did not satisfy all boundary conditions; it has been demonstrated for buckling of cylinders (refs. 37 and 38) that application of the Galerkin method to the governing eighth-order equation on the normal displacement can give incorrect results for the buckling load or mode. Some comments on why application of the Galerkin method to the uncoupled equation can lead to erroneous results have been given by Singer (ref. 39).

Flutter mode shapes.- The effects of cone angle on flutter mode shape is shown in figure 7 for various values of α for isotropic conical shells with cylindrical simple support with $L/R_1 = 2$ and $R_1/h = 200$. The maximum amplitude occurs near the trailing edge, and the position of maximum amplitude moves towards the trailing edge as α increases. The mode shapes are similar to those calculated for flat plates (ref. 29) but differ from the one calculated for a cylinder with $L/R = 1.93$ (ref. 21) in that the cylinder flutter mode did not have a node line away from the boundaries. Figure 8 shows the effect of length-radius ratio L/R_1 on flutter mode shape of isotropic conical shells with cylindrical simple support with $R_1/h = 200$ and $\alpha = 30°$. For large values of L/R_1 $(L/R_1 = 6)$, several node lines occur in the flutter mode as indicated in figure 8(c).

General flutter boundaries.- The variation of λ with R_1/h for conical shells with cylindrical simple supports was found to be well correlated by the parameter $\bar{\lambda}$ determined in reference 33 for cylinders, where, for conical shells,

$$\bar{\lambda} = \frac{\lambda}{\left(1 - \mu^2\right)\left(R_1/h\right)^x} \quad \text{where} \quad x = \tanh\left(0.5 \frac{L}{R_1}\right) \tag{14}$$

The variation of $\bar{\lambda}$ with L/R_1 is shown in figure 9 for several values of α. Supersonic flow over a cone in air at zero angle of attack is dependent on cone angle α and free-stream Mach number M_∞. For example, at $M_\infty = 3$, α must be less than about $46°$ for $M_l > 1$ (ref. 36), and for $M_\infty = \infty$, α must be less than about $57.5°$. However, supersonic flow can occur over part of a cone for $\alpha > 57.5°$ if the cone is at an angle of attack. Since $60°$ cones are of interest as aerodynamic decelerators (ref. 25) which can be at angles of attack, results are presented in figure 9 for $0° \leq \alpha \leq 60°$; the results for $\alpha = 0°$ were obtained from reference 33. The curves represent average values of $\bar{\lambda}$ obtained for values of R_1/h from 100 to 2000. No calculated value of $\bar{\lambda}$ differed by more than about 12 percent from the average values shown in figure 9. Thus, these curves provide a rapid and reasonably accurate means of predicting the flutter characteristics of isotropic conical shells with cylindrical simple support for a wide range of α, L/R_1, and R_1/h. Blunt cones are significantly more susceptible to flutter than cylindrical shells for the same local flow conditions when the radius of the cylinder is

18

equal to R_1. Results for $L/R_1 \leqq 1$ could not be correlated by use of the parameter $\bar{\lambda}$. Difficulty in correlating results in this region might have been expected from the trends exhibited by the variation of $\dfrac{(q/\beta)_{max}}{(q/\beta)_{\alpha=0}}$ with R_1/h for $L/R_1 \leqq 1$ (fig. 5).

Effects of applied load.- Some effects of hydrostatic pressure and axial load on the flutter of isotropic conical shells with cylindrical simple support are shown in figure 10 in terms of λ as a function of the ratios p/p_{cr} (positive for external pressure) or P/P_{cr} (positive for compression) for $\alpha = 10^{\circ}$ and 30°. The variation of λ with applied load is nearly linear for both hydrostatic pressure and axial load. The effect of hydrostatic pressure is slight, whereas the effect of axial load is pronounced. Compressive axial load can decrease λ by up to an order of magnitude from the value for no load; similar trends have been shown for cylinders (refs. 40 and 41). Thus the effect of N_{yA} (the only stress for axial load) is considerably greater than the effect of $N_{\theta A}$ (the predominate stress for hydrostatic pressure). Results for flat plates also indicate that the effect of the stress in the direction of the airflow is much more significant than the stress in the cross-flow direction (ref. 42).

Effects of compressive axial load on flutter mode shape are shown in figure 11 for a conical shell with cylindrical simple support for $\alpha = 10^{\circ}$. As can be seen, the effect of axial load is to move the point of maximum amplitude toward the leading edge and to increase the amplitude over the forward part of the shell. Similar effects of compressive load have been observed both theoretically and experimentally for flat plates (ref. 43).

Effects of ring or stringer stiffening.- In order to analyze a ring- or stringer-stiffened cone by use of the present analysis, it is necessary to calculate equivalent orthotropic stiffness properties. Stiffness properties which neglect eccentricity effects were calculated from the formulas given in table I. Some flutter trends for ring- and stringer-stiffened shells are shown in figure 12 for $\alpha = 30^{\circ}$ with stiffener details also given. Stiffener size and spacing was such that the ring- or stringer-stiffened shells were essentially of equal weight. The stringer spacing, which actually varies along the length of the shell, was assumed to be the constant value of the spacing at the small end of the shell in calculating the equivalent orthotropic stiffness constants. Buckling and vibration results for the same shells are presented in appendixes C and D for $5^{\circ} \leqq \alpha \leqq 60^{\circ}$ and in reference 44 for $\alpha = 0$.

The flutter results are presented in figure 12 in terms of the ratio of the value of q/β for the stiffened cone to the value of q/β for the unstiffened cone plotted against L/R_1. The addition of either rings or stringers for the present configuration increases the value of q/β required for flutter compared to the value for the unstiffened shell. The effect of stringer stiffening decreases rapidly with L/R_1 up to about 3 and becomes essentially independent of L/R_1 for $L/R_1 > 5$. On the other hand, the effect of ring

stiffening increases with L/R_1 for the entire range of L/R_1. The results presented in figure 12 suggest for the present configuration that, for L/R_1 less than about 1, stringers may have more effect than rings. The effect of both rings and stringers decreases with increasing cone angle as shown in figure 13; the reduction is more pronounced for rings. The addition of stringers has a larger effect on flutter than on either buckling or vibration. This result is attributed to the fact that the effect of stringers increases with the number of axial half-waves m, and vibration modes with $m > 1$ have a pronounced effect on flutter characteristics.

The results presented in figures 12 and 13 neglect the effects of stiffener eccentricity. Two mode results for the flutter of flat plates with the same stiffener details shown in figure 12 are presented in reference 44. These results indicated that consideration of stiffener eccentricity increased the flutter resistance by nearly a factor of 2. Thus it would appear that stiffener eccentricity effects would be significant for the flutter of shells also, although there are no results available to verify this conjecture.

Elastically Supported Isotropic Shells

<u>Effects of axial and rotational restraint.</u>- Effects of axial restraint $\left(k_1\right)$ are shown in figure 14, which gives the variation of λ and Δ with the ratio k_1/E; shell properties are also given. Increasing axial restraint results in decreases in λ of up to about 10 percent for $k_1/E = 1$. This result is in marked contrast to the trends for buckling (appendix C) and vibration (appendix D); the buckling load and natural frequencies always increased with increasing k_1/E. The decrease in λ with k_1/E is attributed to the dependence of shell flutter characteristics on the frequency spectrum as well as magnitude. The decrease of Δ with k_1/E indicates that the effect of decreases in frequency spacing with k_1/E is greater than the effect of increases in frequency magnitude. These results illustrate again that trends established for buckling and vibration do not necessarily hold for flutter.

Some effects of rotational restraint are shown in figure 15, in terms of λ and $\dfrac{R_1 k_4}{D_y}$ for the same shell considered in figure 14. The lower curve is for complete axial constraint, the upper curve for no axial restraint. Figure 15 shows that λ increases only slightly with increasing rotational restraint. Calculations (not presented) revealed that Δ also increased with increasing rotational restraint. The increase of λ with $\dfrac{R_1 k_4}{D_y}$ is similar to the trends for buckling and vibration. The results also indicate that the value of λ for the essentially clamped cone is about 6 percent less than the value of λ for the simply supported cone. However, additional calculations (not presented) indicated that the effects of edge clamping depend on cone angle α. As α approached zero

$(\alpha < 15^{\circ})$, the effects of edge clamping (primarily axial restraint) became stabilizing as for cylindrical shells (ref. 26).

Effects of circumferential and radial restraint.- Effects of elastic circumferential restraint k_2 and radial restraint k_3 are shown in figure 16, which gives the variation of λ with the ratio k_3/E; shell properties are also given. The upper curve is for $k_2/E = 1$ $\left(v_B = 0\right)$, the lower curve for $k_2/E = k_3/E$; for both curves $k_1 = k_4 = 0$. The numbers on the curves represent the number of circumferential waves in the flutter mode. The open circles and squares at $k_3/E = 1$ $\left(u_{HB} = 0\right)$ show the slight effect of changing the circumferential restraint from complete constraint $\left(v_B = 0\right)$ to no restraint $\left(N_{y\theta B} = 0\right)$ for no radial displacement. The effect of decreasing the radial restraint becomes significant for $k_3/E \leqq 10^{-3}$. For $k_2/E = 1$, decreasing k_3/E to 0 decreases λ by over a factor of 2 as indicated by the solid square. However, when $k_2/E = k_3/E$, decreasing k_3/E to 0 decreases λ by over 2 orders of magnitude as indicated by the solid circle, and the flutter mode changes from $\eta = 8$ to an essentially inextensional mode at $\eta = 2$. The reason for the large effect of circumferential restraint as the radial restraint becomes weak is that the constraint $v_B = 0$ prevents the inextensional form of flutter ($\eta = 2$), which is the critical mode of instability when all edge restraints are relatively weak. The flutter trends shown in figure 16 are similar to the trends for free vibration for the same shell given in appendix D. Since the critical value of η becomes small as the edge restraint becomes relatively weak, the present Donnell type theory becomes more approximate. Hence it might be desirable to use more exact shell theories in analysis of flutter of shells with weak edge restraint.

Calculations for the variation of Δ with the various edge restraints considered in figures 14, 15, and 16 indicated that the qualitative effects of edge restraint on λ apparently can be determined by merely examining the effect of edge restraint on Δ for the appropriate range of η.

CONCLUDING REMARKS

The flutter, vibration, and buckling characteristics of orthotropic truncated conical shells with generalized elastic edge restraint have been investigated theoretically. The problem was simplified by making certain assumptions which have been found admissible for flutter analyses of cylinders. The shell analysis utilized the classical Donnell type theory, in-plane inertias and structural damping were neglected, and the aerodynamic loading was represented by the inviscid two-dimensional quasi-steady approximation (modified piston theory). The principle of virtual work was utilized to formulate the problem. An approximate solution was obtained by the generalized Galerkin method in terms of assumed displacement functions that had to satisfy only geometric constraints. A stress function was introduced so that only the normal displacement needed to be

assumed. The equation for the stress function was solved exactly in terms of the arbitrary coefficients in the assumed displacement.

Numerical results for flutter of conical shells revealed that trends established for buckling and vibration do not necessarily hold for flutter. Increasing cone semivertex angle (up to about 15°) for length-radius ratios greater than about 1 increased the resistance to flutter even though the buckling load and natural frequencies decreased. Also, increasing the axial edge restraint could decrease the resistance to flutter even though both the buckling load and natural frequencies were increased. These phenomena were attributed to the fact that flutter depends on frequency spectrum as well as magnitude. The flutter resistance for a given circumferential wave number was shown to be proportional to the difference in the square of the first two in vaccuo natural frequencies. Thus the effect of a given parameter on the flutter of a conical shell can be determined qualitatively by considering its effect on the natural frequencies (magnitude and spectrum) of the shell for the appropriate range of wave numbers. Although slightly conical shells (semivertex angles less than about 15°) have more flutter resistance than cylinders with the same thickness and length and a radius equal to the smaller radius of the conical shell, blunt cones (semivertex angles greater than about 45°) are significantly more susceptible to flutter than cylinders. Sufficient numerical results are presented in the form of general flutter boundaries to permit the determination of the flutter condition for simply supported isotropic conical shells for a wide range of cone semivertex angle, length-radius ratio, and radius-thickness ratio. Results are also presented to indicate some effects of finite axial, radial, circumferential, and rotational edge restraints, hydrostatic pressure, axial load, and rings and stringers on the flutter, vibration, and buckling characteristics of conical shells.

Langley Research Center,
National Aeronautics and Space Administration,
Hampton, Va., March 18, 1970.

APPENDIX A

CONVERSION OF U.S. CUSTOMARY UNITS TO SI UNITS

The International System of Units (SI) was adopted by the Eleventh General Conference on Weights and Measures, Paris, October 1960 (ref. 45). Conversion factors for the units used herein are given in the following table:

Physical quantity	U.S. Customary Unit	Conversion factor (*)	SI Unit
Area	in^2	0.6451×10^{-3}	$meters^2$ (m^2)
Length	in.	0.0254	meters (m)
Moment of inertia	in^4	0.4161×10^{-6}	$meters^4$ (m^4)
Young's and shear moduli . . .	lb/in^2	6.895×10^3	newtons/$meter^2$ (N/m^2)

*Multiply value given in U.S. Customary Unit by conversion factor to obtain equivalent value in SI unit.

Prefixes to indicate multiple of units are as follows:

Prefix	Multiple
giga (G)	10^9
kilo (k)	10^3
centi (c)	10^{-2}
milli (m)	10^{-3}

23

APPENDIX B

GOVERNING EQUATIONS

The principle of virtual work is used to formulate the problem of flutter of an orthotropic conical shell with generalized elastic edge restraint. Such a formulation admits a solution by the generalized Galerkin method in terms of assumed displacements that must satisfy only geometric constraints. For a generalized elastic edge restraint there are no geometric constraints (only force or natural constraints); thus a rather simple series can be used for the assumed displacements. Such a procedure is straightforward and well known (for example, refs. 15 and 16) but has been used only sparingly (for example, refs. 46 and 47). Instead, investigators of flutter problems have obtained displacement functions that satisfy all boundary conditions (sometimes going to great lengths, for example, ref. 48), or have relied on psuedo energy methods (for example, refs. 32 and 49).

Although the use of complicated series representations can result in fewer terms required for convergence, and thus possibly justify the effort, the modification of potential energy methods for nonconservative problems seems unjustified. As pointed out in references 39 and 50, investigators have applied the Galerkin method to single uncoupled equations for systems properly defined by two or more coupled equations and obtained erroneous results. The erroneous results are due to inadequate attention to the boundary conditions that result from the manipulations required to obtain the single uncoupled equation. Thus in the present investigation the derivation and solution of equations is given in some detail to emphasize the straightforward yet completely general character of the virtual work (generalized Galerkin method) approach to nonconservative problems.

General Nonlinear Equilibrium Equations

Donnell type expressions for middle surface strains and curvatures of a deformed conical shell are given by Seide in reference 27. For this paper, these expressions are given in the following form:

$$\left.\begin{array}{l} \epsilon_y = u_{,y} + \frac{1}{2}\left(w_{,y}\right)^2 \\[2em] \epsilon_\theta = \dfrac{u - w\cot\alpha}{y} + \dfrac{1}{y}\,v_{,\phi} + \dfrac{1}{2y^2}\left(w_{,\phi}\right)^2 \\[2em] \epsilon_{y\theta} = v_{,y} - \dfrac{v}{y} + \dfrac{1}{y}\,u_{,\phi} + \dfrac{1}{y}\,w_{,y}w_{,\phi} \end{array}\right\} \tag{B1}$$

$$\left.\begin{aligned}
\chi_y &= w{,}_{yy} \\
\chi_\theta &= \frac{1}{y}\, w{,}_y + \frac{1}{y^2}\, w{,}_{\phi\phi} \\
\chi_{y\theta} &= \frac{1}{y}\, w{,}_{y\phi} - \frac{1}{y^2}\, w{,}_\phi
\end{aligned}\right\} \tag{B2}$$

Middle-surface force and moment resultants are defined as

$$\left.\begin{aligned}
N_y &= B_y\!\left(\epsilon_y + \mu'_\theta \epsilon_\theta\right) \\
N_\theta &= B_\theta\!\left(\epsilon_\theta + \mu'_y \epsilon_y\right) \\
N_{y\theta} &= B_{y\theta}\,\epsilon_{y\theta}
\end{aligned}\right\} \tag{B3}$$

$$\left.\begin{aligned}
M_y &= -D_y\!\left(\chi_y + \mu_\theta \chi_\theta\right) \\
M_\theta &= -D_\theta\!\left(\chi_\theta + \mu_y \chi_y\right) \\
M_{y\theta} &= -D_{y\theta}\,\chi_{y\theta}
\end{aligned}\right\} \tag{B4}$$

The equations of equilibrium will be obtained by the principle of virtual work, which requires that

$$\delta\Omega_t = \delta U_s \tag{B5}$$

where $\delta\Omega_t$ represents the total virtual work of all the external forces and the restoring forces of the elastic edge restraint, and δU_s represents the change in the internal strain energy of the system corresponding to the virtual displacements.

The virtual work of the total surface pressure can be expressed by the surface integral

$$\delta\Omega_p = \int_{y_1}^{y_2} \int_0^{2\pi \sin\alpha} p_t \delta w \, y \, d\phi \, dy \tag{B6}$$

while the virtual work of the boundary forces can be expressed as

$$\delta\Omega_f = \int_0^{2\pi \sin\alpha} \left(\overline{N}_y \delta u + \overline{N}_{y\theta} \delta v + \overline{Q}_y \delta w - \overline{M}_y \delta w{,}_y + \overline{M}_{y\theta} \frac{\delta w{,}_\phi}{y}\right) y \Bigg|_{y_1}^{y_2} d\phi \tag{B7}$$

where δ represents virtual change in variable and $\phi = \theta \sin\alpha$. The effects of the generalized elastic edge restraint can be introduced into the analysis by the virtual work expression

$$\delta\Omega_e = \int_0^{2\pi \sin\alpha} \left(F_u \delta u + F_v \delta v + F_w \delta w - M_w \delta w,_y\right) y \bigg|_{y_1}^{y_2} d\phi \tag{B8}$$

where F_u, F_v, F_w, and M_w are the forces and bending moment exerted on the shell by the elastic support at the shell edge. The total virtual work of all the external forces is given by

$$\delta\Omega_t = \delta\Omega_p + \delta\Omega_f + \delta\Omega_e \tag{B9}$$

The strain energy of the shell can be expressed in terms of middle surface force and moment resultants by the surface integral

$$U_S = \frac{1}{2} \int_{y_1}^{y_2} \int_0^{2\pi \sin\alpha} \left(N_y \epsilon_y + N_\theta \epsilon_\theta + N_{y\theta} \epsilon_{y\theta} - M_y \chi_y - M_\theta \chi_\theta - 2M_{y\theta} \chi_{y\theta}\right) y \, d\phi \, dy \tag{B10}$$

If the force and moment resultants, strains, and curvatures are expressed in terms of displacements by equations (B1) to (B4), if the variation of U_S is taken with respect to these displacements, and if equation (B9) is utilized, equation (B5) becomes, after integration by parts,

$$\int_{y_1}^{y_2} \int_0^{2\pi \sin\alpha} \left\{\Big[\text{eq. (B12)}\Big]\delta u + \Big[\text{eq. (B13)}\Big]\delta v + \Big[\text{eq. (B14)}\Big]\delta w\right\} d\phi \, dy$$

$$- \int_0^{2\pi \sin\alpha} \left\{\Big[\text{eq. (B16a)}\Big]\delta u + \Big[\text{eq. (B16b)}\Big]\delta v + \Big[\text{eq. (B16c)}\Big]\delta w\right.$$

$$\left. - \Big[\text{eq. (B16d)}\Big]\delta w,_y\right\} y \bigg|_{y_1}^{y_2} d\phi = 0 \tag{B11}$$

where the general nonlinear equilibrium equations are given by

$$\left(yN_y\right),_y + N_{y\theta},_\phi - N_\theta = 0 \tag{B12}$$

$$N_\theta,_\phi + \left(yN_{y\theta}\right),_y + N_{y\theta} = 0 \tag{B13}$$

$$D_y L_1(w) - N_\theta \cot\alpha - \left(yN_y w,_y\right),_y - \frac{1}{y}\left(N_\theta w,_\phi\right),_\phi - \left(N_{y\theta} w,_y\right),_\phi - \left(N_{y\theta} w,_\phi\right),_y - p_t y = 0 \tag{B14}$$

with

$$L_1(\ ) = y(\ )_{,yyyy} + 2(\ )_{,yyy} + \frac{D_\theta}{D_y}\left[\frac{1}{y^3}(\ )_{,\phi\phi\phi\phi} + \frac{2}{y^3}(\ )_{,\phi\phi} + \frac{1}{y^2}(\ )_{,y} - \frac{1}{y}(\ )_{,yy}\right]$$

$$+ 2\left[\frac{D_{y\theta}}{D_y} + \mu_\theta\right]\left[\frac{1}{y^3}(\ )_{,\phi\phi} - \frac{1}{y^2}(\ )_{,y\phi\phi} + \frac{1}{y}(\ )_{,yy\phi\phi}\right] \tag{B15}$$

and the boundary conditions on an edge $y = $ Constant are to prescribe

$$N_y - F_u - \overline{N}_y = 0 \qquad\qquad \text{or} \qquad u \tag{B16a}$$

$$N_{y\theta} - F_v - \overline{N}_{y\theta} = 0 \qquad\qquad \text{or} \qquad v \tag{B16b}$$

$$Q_y - F_w - \overline{Q}_y + \frac{1}{y}\left(\overline{M}_{y\theta}\right)_{,\phi} = 0 \qquad\qquad \text{or} \qquad w \tag{B16c}$$

$$M_y - M_w - \overline{M}_y = 0 \qquad\qquad \text{or} \qquad w_{,y} \tag{B16d}$$

with

$$Q_y = N_y w_{,y} + \frac{N_{y\theta}w_{,\phi}}{y} - \frac{M_\theta}{y} + \frac{\left(yM_y\right)_{,y}}{y} + \frac{2M_{y\theta,\phi}}{y} \tag{B17}$$

Linearized Stability Equations

The total surface pressure loading p_t can be expressed as

$$p_t = p + p_s \tag{B18}$$

where p represents an axisymmetric uniform lateral pressure loading that exists prior to flutter and p_s represents the asymmetric surface loading resulting from vibration and flutter of the shell. Because the loading prior to flutter is axisymmetric

$$N_{y\theta A} = v_A = (\ )_{A,\phi} = 0 \tag{B19}$$

where the subscript A denotes quantities that exist prior to flutter, vibration, or buckling. If equations (B19) are utilized, equation (B13) is identically satisfied and equations (B12) and (B14) become

$$\left(yN_{yA}\right)_{,y} - N_{\theta A} = 0 \tag{B20a}$$

$$D_y\left[yw_{A,yyyy} + 2w_{A,yyy} + \frac{D_\theta}{D_y}\left(\frac{1}{y^2}w_{A,y} - \frac{1}{y}w_{A,yy}\right)\right] - N_{\theta A}\cot\alpha$$

$$- \left(yN_{yA}w_{A,y}\right)_{,y} - yp = 0 \tag{B20b}$$

and the boundary conditions on an edge y = Constant are to prescribe

$$N_{yA} - F_{uA} - \overline{N}_y = 0 \qquad \text{or} \qquad u_A \qquad \text{(B21a)}$$

$$v_A = 0 \qquad \qquad \text{(B21b)}$$

$$Q_{yA} - F_{wA} - \overline{Q}_y = 0 \qquad \text{or} \qquad w_A \qquad \text{(B21c)}$$

$$M_{yA} - M_{wA} - \overline{M}_y = 0 \qquad \text{or} \qquad w_{A,y} \qquad \text{(B21d)}$$

If the exact nonlinear stress distribution prior to flutter were desired, it would be necessary to solve equations (B20) subject to the boundary conditions given by equations (B21).

To investigate flutter, the total displacements are expressed as the sum of the axisymmetric displacements that exist prior to flutter and the infinitesimal asymmetric displacements u_B, v_B, and w_B that occur at flutter. Thus

$$\left. \begin{aligned} u &= u_A + u_B \\ v &= v_B \\ w &= w_A + w_B \end{aligned} \right\} \qquad \text{(B22)}$$

Similar expressions can be developed for the stress resultants, moments, and forces applied by the elastic edge support.

If these expressions and equations (B18) and (B22) are substituted into equation (B11), if equations (B19), (B20), and (B21) relating subscript A terms are subtracted out, if products of the displacement w_A and the stresses N_{yB} and $N_{y\theta B}$ are omitted, and if terms nonlinear with respect to subscript B are neglected, the virtual work expression governing stability of the conical shell becomes

$$\int_{y_1}^{y_2} \int_0^{2\pi \sin\alpha} \left\{ \Big[\text{eq. (B24)}\Big] \delta u_B + \Big[\text{eq. (B25)}\Big] \delta v_B + \Big[\text{eq. (B26)}\Big] \delta w_B \right\} d\phi \, dy$$

$$- \int_0^{2\pi \sin\alpha} \left\{ \Big[\text{eq. (B27a)}\Big] \delta u_B + \Big[\text{eq. (B27b)}\Big] \delta v_B + \Big[\text{eq. (B27c)}\Big] \delta w_B \right.$$

$$\left. - \Big[\text{eq. (B27d)}\Big] \delta w_{B,y} \right\} y \Big|_{y_1}^{y_2} d\phi = 0 \qquad \text{(B23)}$$

where the linear stability equations are

$$\left(yN_{yB}\right)_{,y} + N_{y\theta B,\phi} - N_{\theta B} = 0 \tag{B24}$$

$$N_{\theta B,\phi} + \left(yN_{y\theta B}\right)_{,y} + N_{y\theta B} = 0 \tag{B25}$$

$$D_y L_1\left(w_B\right) - N_{\theta B}\cot\alpha - yN_{yA}w_{B,yy} - N_{\theta A}\left(\frac{1}{y}w_{B,\phi\phi} + w_{B,y}\right) - yp_s = 0 \tag{B26}$$

and the boundary conditions on an edge $y = \text{Constant}$ are to prescribe

$$N_{yB} - F_{uB} = 0 \qquad \text{or} \qquad u_B \tag{B27a}$$

$$N_{y\theta B} - F_{vB} = 0 \qquad \text{or} \qquad v_B \tag{B27b}$$

$$Q_{yB} - F_{wB} = 0 \qquad \text{or} \qquad w_B \tag{B27c}$$

$$M_{yB} - M_{wB} = 0 \qquad \text{or} \qquad w_{B,y} \tag{B27d}$$

In obtaining equation (B26), use has been made of the identity

$$\left(yN_{yA}w_{B,y}\right)_{,y} + \frac{1}{y}\left(N_{\theta A}w_{B,\phi}\right)_{,\phi} = yN_{yA}w_{B,yy} + N_{\theta}\left(\frac{1}{y}w_{B,\phi\phi} + w_{B,y}\right)$$

$$+ w_{B,y}\left[\left(yN_{yA}\right)_{,y} - N_{\theta A}\right] \tag{B28}$$

From equation (B20a), the term in brackets in equation (B28) is 0.

Equations (B24) and (B25) are identically satisfied if the stress functions F or F_0 (refs. 27 and 28) are introduced such that, for $\eta > 0$,

$$\left.\begin{array}{l} N_{\theta B} = F_{,yy} \\[2mm] N_{yB} = \dfrac{1}{y}F_{,y} + \dfrac{1}{y^2}F_{,\phi\phi} \\[2mm] N_{y\theta B} = \dfrac{1}{y^2}F_{,\phi} - \dfrac{1}{y}F_{,y\phi} \end{array}\right\} \tag{B29}$$

and, for $\eta = 0$,

$$\left. \begin{aligned} N_{\theta B} &= F_{o,y} \\[6pt] N_{yB} &= \frac{F_o}{y} \\[6pt] N_{y\theta B} &= 0 \end{aligned} \right\} \tag{B30}$$

where η is the number of circumferential waves.

Thus, the number of unknowns is reduced from three $\left(u_B, \ v_B, \text{ and } w_B\right)$ to two $\left(F \text{ and } w_B\right)$. However, in order to use the stress-function approach an equation is needed to define F. The appropriate equation is the compatibility equation which is obtained by eliminating u_B and v_B from the linear form of the middle-surface strain-displacement relations and is given as follows:

$$\left(y\epsilon_{y\theta B,\phi}\right)_{,y} - \epsilon_{yB,\phi\phi} - \left(y^2\epsilon_{\theta B,y}\right)_{,y} + y\epsilon_{yB,y} = y \cot \alpha \ w_{B,yy} \tag{B31}$$

or, in terms of F,

$$L_2(F) = -B_\theta\left(1 - \mu'_\theta\mu'_y\right)w_{B,yy} \cot \alpha \tag{B32}$$

where

$$L_2(\ ) = y(\ )_{,yyyy} + \frac{B_\theta}{By}\left[\frac{1}{y^3}(\ )_{,\phi\phi\phi\phi} + \frac{2}{y^3}(\ )_{,\phi\phi} + \frac{1}{y^2}(\ )_{,y} - \frac{1}{y}(\ )_{,yy}\right]$$

$$+ \left[\frac{B_\theta}{By\theta}\left(1 - \mu'_\theta\mu'_y\right) - 2\mu'_\theta\right]\left[\frac{1}{y^3}(\ )_{,\phi\phi} - \frac{1}{y^2}(\ )_{,y\phi\phi} + \frac{1}{y}(\ )_{,yy\phi\phi}\right] \tag{B33}$$

The boundary conditions for F are the boundary conditions for u_B and v_B (eqs. (B27a) and (B27b)). For $\eta = 0$, the symmetry conditions $N_{y\theta B} = v_B = (\ )_{B,\phi} = 0$ exist and the compatibility equation becomes

$$\left(y\epsilon_{\theta B}\right)_{,y} - \epsilon_{yB} = -w_{B,y} \cot \alpha \tag{B34}$$

or, in terms of F_o,

$$F_{o,yy} + \frac{1}{y} F_{o,y} - \frac{B_\theta}{By}\frac{F_o}{y^2} = -\frac{1}{y} B_\theta\left(1 - \mu'_\theta\mu'_y\right) \cot \alpha \ w_{B,y} \tag{B35}$$

The boundary condition for F_o is the boundary condition for u_B (eq. (B27a)). The linear membrane stress distribution is adequate to express $N_{\theta A}$ and N_{yA} in terms of

the external hydrostatic pressure p and externally applied axial load P (positive in compression). Thus,

$$\left.\begin{array}{l} N_{\theta A} = -y \tan \alpha \; p \\[2ex] N_{yA} = -\dfrac{y}{2} \tan \alpha \; p - \dfrac{P}{2\pi \sin \alpha \cos \alpha} \end{array}\right\} \tag{B36}$$

To investigate flutter it is necessary that p_S represent the inertial and aerodynamic loading. If the modified piston theory aerodynamic approximation is used to represent the aerodynamic forces (ref. 29), p_S can be expressed as

$$p_S = -\gamma w_{B,tt} - \frac{2q}{\beta} w_{B,y} - \rho c_{air} w_{B,t} \tag{B37}$$

where the first term on the right is the inertia loading, the second term is the static aerodynamic loading, and the last term is a viscous loading corresponding to the aerodynamic damping. In the denominator of the second term on the right, the Mach number M_l has been replaced by $\beta = \sqrt{M_l^2 - 1}$. Preference for the compressibility factor β is based on its demonstrated usefulness for flutter of flat panels.

With the introduction of the stress function and equations (B36) and (B37), the virtual work stability criterion becomes

$$\int_{y_1}^{y_2} \int_0^{2\pi \sin \alpha} \Big[\text{eq. (B39)}\Big] \delta w_B \; d\phi \; dy + \int_0^{2\pi \sin \alpha} \left\{ \Big[\text{eq. (B27c)}\Big] \delta w_B \right.$$

$$\left. - \Big[\text{eq. (B27d)}\Big] \delta w_{B,y} \right\} y \Big|_{y_1}^{y_2} d\phi = 0 \tag{B38}$$

where the governing equation for the normal displacement w_B is given by

$$D_y L_1\big(w_B\big) - \cot \alpha \; F_{,yy} + \left(y \frac{\tan \alpha}{2} p + \frac{P}{2\pi \sin \alpha \cos \alpha}\right) y w_{B,yy} + y \tan \alpha \; p\left(\frac{1}{y} w_{B,\phi\phi} + w_{B,y}\right)$$

$$+ y\left(\gamma w_{B,tt} + \frac{2q}{\beta} w_{B,y} + \rho c_{air} w_{B,t}\right) = 0 \tag{B39}$$

For $\eta = 0$ the term $F_{,yy}$ is replaced by $F_{0,y}$.

Solution of Equations

The equations for the stress functions (eqs. (B32) and (B35)) and the equation for the normal displacement (eq. (B38)) are solved by an assumed displacement method. Equation (B32) has variable coefficients that reduce to constant coefficients by use of the transformation of coordinates (ref. 51)

$$y = y_1 e^x \tag{B40}$$

Thus, $y = y_1$ corresponds to $x = 0$ and $y = y_2$ corresponds to $x = x_1 = \ln \dfrac{y_2}{y_1}$. For simple harmonic motion the displacement w_B is assumed to be

$$w_B = w_B^*(x) \cos n\phi \, e^{i\omega t} \tag{B41}$$

where

$$w_B^*(x) = a_0 + \bar{a}_0 x + \sum_{m=1}^{M} a_m \sin \frac{m\pi x}{x_1} \tag{B42}$$

and

$$n = \frac{\eta}{\sin \alpha} \tag{B43}$$

The expression for w_B is continuous in the circumferential direction and permits deflections and rotations to exist at the ends of the cone.

The boundary conditions (eqs. (B27)) are now specialized. The shell stresses and displacements are of the form $\left(\text{neglecting the term } e^{i\omega t}\right)$

$$\left.\begin{aligned}
u_B &= u_B^* \cos n\phi \\[6pt]
v_B &= v_B^* \sin n\phi \\[6pt]
w_B &= w_B^* \cos n\phi \\[6pt]
N_{yB} &= N_{yB}^* \cos n\phi \\[6pt]
N_{\theta B} &= N_{\theta B}^* \cos n\phi \\[6pt]
N_{y\theta B} &= N_{y\theta B}^* \sin n\phi
\end{aligned}\right\} \tag{B44}$$

From equations (B27) it follows that $\left(\text{the expressions for } Q_{yB} \text{ and } M_{yB} \text{ being considered}\right)$

$$\left.\begin{array}{l} F_{uB} = F^*_{uB} \cos n\phi \\[10pt] F_{vB} = F^*_{vB} \sin n\phi \\[10pt] F_{wB} = F^*_{wB} \cos n\phi \\[10pt] M_{wB} = M^*_{wB} \cos n\phi \end{array}\right\} \qquad\qquad \text{(B45)}$$

The forces F^*_{uB}, F^*_{vB}, F^*_{wB}, and M^*_{wB} are now expressed in terms of the shell displacements u^*_B, v^*_B, w^*_B, and $w^*_{B,y}$. The most general relations for a shell of revolution supported by some generalized unloaded elastic support at its boundaries can be written in matrix form as (ref. 17)

$$\begin{Bmatrix} F^*_{uB} \\[8pt] F^*_{vB} \\[8pt] F^*_{wB} \\[8pt] -M^*_{wB} \end{Bmatrix} = \begin{bmatrix} K_{ijB} - \omega^2 G_{ijB} \end{bmatrix} \begin{Bmatrix} u^*_B \\[8pt] v^*_B \\[8pt] w^*_B \\[8pt] w^*_{B,y} \end{Bmatrix} \qquad\qquad \text{(B46)}$$

The term K_{ij} represents the elastic restraint of the support at the shell edge, and the term G_{ij} represents the mass effects of the elastic support. By utilizing equations (B44) to (B46), the boundary conditions (eqs. (B27)) become

$$\begin{Bmatrix} N^*_{yB} \\[8pt] N^*_{y\theta B} \\[8pt] Q^*_{yB} \\[8pt] -M^*_{yB} \end{Bmatrix} \mp \begin{bmatrix} K_{ijB} - \omega^2 G_{ijB} \end{bmatrix} \begin{Bmatrix} u^*_B \\[8pt] v^*_B \\[8pt] w^*_B \\[8pt] w^*_{B,y} \end{Bmatrix} = 0 \qquad (i,j=1,2,3,4) \quad \text{(B47)}$$

where the minus sign applies at $y = y_1$.

APPENDIX B

For uncoupled massless springs all G_{ijB} terms are 0, and, for conical coordinates,

$$K_{ijB} = \begin{bmatrix} \bar{k}_1 & 0 & 0 & 0 \\ 0 & k_2 & 0 & 0 \\ 0 & 0 & \bar{k}_3 & 0 \\ 0 & 0 & 0 & k_4 \end{bmatrix} \tag{B48}$$

or, for cylindrical coordinates,

$$K_{ijB} = \begin{bmatrix} k_1 & 0 & k_{13} & 0 \\ 0 & k_2 & 0 & 0 \\ k_{13} & 0 & k_3 & 0 \\ 0 & 0 & 0 & k_4 \end{bmatrix} \tag{B49}$$

where

$$k_{13} = \left(k_1 - k_3\right) \cos \alpha \sin \alpha \tag{B50}$$

and k_i and $\bar{k}_i$ are spring constants.

The nondimensional forms of K_{ij} and G_{ij} are S_{ij} and M_{ij}; expressions for S_{ij} and M_{ij} relating the stiffness and inertia characteristics of end rings to the ring and shell material properties and geometry were obtained from equations (A5) to (A8) of reference 17 and are presented in the supplement to NASA TN D-5759. For flutter (or vibration), the eigenvalue ω^2 appears in the boundary conditions unless all G_{ij} terms are 0; thus, it is necessary to iterate on the eigenvalue until the value used in the boundary conditions differs by a negligible amount from the calculated eigenvalue.

Compatibility equations.- The procedure for solving the compatibility equation for the stress functions is outlined in this section. The details of the solutions are given in the supplement to NASA TN D-5759. If the stress function F is taken to be

$$\dot{F} = e^x f(x) \cos n\phi \; e^{i\omega t} \tag{B51}$$

and equations (B40) and (B41) are utilized, equation (B32) reduces to the ordinary differential equation

$$f_{,xxxx} + P_1 f_{,xx} + P_2 f = -B_\theta\left(1 - \mu'_\theta \mu'_y\right) y_1 \cos \alpha \left(w^*_{B,xx} - w^*_{B,x}\right) \tag{B52}$$

where

$$P_1 = -\left(1 + \frac{B_\theta}{B_y}\right) - n^2 \left[\frac{B_\theta}{B_{y\theta}}\left(1 - \mu'_\theta\mu'_y\right) - 2\mu'_\theta\right]$$

$$P_2 = \frac{B_\theta}{B_y}\left(n^2 - 1\right)^2$$

(B53)

By use of equation (B51), equation (B52) contains only even derivatives of f with respect to x. The homogeneous solution is readily found to be

$$f_h = A_1 e^{\lambda_1 x} + A_2 e^{-\lambda_1 x} + A_3 e^{\lambda_2 x} + A_4 e^{-\lambda_2 x}$$

(B54)

where

$$\lambda_1 = \left[\frac{-P_1 + \left(P_1^2 - 4P_2\right)^{1/2}}{2}\right]^{1/2}$$

$$\lambda_2 = \left[\frac{-P_1 - \left(P_1^2 - 4P_2\right)^{1/2}}{2}\right]^{1/2}$$

(B55)

and A_1 to A_4 are constants of integration. The particular solution for an M-term approximation in w_B^* is obtained by substituting

$$f_p = d_o + \sum_{m=1}^{M}\left(d_m \cos \frac{m\pi x}{x_1} + e_m \sin \frac{m\pi x}{x_1}\right)$$

(B56)

into equation (B52) and matching coefficients. With $f = f_h + f_p$ known in terms of A_1 to A_4, the stress resultants are obtained from equations (B29) and (B30), the strains are obtained from the constitutive equations (B3), and the displacements u_B and v_B are obtained from the linearized strain-displacement relations (eqs. (B1)). The constants of integration A_1 to A_4 are determined from the boundary conditions for u_B and v_B, the first two of equations (B47). Expressions for the stress function, stress resultants, displacements, and constants of integration are given in the supplement to NASA TN D-5759.

Stability equations.- By utilizing the transformation of coordinates (eq. (B40)) the virtual work expression for the stability of the conical shell becomes

$$\int_0^{x_1} \int_0^{2\pi \sin \alpha} \left[\text{eq. (B58)}\right] \delta w_B \, d\phi \, y_1 e^x \, dx$$

$$+ \int_0^{2\pi \sin \alpha} \left\{ \left[\text{eq. (B27c)}\right] \delta w_B - \left[\text{eq. (B27d)}\right] \frac{\delta w_{B,x}}{y_1 e^x} \right\} y_1 e^x \bigg|_0^{x_1} d\phi = 0 \qquad (B57)$$

where the equation for w_B is given by

$$D_y L_3(w_B) - \frac{\cot \alpha \left(f_{,xx} + f_{,x}\right)}{y_1^2 e^x} + \left[\tan \alpha \, \frac{p}{2} + \frac{P}{2\pi \left(y_1 e^x\right)^2 \sin \alpha \cos \alpha} \right] \left(w_{B,xx} - w_{B,x}\right)$$

$$+ \tan \alpha \, p \left(w_{B,\phi\phi} + w_{B,x}\right) - y_1 e^x \left(\gamma \omega^2 - i\rho c_{air}\omega\right) w_B + \frac{2q}{\beta} w_{B,x} = 0 \qquad (B58)$$

and $L_3(\ )$ is defined as

$$L_3(\ ) = \frac{1}{\left(y_1 e^x\right)^3} \Bigg[(\ )_{,xxxx} - 4(\ )_{,xxx} + \left(5 - \frac{D_\theta}{D_y}\right)(\ )_{,xx} + 2\left(\frac{D_\theta}{D_y} - 1\right)(\ )_{,x}$$

$$+ \frac{2D_\theta}{D_y}(\ )_{,\phi\phi} + \frac{D_\theta}{D_y}(\ )_{,\phi\phi\phi\phi} \Bigg] + \frac{2}{\left(y_1 e^x\right)^3} \left(\frac{D_{y\theta}}{D_y} + \mu_\theta\right) \Big[(\ )_{,\phi\phi}$$

$$- 2(\ )_{,\phi\phi x} + (\ )_{,\phi\phi xx} \Big] \qquad (B59)$$

For $\eta = 0$ the term $\dfrac{\cot \alpha \left(f_{,xx} + f_{,x}\right)}{y_1^2 e^x}$ in equation (B58) is replaced by $\dfrac{\cot \alpha \, F_{0,x}}{y_1 e^x}$.

If F_{wB} and M_{wB} in equations (B27c) and (B27d) are expressed in terms of K_{ij}, G_{ij}, and the shell displacements by use of equation (B46), if the moments, transverse shear, f, u_B, v_B, and w_B are expressed in terms of the assumed series for w_B, and if the integration with respect to ϕ is performed, equation (B57) becomes the generalized Galerkin solution of equation (B58) where δw_B^* and $\delta w_{B,x}^*$ are taken successively as

$$\delta w_B^* = \delta a_o \qquad \delta w_{B,x}^* = 0$$

$$\delta w_B^* = \delta \bar{a}_o x \qquad \delta w_{B,x}^* = \delta \bar{a}_o \qquad\qquad (B60)$$

$$\delta w_B^* = \delta a_p \sin \frac{p\pi x}{x_1} \qquad \delta w_{B,x}^* = \delta a_p \frac{p\pi}{x_1} \cos \frac{p\pi x}{x_1} \quad (p=1,2,3,\ldots,M)$$

If the integration with respect to x is also performed, equation (B57) becomes $M + 2$ simultaneous algebraic equations which can be written as

$$\left[\left[b_{ij} \right] + \frac{C_P}{2\pi \sin^2\alpha \cos \alpha} \left[c_{ij} \right] + \frac{C_p}{\sin^2\alpha \cos \alpha} \left[d_{ij} \right] - \frac{C_\omega}{\sin^4\alpha} \left[e_{ij} \right] + \frac{\lambda}{\sin^3\alpha} \left[f_{ij} \right] \right] \begin{Bmatrix} a_o \\ \bar{a}_o \\ a_1 \\ \cdot \\ \cdot \\ \cdot \\ a_M \end{Bmatrix} = 0$$

$$(B61)$$

where

$$C_P = \frac{R_1 P}{D_y}$$

$$C_p = \frac{R_1^3 p}{D_y}$$

$$C_\omega = \left(\frac{\omega}{\omega_r}\right)^2 - i g_a \left(\frac{\omega}{\omega_r}\right)$$

$$g_a = \frac{\rho c_{air}}{\gamma \omega_r} \qquad\qquad\qquad (B62)$$

$$\lambda = \frac{2q R_1^3}{\beta D_y}$$

$$\omega_r^2 = \frac{D_y}{\gamma R_1^4}$$

and b_{ij}, c_{ij}, d_{ij}, e_{ij}, and f_{ij} are given in the supplement.

APPENDIX C

BUCKLING RESULTS

Simply Supported Shells

Effects of conicity.- Some effects of conicity on the buckling of isotropic truncated conical shells with cylindrical simple support subjected to hydrostatic pressure are shown in figure 17. Figure 17(a) shows the variation of C_p with cone angle α for two values of L/R_1. The dashed portion of the curves represent extrapolation to zero cone angle. These results are in excellent agreement with the results obtained in reference 44 indicated by the circles. As would be expected, the buckling load for a fixed small-end radius R_1 decreases considerably with increasing α; for $\alpha = 45^o$ the buckling pressure is about an order of magnitude less than the pressure required to buckle a cylinder with the same L/R_1 and R_1/h. Figure 17(b) shows the decrease of C_p with increasing L/R_1 for $\alpha = 0^o$ and 30°. Again, the extrapolated results for $\alpha = 0$ are in excellent agreement with the results of reference 44.

Buckling results for isotropic conical shells have been correlated (ref. 52) by use of the taper ratio $1 - \dfrac{R_1}{R_2}$ where

$$\frac{R_2}{R_1} = 1 + \frac{L}{R_1} \tan \alpha \tag{C1}$$

and the concept of an equivalent cylinder. Calculated results for $3^o \leqq \alpha \leqq 75^o$, $1 \leqq \dfrac{L}{R_1} \leqq 6.28$, and $250 \leqq \dfrac{R_1}{h} \leqq 1000$ are presented in figure 18 in terms of the ratio $\dfrac{p}{p_{cyl}}$ as a function of the taper ratio $1 - \dfrac{R_1}{R_2}$ where p_{cyl} is the buckling pressure for an equivalent cylinder. If the normal equivalent cylinder transformations

$$\left.\begin{array}{c} R \rightarrow \dfrac{R_1 + R_2}{2 \cos \alpha} \\[3mm] L \rightarrow \dfrac{R_2 - R_1}{\sin \alpha} \\[3mm] h \rightarrow h \\[3mm] \eta \rightarrow \dfrac{\eta}{\cos \alpha} \end{array}\right\} \tag{C2}$$

are substituted into the cylinder buckling equation (eq. (17) of ref. 53), the following expression for p_{cyl} for unstiffened or ring-stiffened shells is obtained for buckling into one-half wave (m = 1):

$$p_{cyl} = \frac{2\pi^2 \sin^2 \alpha \cos \alpha\, E}{12\left(1 - \mu^2\right)\left(R_1/h\right)^3 \left[\left(R_2/R_1\right) - 1\right]^2 \left[\left(R_2/R_1\right) + 1\right]\left[(1/2) + \bar{\beta}^2\right]}\left[\left(1 + \bar{\beta}^2\right)^2 + \bar{\beta}^2 \frac{G_R J_R}{d_R}\right.$$

$$\left. + \bar{\beta}^4 \frac{E_R I_R}{d_R} + \frac{\frac{48\left(1 - \mu^2\right)}{\pi^4 \cos^2 \alpha}\left(R_1/h\right)^2 \left[\left(R_2/R_1\right) + 1\right]^2 \left[\frac{\left(R_2/R_1\right) - 1}{\left(R_2/R_1\right) + 1}\right]^4 \cot^4 \alpha}{\left(1 + \bar{\beta}^2\right)^2 + \frac{E_R A_R}{Ehd_R}\left[2\bar{\beta}^2(1 + \mu) + \bar{\beta}^4\left(1 - \mu^2\right)\right]}\right.$$

$$\left. \times \left(1 + \frac{E_R A_R}{Ehd_R}\left\{1 + \frac{4\eta^4}{\cos^2 \alpha}\frac{\left(1 + \bar{\beta}^2\right)\left(\bar{z}_R/R_1\right)^2}{\left[\left(R_2/R_1\right) + 1\right]^2}\right\}\right)\right] \tag{C3}$$

where

$$\bar{\beta} = \frac{2\eta}{\pi \sin \alpha}\frac{\left(R_2/R_1\right) - 1}{\left(R_2/R_1\right) + 1} \tag{C4}$$

It should be noted that equation (17) of reference 53 contains expressions multiplied by $\bar{z}_R$, which can be either positive or negative. These terms, which account for eccentricity (one-sided) effects, are omitted in equation (C3).

Equation (C3) is a function of η, which must be varied to find the minimum values of p_{cyl}. An approximate expression for p_{cyl}, based in part on the assumption that

$$\frac{\left[\left(R_2/R_1\right) + 1\right]}{\left[\left(R_2/R_1\right) - 1\right]} \ll \frac{2\eta}{\pi \sin \alpha} \tag{C5}$$

is (ref. 54)

$$p_{cyl} = \left\{ \left(\frac{D_\theta}{D_y}\right)^{3/4} - \frac{\left[\left(D_\theta/D_y\right) - 1\right]\sin\alpha}{\left(R_1/h\right)^{1/2}\left[\left(R_2/R_1\right) - 1\right]} \left[\frac{\left(R_2/R_1\right) + 1}{2\cos\alpha}\right]^{1/2} \right\}$$

$$\times \quad \frac{\pi\sqrt{6}\ E\tan\alpha \Big/ 9\left(1 - \mu^2\right)^{3/4}}{\left(1 - \dfrac{R_1}{R_2}\right)\left[\dfrac{1 + \left(R_1/R_2\right)}{2}\right]^{3/2}\left(\dfrac{R_2}{h\cos\alpha}\right)^{5/2}} \tag{C6}$$

where for ring-stiffened shells

$$\frac{D_\theta}{D_y} = 1 + 12\left(\frac{z_{cR}}{h}\right)^2 + 12\left(1 - \mu^2\right)\frac{E_R}{E}\left[\frac{I_R}{d_R h^3} + \frac{A_R}{d_R h}\left(\frac{z_{sR}}{h}\right)^2\right] \tag{C7}$$

When $D_\theta/D_y = 1$, equation (C6) reduces to the expression obtained by Seide (ref. 52) for unstiffened shells. Note that equation (C6) gives the minimum value of p_{cyl} directly.

The correlation curve in figure 18 was obtained by Seide (ref. 52). The open symbols represent results from the present investigation for unstiffened shells; values of p_{cyl} obtained from equations (C3) and (C6) were essentially the same. The agreement is quite good. Most of the scatter is for $\alpha \geqq 45^O$; Singer (ref. 55) has shown that the correlation curve overestimates the ratio p/p_{cyl} somewhat for this range of α. Results presented in reference 54 indicate the correlation curve can also be used to correlate data for orthotropic and ring-stiffened conical shells. Accordingly, results for ring-stiffened shells are also shown in figure 18 as solid symbols. Equivalent orthotropic stiffness properties were calculated from the formulas given in table I, which neglect eccentricity effects.

The solid squares in figure 18 represent results from reference 56 (based on eq. (C6)) for $D_\theta/D_y \leqq 25$ and agree quite well with the correlation curve. Results from the present investigation for $D_\theta/D_y = 316$ (ring details are given in fig. 12) are indicated by the solid circles for p_{cyl} defined by equation (C6) and by the solid symbols with ticks for p_{cyl} defined by equation (C3). The scatter shown by these results suggest that the correlation curve becomes more approximate as D_θ/D_y increases and that a family of curves would probably be required for proper correlation, particularly for larger values of the taper ratio $\left(1 - R_1/R_2 > 0.6\right)$. Use of the more exact definition of p_{cyl} (eq. (C3)) resulted in larger values of p/p_{cyl} and somewhat better correlation than the results obtained by the use of the approximate expression (eq. (C6)).

Effects of ring or stringer stiffening.- The relative magnitudes of the effects of ring and stringer stiffening are indicated in figure 19 in terms of the ratio of the buckling load

of the stiffened shell to that of the unstiffened shell and L/R_1. Flutter results for the same shells are given in figure 12. The open symbols are for ring stiffeners and the solid symbols are for stringer stiffeners; stiffener details are given in figure 12. The equivalent orthotropic stiffnesses were based on the stringer spacing at the small end of the cone. Stiffener size and spacing was such that the ring- or stringer-stiffened shells were essentially of equal weight. The vertical lines connecting the open symbols in figure 19 represent the variation in the ratio of the buckling loads with cone angle α; in general, the ratio decreased with increasing cone angle. The variations with cone angle for stringer stiffening was not significant. The advantage of ring stiffening $\left(\text{or orthotropic stiffening for } D_\theta/D_y > 1\right)$ for hydrostatic pressure loading is obvious. The curves shown in figure 19 were obtained from the expressions for equivalent cylinders (eqs. (C3) and (C6)). The variation with α $\left(\text{for fixed } L/R_1\right)$ was not significant; thus, only a single curve (for each equation) is shown. The qualitative effect of stiffening indicated by the equivalent cylinder equations is in reasonable agreement with the actual, calculated cone results.

Elastically Supported Shells

The results of the preceding sections show that from a theoretical standpoint the buckling of a simply supported unstiffened conical shell subjected to hydrostatic pressure is adequately described by equation (C6) in conjunction with the correlation curve shown in figure 18. Furthermore, the buckling of ring-stiffened shells is fairly well described by equation (C3) or (C6), and the results obtained, if not sufficiently accurate for final buckling criteria, should at least prove useful for preliminary calculations. On the other hand, the considerable scatter in available experimental data is such that experimental values range from 60 percent to 140 percent of the values predicted for simply supported edges (ref. 3); the scatter is attributed to variation in cone edge conditions and to initial imperfections. In the next three sections, the effects of variations in edge conditions are shown to have a significant effect on the buckling of conical shells.

Effects of axial and rotational restraint.- Some effects of axial restraint $\left(k_1\right)$ are shown in figure 20, which gives the variation of the buckling pressure coefficient C_p with the ratio k_1/E. Fairly large values of axial restraint $\left(k_1/E > 0.001\right)$ are required to noticeably affect C_p, but as the restraint approaches complete constraint the effect is appreciable. The value of C_p for complete constraint is about 40 percent greater than the value for no axial restraint. The symbols shown in figure 20 represent buckling results for no axial restraint and complete axial restraint obtained previously by Thurston (ref. 24) who used a very accurate prebuckling state. The results of the present investigation are in excellent agreement with the results of reference 24. (See fig. 20.) This agreement suggests that the extra computation involved in considering the accurate prebuckling state is not necessary, at least for hydrostatic pressure loading and the edge

conditions considered. Similar results and conclusions for no axial restraint and complete axial constraint were presented in reference 57.

The variation of the effects of complete axial restraint with L/R_1 are shown in figure 21. The variation of the buckling ratio $\dfrac{p_{u_{V_B=0}}}{p_{V_B=0}}$ increases rapidly with L/R_1 up to about 2 and apparently would reach a limiting value of between 1.4 and 1.5 for very large values of L/R_1. More complete results on the variation of the effects of no axial restraint and complete axial constraint with L/R_1, R_1/h, and α are given in reference 57 where similar trends are indicated.

Figure 22 shows some effects of rotational restraint in terms of C_p as a function of $\dfrac{R_1 k_4}{D_y}$. The lower curve is for no axial restraint, and the upper curve is for complete axial constraint. The results show that increasing rotational restraint increases the buckling pressure about 8 percent for no axial restraint but only about 2 percent for complete axial constraint. This tends to confirm the results of other investigations (for example, ref. 11) that the effect of a given edge restraint depends on the magnitudes and types of other restraints acting on the shell edges. For complete axial constraint and $\dfrac{R_1 k_4}{D_y}$ greater than about 500, the restraint approaches the fully clamped condition. The square represents buckling results for the fully clamped condition previously obtained by Singer (ref. 58); the computation is in excellent agreement with the results of the present investigation. The results shown in figure 22 indicate that the large increase in buckling pressure for clamped edges (square) compared with the results for cylindrical simple support (circle) is primarily caused by axial constraint. The effect of axial restraint is sufficiently large to preclude neglecting it in comparisons of theoretical and experimental results. Indeed, improved predictions of experimental results have been shown to occur when the axial constraint present in the experiment is considered in the analytical computations (ref. 57).

Effects of circumferential and radial restraint.- Some effects of finite circumferential $\left(k_2\right)$ and radial $\left(k_3\right)$ elastic restraint are shown in figure 23, which gives the variation of C_p with k_3/E for a sandwich shell subjected to lateral pressure and axial load such that the large end of the cone is free of stress. Shell structural properties are given in table II. The upper curve in figure 23 is for $k_2/E = 1$ and the lower curve is for $k_2/E = k_3/E$; for both curves $k_1 = k_4 = 0$. The circle and square at $k_2/E = 1$ show the slight effect of changing the circumferential restraint from complete constraint $\left(v_B = 0\right)$ to no restraint $\left(N_{y\theta B} = 0\right)$ for no radial displacement. The two symbols (diamond and triangle) at $k_3/E = 0$ show the effect of changing the circumferential boundary condition from $v_B = 0$ to $N_{y\theta B} = 0$ for no radial restraint; the effect is in marked contrast to the effect when there is complete radial constraint. The reason for the large effect of

APPENDIX C

circumferential restraint as the radial restraint becomes weak is that the constraint $v_B = 0$ prevents the inextensional form of buckling ($\eta = 2$), which is the critical mode of buckling when all edge restraints are relatively weak (refs. 25 and 59). Since the critical value of η becomes small as the edge restraint becomes relatively weak, the present Donnell type theory becomes more approximate. Hence it might be desirable to use more exact shell theories in analyses of buckling of shells with weak edge restraint.

The sandwich shell considered in figure 23 has previously been analyzed by Cohen (ref. 25) who utilized Novozhilov shell theory (ref. 60) and very accurate prebuckling stresses and deformations. Although the main purpose of the analysis was to consider the effects of the edge restraint imposed by rings, results for simply supported edges were also presented and are indicated in figure 23 by the solid symbol. The result of the present investigation for simply supported edges is in good agreement with the result from the more rigorous analysis of Cohen, the difference being only about 6 percent.

Effects of restraint of end rings.- Results for the sandwich shell considered in the previous section and a similarly loaded ring-stiffened shell are presented in figure 24 in terms of C_p as a function of the ratio of the radius of the tubular end ring (of circular cross section) to the radius of the shell at the large end $(r/R)_2$. The ratio $(r/R)_1$ for both shells was constant and equal to 0.0312; structural details of the shells are given in table II. For the end rings, $r_1 = 1.25$ in. (3.18 cm), $\tau_1 = \tau_2 = 0.125$ in. (0.318 cm), and r_2 is varied. When the edge restraint is weak $\left(\text{small values of } (r/R)_2\right)$, the shell tends to buckle inextensionally into two circumferential waves, but when the edge restraint becomes large, the shell buckles extensionally into seven circumferential waves. The intersection of the curves for $\eta = 2$ and $\eta = 7$ gives the minimum base-ring radius ratio $(r/R)_2$ required to suppress inextensional buckling; further stiffening would not have a significant effect on the buckling pressure. The minimum value of $(r/R)_2$ to suppress inextensional buckling obtained from the present analysis is conservative in that it is approximately 35 percent larger than the value predicted by the more rigorous analysis of reference 25 for the sandwich shell and 18 percent larger for the ring-stiffened shell. These differences are due primarily to use of Donnell theory and the membrane stress state in the present analysis and, also, to neglect of ring eccentricity.

The results of figure 24 indicate that the present analysis gives fair predictions (compared with the more rigorous analysis of ref. 25) of the buckling pressure for ring-stiffened pressure-loaded shells. However, for axial load or stringer stiffening the neglect of eccentricity effects and the use of the membrane prebuckling state can lead to extremely inaccurate results. For example, in reference 61, which utilizes a Donnell type buckling analysis, it is shown that either eccentricity effects or the use of a very accurate prebuckling state can cause over a factor of 1.5 change in the buckling load. Results of the present analysis differed by about a factor of 2 from the results of

reference 61 for a clamped shell with $\alpha = 5^O$ and external stringers. Thus, the present analysis should be used with caution for configuration and loading combinations sensitive to prebuckling and eccentricity effects.

APPENDIX D

VIBRATION RESULTS

Simply Supported Shells

Effects of conicity.- Some effects of conicity on the vibration characteristics of shells with cylindrical simple support are shown in figure 25. The decrease of $(\omega/\omega_r)^2$ with increasing α (fig. 25(a)) and L/R_1 (fig. 25(b)) is similar to the trends for buckling (fig. 17). Extrapolated results for zero cone angle are seen to be in excellent agreement with the cylinder results obtained from equation (43) of reference 62, indicated by the circles in figure 25.

The minimum frequencies for isotropic conical shells have been correlated (ref. 63) by use of the taper ratio $1 - \dfrac{R_1}{R_2}$ and the concept of equivalent cylinders. Results from the present analysis for $5^O \leq \alpha \leq 60^O$, $1.26 \leq L/R_1 \leq 6.28$, and $107 \leq R_1/h \leq 341$ are compared with the correlation curve of reference 63 in figure 26 which gives the variation of $\omega_{min}/(\omega_{cyl})_{min}$ with $1 - \dfrac{R_1}{R_2}$. An expression for the natural frequency of an equivalent cylinder ω_{cyl} applicable for unstiffened or ring stiffened shells can be obtained by substituting equations (C2) into the cylindrical vibration equation (eq. (43) of ref. 62). The result for the lowest frequency (m = 1) for a given value of η is

$$\omega_{cyl} = \frac{4\omega_r \cos^2 \alpha}{\left[(R_2/R_1) + 1\right]^2} \left[\frac{\pi^4 \tan^4 \alpha}{16} \left[\frac{(R_2/R_1) + 1}{(R_2/R_1) - 1} \right]^4 \left[\left(1 + \bar{\beta}^2\right)^2 + \bar{\beta}^2 \frac{G_R J_R}{D d_R} + \bar{\beta}^4 \frac{E_R I_R}{D d_R} \right] \right.$$

$$+ \frac{\dfrac{3\left(1 - \mu^2\right)}{\cos^2 \alpha} \left(R_1/h\right)^2 \left[(R_2/R_1) + 1\right]^2}{\left(1 + \bar{\beta}^2\right)^2 + \dfrac{E_R A_R}{E h d_R}\left[2\bar{\beta}^2(1 + \mu) + \left(1 - \mu^2\right)\bar{\beta}^4\right]}$$

$$\times \left. \left(1 + \frac{E_R A_R}{E h d_R} \left\{ 1 + 4 \frac{\eta^4}{\cos^2 \alpha} \frac{\left(1 + \bar{\beta}^2\right)^2 \left(\bar{z}_R/R_1\right)^2}{\left[(R_2/R_1) + 1\right]^2} \right\} \right) \right]^{1/2} \tag{D1}$$

45

where $\bar{\beta}$ is defined by equation (C4). It should be noted that equation (43) of reference 62 contains expressions multiplied by z_R, which can be either positive or negative. These terms, which account for eccentricity (one-sided) effects, are omitted in equation (D1).

Equation (D1) is a function of η, which must be varied to find $(\omega_{cyl})_{min}$. For unstiffened shells the expression for $(\omega_{cyl})_{min}$ becomes (ref. 63)

$$(\omega_{cyl})_{min} = \omega_r \, 2\pi \, \sin \alpha \, \cos^{1/2} \alpha \, \frac{\left[12(1 - \mu^2)\right]^{1/4} (R_1/h)^{1/2}}{\left[(R_2/R_1) - 1\right]\left[(R_2/R_1) + 1\right]^{1/2}} \qquad (D2)$$

As can be seen from figure 26, the results of the present analysis for unstiffened shells are in good agreement with the correlation curve. Calculations were also made for ring-stiffened shells for which $D_\theta/D_y \leqq 316$ as indicated by the solid circles in figure 26. As can be seen, the equivalent cylinder vibration results for stiffened shells correlate better (fig. 26) than did the buckling results for similar shells (fig. 18). It should be noted that the equivalent cylinder concept has limited usefulness for frequencies $\omega > \omega_{min}$ (ref. 63). As η increases, the mode shapes become more confined to the region near the large end of the cone and, therefore, can deviate considerably from the sinusoidal shape of a vibrating simply supported cylinder. Thus, the difference in the frequencies for actual cones and equivalent cylinders increases as η increases; this trend was also noted by Weingarten (ref. 64) for ring-stiffened conical shells.

Effects of applied loads.- Effects of hydrostatic pressure and axial load on the natural frequencies of an isotropic conical shell with cylindrical simple support are shown in figure 27 in terms of $(\omega/\omega_r)^2$ as a function of the ratio p/p_{cr} or P/P_{cr} for several values of η. As can be seen from figure 27(a), $(\omega/\omega_r)^2$ varies linearly with p/p_{cr} and the slope of the curves increases with increasing η. For the range of η considered, which brackets the value for buckling ($\eta = 10$), $(\omega/\omega_r)^2$ decreases significantly with p/p_{cr}. Weingarten (ref. 65) has presented results which also show significant effects of increasing p/p_{cr} and, in addition, indicate that the frequency is nearly independent of p/p_{cr} for $\eta \leqq 2$.

Some effects of axial load are shown in figure 27(b) for the same shell considered in figure 27(a). In contrast to the results for hydrostatic loading, figure 27(b) reveals that $(\omega/\omega_r)^2$ does not vary linearly with P/P_{cr}; this is attributed to the differences in the axial variation of N_{yA} for hydrostatic loading and axial loading. For $P/P_{cr} < 0.5$ the variation is nearly linear and the slope of the curves again increases with η.

APPENDIX D

Effects of ring or stringer stiffening.- The relative magnitudes of the effects of ring and stringer stiffeners on the minimum frequencies of conical shells are indicated in figure 28 in terms of the ratio of the frequency of the stiffened shell to the frequency of the unstiffened shell as a function of L/R_1. Stiffener size and spacing was such that the shells were of equal total weight; stiffener details and flutter results are given in figure 12, and buckling results are given in figure 19. The equivalent orthotropic stiffnesses were calculated from the formulas given in table I and were based on the stringer spacing at the small end of the shell. The variation of the frequency ratio with α was not significant for the range considered ($5^O \leqq \alpha \leqq 60^O$); thus, an average value is presented. The solid curves represent results for actual conical shells, and the dashed curve represents results for equivalent cylinders; the results for equivalent cylinders are in excellent agreement with the results for actual conical shells. For the particular configuration studied, the effect of rings is to increase the minimum frequencies by a factor of 2 to 3. The addition of stringers has a slight effect, and may even lower the frequency. The effect on vibration results of adding stiffeners can be (and for the configuration studied is) considerably less than the effect for buckling (fig. 19). The reason for the difference is that for vibration the additional mass of the stiffeners can tend to offset the effects of increased stiffness.

Elastically Supported Isotropic Shells

The results of the preceding sections show that simply supported unstiffened or ring-stiffened conical shells are fairly well described by equation (D1), or equation (D2) for unstiffened shells in conjunction with the correlation curve shown in figure 26. Agreement between theoretical and experimental results is generally good (for example, refs. 63 to 66); discrepancies that exist are attributed to effects of edge conditions (ref. 63). In the next two sections it is shown that the effects of variations in edge conditions can have a significant effect on the vibration characteristics of conical shells.

Effects of axial and rotational restraint.- Some effects of variations in elastic axial restraint $\left(k_1\right)$ and rotational restraint $\left(k_4\right)$ are shown in figure 29. Figure 29(a) shows the variation of $(\omega/\omega_r)^2$ with k_1/E for no rotational restraint, and figure 29(b), shows the variation of $(\omega/\omega_r)^2$ with $\dfrac{R_1 k_4}{D_y}$ for no axial restraint and complete axial constraint. As can be seen from figure 29, the effects of axial and rotational restraint on free vibrations are similar to the trends for buckling. (See figs. 20 and 22.) The effect of axial restraint appears to be sufficiently large to preclude neglecting it in comparisons of theoretical and experimental results. For example, in reference 66 the agreement between theoretical and experimental frequencies was improved by relaxing the axial constraint condition in the theoretical calculations. On the other hand, increasing axial restraint improves the agreement between theoretical frequencies and the experimental frequencies

presented in reference 65 as shown in figure 30 in terms of $(\omega/\omega_r)^2$ as a function of η for $p/p_{cr} = -0.446, 0,$ and $0.446;$ p_{cr} is the theoretical buckling pressure. The solid curves are for the conical simple support boundary conditions $N_{yB} = v_B = w_B = M_{yB} = 0$ and agree with the theoretical results presented in reference 65. The dashed curves are for the cylindrical simple support, $V_B = v_B = u_{HB} = M_{yB} = 0,$ and indicate slightly higher frequencies than the solid curves. The long-dash—short-dash curves are for the same support conditions as the dashed curves except that $k_1/E = 0.03;$ this amount of axial restraint was chosen so that the theoretical and experimental results would agree for $\eta_{min} = 6$ and $p = 0.$ As can be seen from figure 30, inclusion of some finite axial restraint in the theoretical calculations improves the agreement between theoretical and experimental frequencies.

Effects of circumferential and radial restraint.- Some effects of variations in elastic circumferential restraint (k_2) and radial restraint (k_3) are shown in figure 31 in terms of $(\omega/\omega_r)^2$ as a function of the ratio $k_3/E.$ The upper curves are for $\eta = 10$ and the lower curves are for $\eta = 6.$ The open circle and square at $k_3/E = 1$ $\left(u_{HB} = 0\right)$ show the slight effect of changing the circumferential restraint from complete constraint $\left(v_B = 0\right)$ to no restraint $\left(N_{y\theta B} = 0\right)$ for no radial displacement. The results of the present investigation are in good agreement with the results of reference 63 as indicated by the solid symbols in figure 31; the results for $u_{HB} = 0$ (present investigation) are slightly higher than the results for $w_B = 0$ (ref. 63). The trends exhibited by the curves for $k_2/E = 1$ $\left(v_B = 0\right)$ and $k_2/E = k_3/E$ as k_3/E decreases are similar to the trends for buckling (fig. 23). Results for other values of η would exhibit similar trends although the magnitude of the change in frequency due to changing the edge restraint would vary with $\eta.$ For example, in reference 63 it is shown that changing the edge restraint from $v_B = 0$ to $N_{y\theta B} = 0$ $\left(\text{for } w_B = 0\right)$ changes the frequency by about 50 percent for $\eta = 2,$ whereas for $\eta \gtrless 10$ the change was about 2 percent or less as indicated in figure 31.

REFERENCES

1. Stocker, James E.: A Review of the Literature on the Buckling Characteristics of Conical Shells. Doc. No. D2-23835-1, Boeing Co., 1965. (Available from DDC as AD 461 869.)

2. Kobayashi, Shigeo: Literature Survey on the Buckling of Conical Shells. Grant No. NsG-18-59, Grad. Aeronaut. Lab., California Inst. Technol., Jan. 1966.

3. Seide, Paul: A Survey of Buckling Theory and Experiment for Circular Conical Shells of Constant Thickness. Collected Papers on Instability of Shell Structures — 1962, NASA TN D-1510, 1962, pp. 401-426.

4. Singer, Josef: Buckling of Orthotropic and Stiffened Conical Shells. Collected Papers on Instability of Shell Structures — 1962, NASA TN D-1510, 1962, pp. 463-479.

5. Hu, William C. L.: A Survey of the Literature on the Vibrations of Thin Shells. Tech. Rep. No. 1 (Contract NASr-94(06)), Southwest Res. Inst., June 30, 1964.

6. Hu, William C. L.: Free Vibrations of Conical Shells. NASA TN D-2666, 1965.

7. Weingarten, V. I.: Free Vibrations of Conical Shells. J. Eng. Mech., Div. Amer. Soc. Civil Eng., vol. 91, no. EM 4, Aug. 1965, pp. 69-87.

8. Almroth, B. O.: Influence of Edge Conditions on the Stability of Axially Compressed Cylindrical Shells. NASA CR-161, 1965.

9. Almroth, B. O.: Influence of Imperfections and Edge Restraint on the Buckling of Axially Compressed Cylinders. NASA CR-432, 1966.

10. Kobayashi, Shigeo: The Influence of the Boundary Conditions on the Buckling Load of Cylindrical Shells Under Axial Compression. NASA CR-558, 1966.

11. Sobel, L. H.: Effects of Boundary Conditions on the Stability of Cylinders Subject to Lateral and Axial Pressures. AIAA J., vol. 2, no. 8, Aug. 1964, pp. 1437-1440.

12. Forsberg, Kevin: Influence of Boundary Conditions on the Modal Characteristics of Thin Cylindrical Shells. AIAA J., vol. 2, no. 12, Dec. 1964, pp. 2150-2157.

13. Singer, J.: The Effect of Axial Constraint on the Instability of Thin Circular Cylindrical Shells Under External Pressure. Trans. ASME, Ser. E: J. Appl. Mech., vol. 27, no. 4, Dec. 1960, pp. 737-739.

14. Johns, D. J.: A Survey on Panel Flutter. AGARD Adv. Rep. 1, Nov. 1965.

15. Mushtari, Kh. M.; and Galimov, K. Z.: Non-Linear Theory of Thin Elastic Shells. NASA TT F-62, Israel Program Sci. Transl., 1961, pp. 54-58. (Available from CFSTI.)

16. Fung, Y. C.: Foundations of Solid Mechanics. Prentice-Hall, Inc., c.1965, pp. 338-339.

17. Cohen, Gerald A.: Computer Analysis of Asymmetric Free Vibrations of Ring-Stiffened Orthotropic Shells of Revolution. AIAA J., vol. 3, no. 12, Dec. 1965, pp. 2305-2312.

18. Dixon, Sidney C.; Weeks, George E.; and Anderson, Melvin S.: Effect of Edge Restraint Coupling on Buckling of Ring-Supported Cylinders. AIAA J. (Tech. Notes), vol. 6, no. 8, Aug. 1968, pp. 1602-1604.

19. Libove, Charles; and Batdorf, S. B.: A General Small-Deflection Theory for Flat Sandwich Plates. NACA Rep. 899, 1948. (Supersedes NACA TN 1526.)

20. Voss, H. M.: The Effect of an External Supersonic Flow on the Vibration Character-istics of Thin Cylindrical Shells. J. Aerosp. Sci., vol. 28, no. 12, Dec. 1961, pp. 945-956, 961.

21. Olson, Mervyn D.; and Fung, Y. C.: Comparing Theory and Experiment for the Supersonic Flutter of Circular Cylindrical Shells. AIAA J., vol. 5, no. 10, Oct. 1967, pp. 1849-1856.

22. Forsberg, Kevin: A Review of Analytical Methods Used To Determine the Modal Characteristics of Cylindrical Shells. NASA CR-613, 1966.

23. Evensen, David A.; and Olson, Mervyn D.: Circumferentially Traveling Wave Flutter of a Circular Cylindrical Shell. AIAA J., vol. 6, no. 8, Aug. 1968, pp. 1522-1527.

24. Thurston, G. A.: Effect of Boundary Conditions on the Buckling of Conical Shells Under Hydrostatic Pressure. Trans. ASME, Ser. E: J. Appl. Mech., vol. 32, no. 1, Mar. 1965, pp. 208-209.

25. Cohen, Gerald A.: The Effect of Edge Constraint on the Buckling of Sandwich and Ring-Stiffened 120 Degree Conical Shells Subjected to External Pressure. NASA CR-795, 1967.

26. Carter, L. L.; and Stearman, R. O.: Some Aspects of Cylindrical Shell Panel Flutter. AIAA J., vol. 6, no. 1, Jan. 1968, pp. 37-43.

27. Seide, Paul: A Donnell Type Theory for Asymmetrical Bending and Buckling of Thin Conical Shells. J. Appl. Mech., vol. 24, no. 4, Dec. 1957, pp. 547-552.

28. Seide, Paul: On the Stability of Internally Pressurized Conical Shells Under Axial Compression. Proceedings of the Fourth U.S. National Congress of Applied Mechanics, Vol. 2, Amer. Soc. Mech. Eng., 1962, pp. 761-773.

29. Houbolt, John Cornelius: A Study of Several Aerothermoelastic Problems of Aircraft Structures in High-Speed Flight. Prom. Nr. 2760, Swiss Fed. Inst. Technol. (Zürich), 1958.

30. Singer, J.: Donnell-Type Equations for Bending and Buckling of Orthotropic Conical Shells. Trans. ASME, Ser. E: J. Appl. Mech., vol. 30, no. 2, June 1963, pp. 303-305.

31. Francis, J. G. F.: The QR Transformation: A Unitary Analogue to the LR Transformation. I. Computer J., vol. 4, 1961/62, pp. 265-271; II., pp. 332-345.

32. Ketter, D. J.: Flutter of Flat, Rectangular, Orthotropic Panels. AIAA J., vol. 5, no. 1, Jan. 1967, pp. 116-124.

33. Dixon, Sidney C.; and Hudson, M. Latrelle: Flutter Boundary for Simply Supported Unstiffened Cylinders. AIAA J. (Tech. Notes), vol. 7, no. 7, July 1969, pp. 1390-1391.

34. Shulman, Yechiel: Vibration and Flutter of Cylindrical and Conical Shells. OSR Tech. Rep. No. 59-776, U.S. Air Force, June 1959.

35. Grigolyuk, É. I.; and Mikhailov, A. P.: Flutter of a Circular Conical Shell Made up of Three Layers. Sov. Phys. — Doklady, vol. 10, no. 8, Feb. 1966, pp. 793-795.

36. Ames Research Staff: Equations, Tables, and Charts for Compressible Flow. NACA Rep. 1135, 1953. (Supersedes NACA TN 1428.)

37. Batdorf, S. B.: A Simplified Method of Elastic-Stability Analysis for Thin Cylindrical Shells. NACA Rep. 874, 1947. (Supersedes NACA TN's 1341 and 1342.)

38. Anderson, Melvin S.: Thermal Buckling of Cylinders. Collected Papers on Instability of Shell Structures — 1962, NASA TN D-1510, 1962, pp. 255-265.

39. Singer, Josef: On the Equivalence of the Galerkin and Rayleigh-Ritz Methods. J. Roy. Aeronaut. Soc., vol. 66, no. 621, Sept. 1962, p. 592.

40. Skurlatov, E. D.: On the Stability of a Circular Cylindrical Shell in a Supersonic Gas Flow. Lockheed Missiles & Space Co. Transl. (From Strength and Stability of Thin-Walled Structures, Mashgiz (Moscow), 1967, pp. 201-209.)

41. Kobayashi, Shigeo: Supersonic Panel Flutter of Unstiffened Circular Cylindrical Shells Having Simply Supported Ends. Trans. Japan Soc. Aeronaut. Space Sci., vol. 6, no. 9, 1963, pp. 27-35.

42. Hedgepeth, John M.: Flutter of Rectangular Simply Supported Panels at High Supersonic Speeds. J. Aeronaut. Sci., vol. 24, no. 8, Aug. 1957, pp. 563-573, 586.

43. Shideler, John L.; Dixon, Sidney C.; and Shore, Charles P.: Flutter at Mach 3 of Thermally Stressed Panels and Comparison With Theory for Panels With Edge Rotational Restraint. NASA TN D-3498, 1966.

44. McElman, John A.; Mikulas, Martin M., Jr.; and Stein, Manual: Static and Dynamic Effects of Eccentric Stiffening of Plates and Cylindrical Shells. AIAA J., vol. 4, no. 5, May 1966, pp. 887-894.

45. Comm. on Metric Pract.: ASTM Metric Practice Guide. NBS Handbook 102, U.S. Dep. Com., Mar. 10, 1967.

46. Matthews, James Benning: Natural Frequencies and Mode Shapes of Circular Cylindrical Shells Determined by a Modified Galerkin Procedure. Ph. D. Thesis, Univ. of Arizona, 1966.

47. Krause, Frederick A.: Natural Frequencies and Mode Shapes of the Truncated Conical Shell With Free Edges. SSD-TR-66-201, U.S. Air Force, Oct. 1966. (Available from DDC as AD 803 426.)

48. Bohon, Herman L.; and Anderson, Melvin S.: Role of Boundary Conditions on Flutter of Orthotropic Panels. AIAA J., vol. 4, no. 7, July 1966, pp. 1241-1248.

49. Calligeros, John M.; and Dugundji, John: Supersonic Flutter of Rectangular Orthotropic Panels With Arbitrary Orientation of Orthotropicity. OSR Tech. Rep. No. AFOSR 5328, U.S. Air Force, June 1963. (Available from DDC as AD 421 977.)

50. Yu, Yi-Yuan; and Lai, Jai-Lue: Application of Galerkin's Method to the Dynamic Analysis of Structures. AIAA J. (Tech. Notes), vol. 5, no. 4, Apr. 1967, pp. 792-795.

51. Mushtari, Kh. M.; and Sachenkov, A. V.: Stability of Cylindrical and Conical Shells of Circular Cross Section, With Simultaneous Action of Axial Compression and External Normal Pressure. NACA TM 1433, 1958.

52. Seide, P.: On the Buckling of Truncated Conical Shells Under Uniform Hydrostatic Pressure. The Theory of Thin Elastic Shells, W. T. Koiter, ed., Interscience Publ., Inc., 1960, pp. 363-388.

53. Block, David L.; Card, Michael F.; and Mikulas, Martin M., Jr.: Buckling of Eccentrically Stiffened Orthotropic Cylinders. NASA TN D-2960, 1965.

54. Baruch, M.; and Singer, J.: General Instability of Stiffened Circular Conical Shells Under Hydrostatic Pressure. Aeronaut. Quart., vol. XVI, pt. 2, May 1965, pp. 187-204.

55. Singer, Josef: Correlation of the Critical Pressure of Conical Shells With That of Equivalent Cylindrical Shells. AIAA J. (Tech. Notes Comments), vol. 1, no. 11, Nov. 1963, pp. 2675-2676.

56. Singer, J.; and Fersht-Scher, R.: Buckling of Orthotropic Conical Shells Under External Pressure. Aeronaut. Quart., vol. XV, pt. 2, May 1964, pp. 151-168.

57. Baruch, Menahem; Harari, Ovadia; and Singer, Josef: Influence of In-Plane Boundary Conditions on the Stability of Conical Shells Under Hydrostatic Pressure. Israel J. Technol., vol. 5, no. 1-2, 1967, pp. 12-24.

58. Singer, Josef: Buckling of Clamped Conical Shells Under External Pressure. AIAA J., vol. 4, no. 2, Feb. 1966, pp. 328-337.

59. Cohen, Gerald A.: Buckling of Axially Compressed Cylindrical Shells With Ring-Stiffened Edges. AIAA J. (Tech. Notes), vol. 4, no. 10, Oct. 1966, pp. 1859-1862.

60. Novozhilov, V. V. (P. G. Lowe, transl.): The Theory of Thin Shells. P. Noordhoff Ltd. (Groningen, Neth.), 1959, pp. 1-60.

61. Almroth, B. O.; and Bushnell, D.: Computer Analysis of Various Shells of Revolution. AIAA J., vol. 6, no. 10, Oct. 1968, pp. 1848-1855.

62. Mikulas, Martin M., Jr.; and McElman, John A.: On Free Vibrations of Eccentrically Stiffened Cylindrical Shells and Flat Plates. NASA TN D-3010, 1965.

63. Seide, Paul: On the Free Vibrations of Simply Supported Truncated Conical Shells. SSD-TDR-64-15, U.S. Air Force, Feb. 27, 1964. (Available from DDC as AD 600 939.)

64. Weingarten, V. I.: Free Vibrations of Ring-Stiffened Conical Shells. AIAA J., vol. 3, no. 8, Aug. 1965, pp. 1475-1481.

65. Weingarten, V. I.: The Effect of Internal or External Pressure on the Free Vibrations of Conical Shells. Int. J. Mech. Sci., vol. 8, no. 2, Feb. 1966, pp. 115-124.

66. Lindholm, Ulric S.; and Hu, William C. L.: Non-Symmetric Transverse Vibrations of Truncated Conical Shells. Int. J. Mech. Sci., vol. 8, no. 9, Sept. 1966, pp. 561-579.

TABLE I

ELASTIC CONSTANTS FOR RING OR STRINGER

STIFFENED CONICAL SHELL

Constant	Formula
D_y	$D\left[1 + 12\left(\dfrac{z_{cS}}{h}\right)^2\right] + \dfrac{E_S}{d_S}\left(I_S + z_{sS}^2 A_S\right)$
D_θ	$D\left[1 + 12\left(\dfrac{z_{cR}}{h}\right)^2\right] + \dfrac{E_R}{d_R}\left(I_R + z_{sR}^2 A_R\right)$
$D_{y\theta}$	$(1 - \mu)D + \dfrac{E_S J_S}{4d_S\left(1 + \mu_S\right)} + \dfrac{E_R J_R}{4d_R\left(1 + \mu_R\right)}$
B_y	$\dfrac{Eh}{1 - \mu^2} + \dfrac{E_S A_S}{d_S}$
B_θ	$\dfrac{Eh}{1 - \mu^2} + \dfrac{E_R A_R}{d_R}$
$B_{y\theta}$	$\dfrac{Eh}{1 - \mu^2}\left(\dfrac{1 - \mu}{2}\right)$
μ_θ	μ, ring stiffened $\mu\,\dfrac{D_\theta}{D_y}$, stringer stiffened
μ'_θ	μ, ring stiffened $\mu\,\dfrac{B_\theta}{B_y}$, stringer stiffened

TABLE II

STRUCTURAL PROPERTIES OF CONICAL MODELS

STUDIED IN REFERENCE 25

Sandwich shell	
Face sheets	Core
$E = 10.5 \times 10^6$ psi $\quad$ (72.5 GN/m^2)	$E = 0$
$G = 3.98 \times 10^6$ psi $\quad$ (27.5 GN/m^2)	$G = 0$
$\mu = 0.32$	$\mu = 0$
$h = 0.020$ in. $\quad$ (0.051 cm)	$h = 0.50$ in. $\quad$ (1.27 cm)
Ring-stiffened shell	
Skin	Ring stiffeners
$E = 6.5 \times 10^6$ psi $\quad$ (44.8 GN/m^2)	$E_R = 6.5 \times 10^6$ psi $\quad$ (44.8 GN/m^2)
$G = 2.4 \times 10^6$ psi $\quad$ (16.6 GN/m^2)	$G_R = 2.4 \times 10^6$ psi $\quad$ (16.6 GN/m^2)
$\mu = 0.35$	$\mu_R = 0.35$
$h = 0.051$ in. $\quad$ (1.30 cm)	$I_R = 0.00414$ in^4 $\quad$ (0.172 cm^4)
	$J_R = 2I_R$
	$A_R = 0.0635$ in^2 $\quad$ (0.410 cm^2)
	$d_R = 1.8$ in. $\quad$ (4.57 cm)
	$z_{cR} = 0.164$ in. $\quad$ (0.418 cm)
	$z_{sR} = 0.236$ in. $\quad$ (0.600 cm)
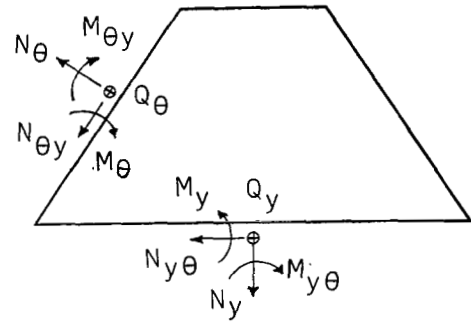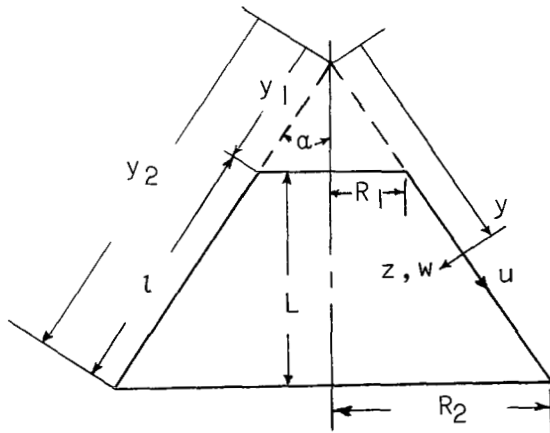
(b) Force and moment resultants.
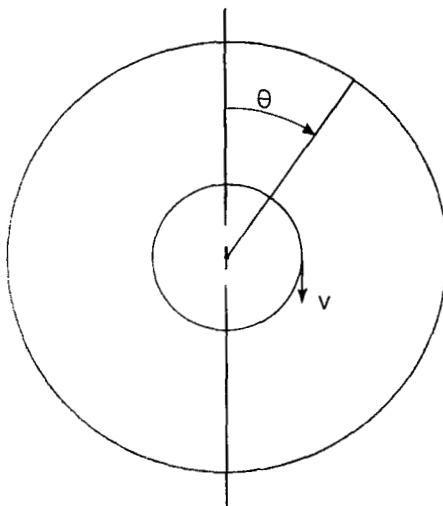
(a) Configuration; coordinates and displacements.
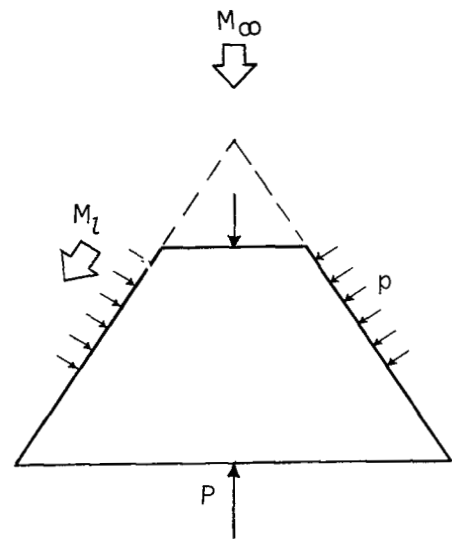
(c) Loads.

Figure 1.- Configuration and notation for coordinates and displacements, force and moment resultants, and loads.

56

$$\lambda = \frac{2qR_1^3}{\beta D_y}$$

Flutter

No flutter

———— $g_a = 0$

– – – – $g_a = 0.0538\lambda^{2/3}$; based on
aluminum at sea level
$M_l = 3$

η
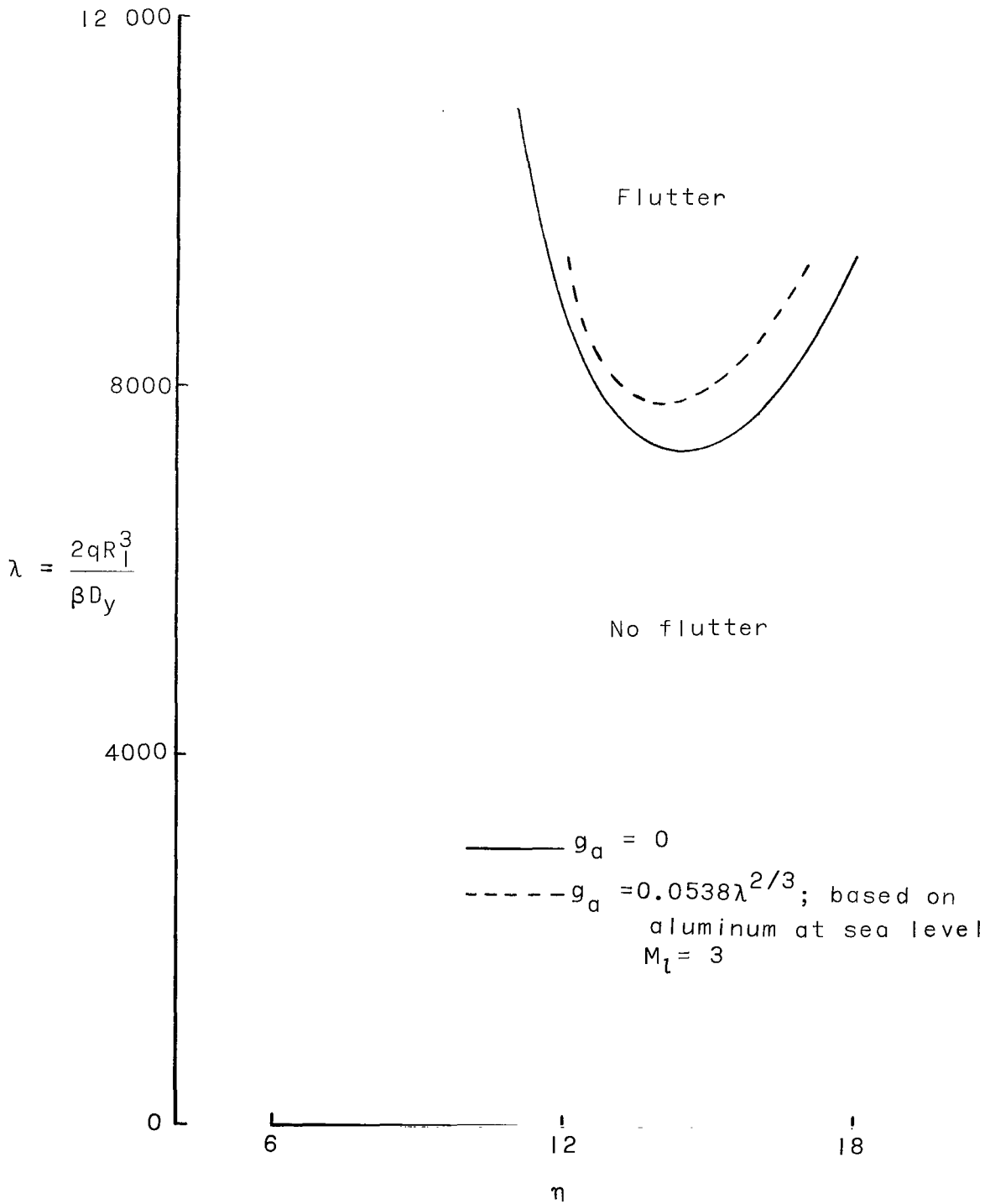
Figure 2.- Variation of flutter parameter λ with wave number η for isotropic conical shell with cylindrical simple support.
$L/R_1 = 1$; $R_1/h = 200$; $\alpha = 20°$; $p = P = 0$.

$$\lambda = \frac{2qR_1^3}{\beta D_y}$$

(a) Cone angle.

$$\lambda = \frac{2qR_1^3}{\beta D_y}$$
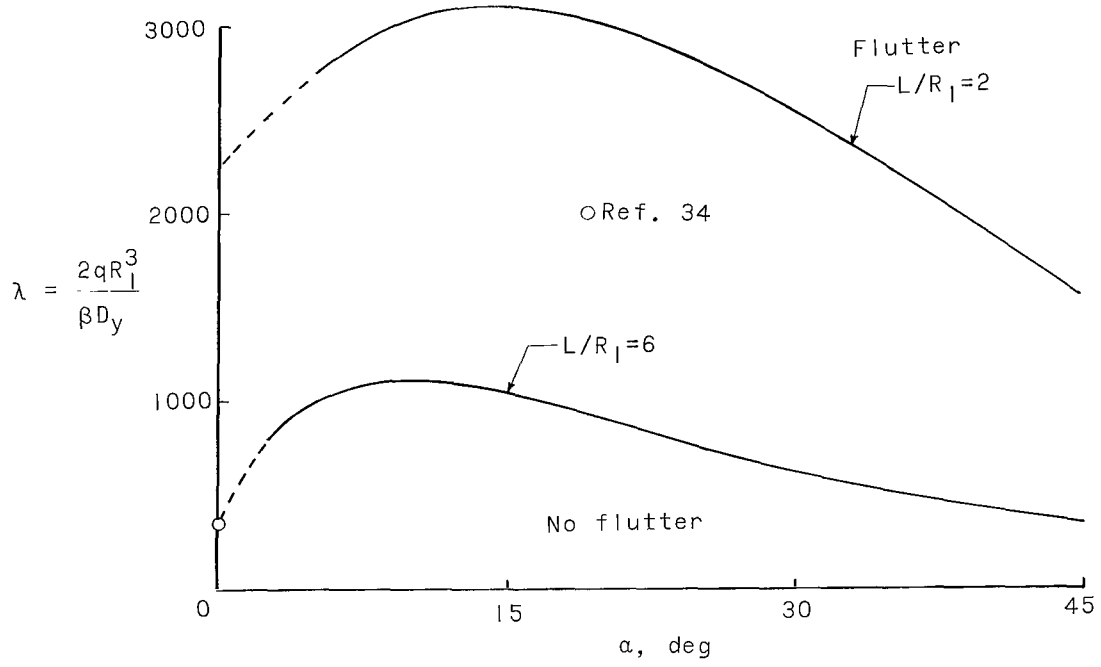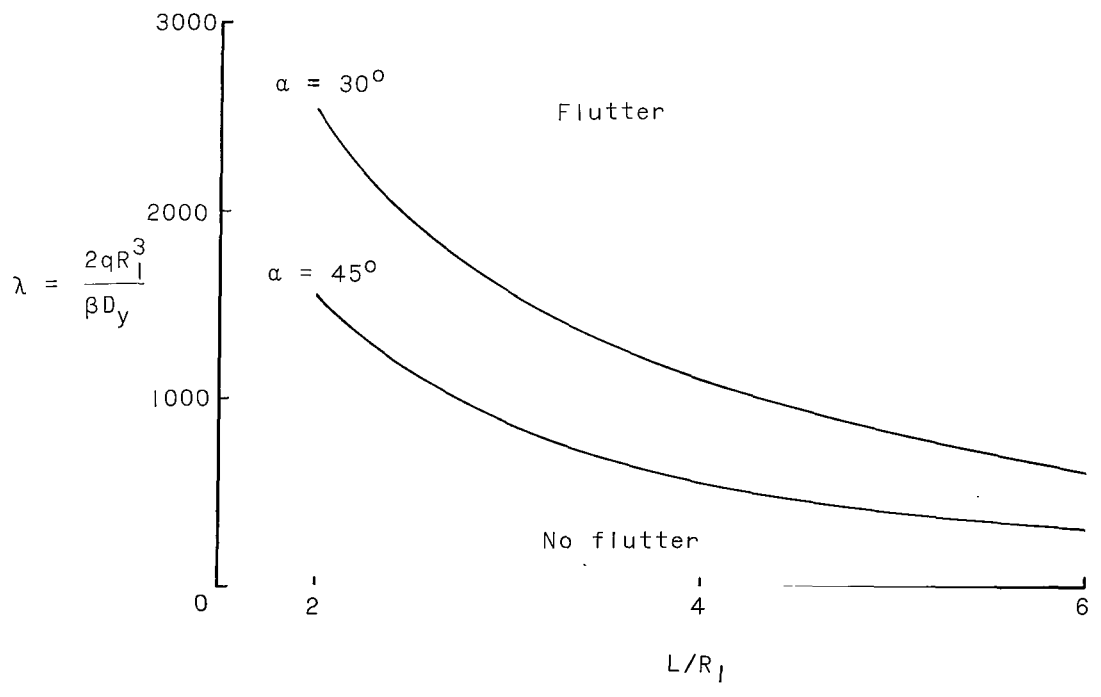
(b) Length-radius ratio.

Figure 3.- Some effects of conicity on flutter of isotropic conical shells with cylindrical simple support. $R_1/h = 200$; $p = P = 0$; $g_a = 0$.

$$\Delta = \frac{\omega_2^2 - \omega_1^2}{\omega_r^2}$$
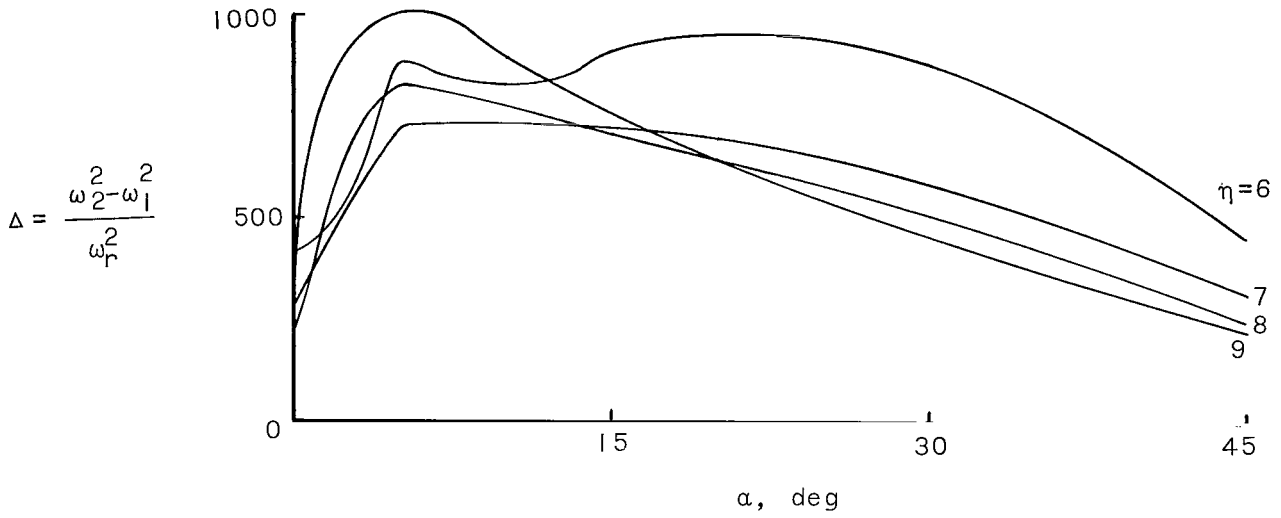
Figure 4.- Variation of frequency spectrum parameter Δ with semivertex angle α for isotropic conical shell with cylindrical simple support. $L/R_1 = 6$; $R_1/h = 200$; $p = P = 0$; $\lambda = 0$.
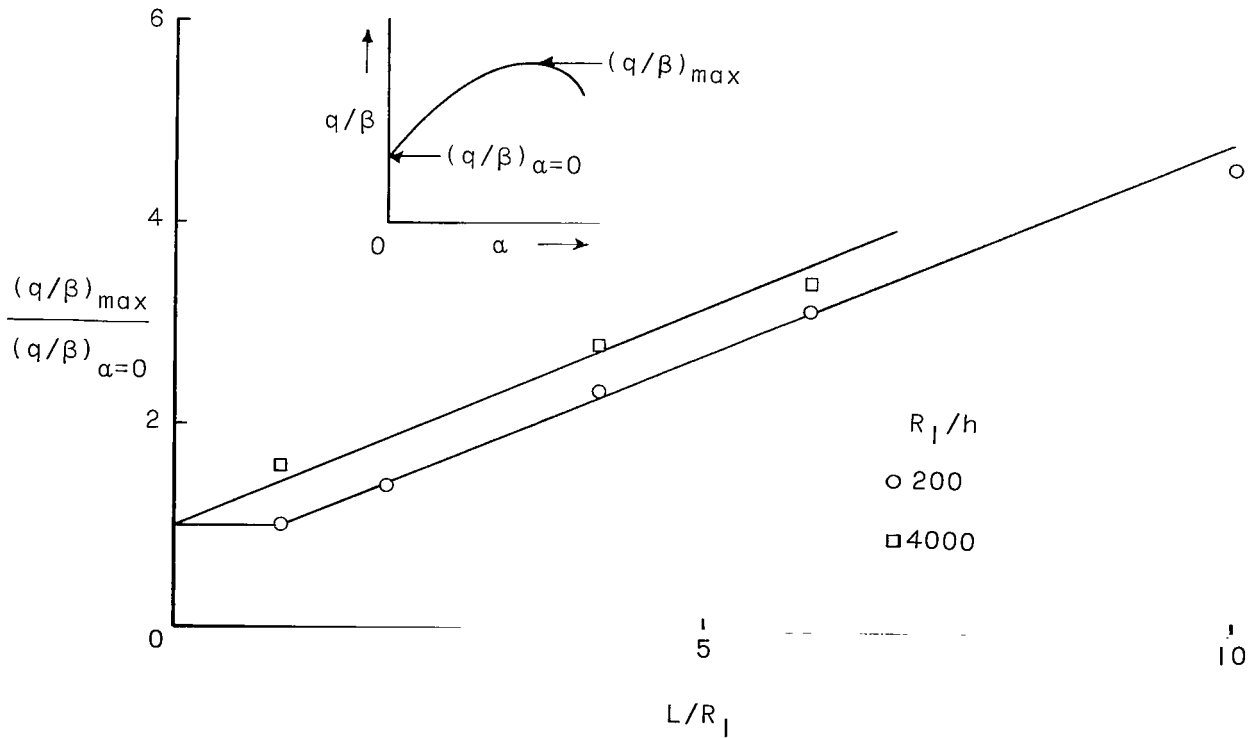
Figure 5.- Variation of $(q/\beta)_{max}/(q/\beta)_{\alpha=0}$ with L/R_1 for isotropic conical shells with cylindrical simple support. $p = P = 0$; $g_a = 0$.
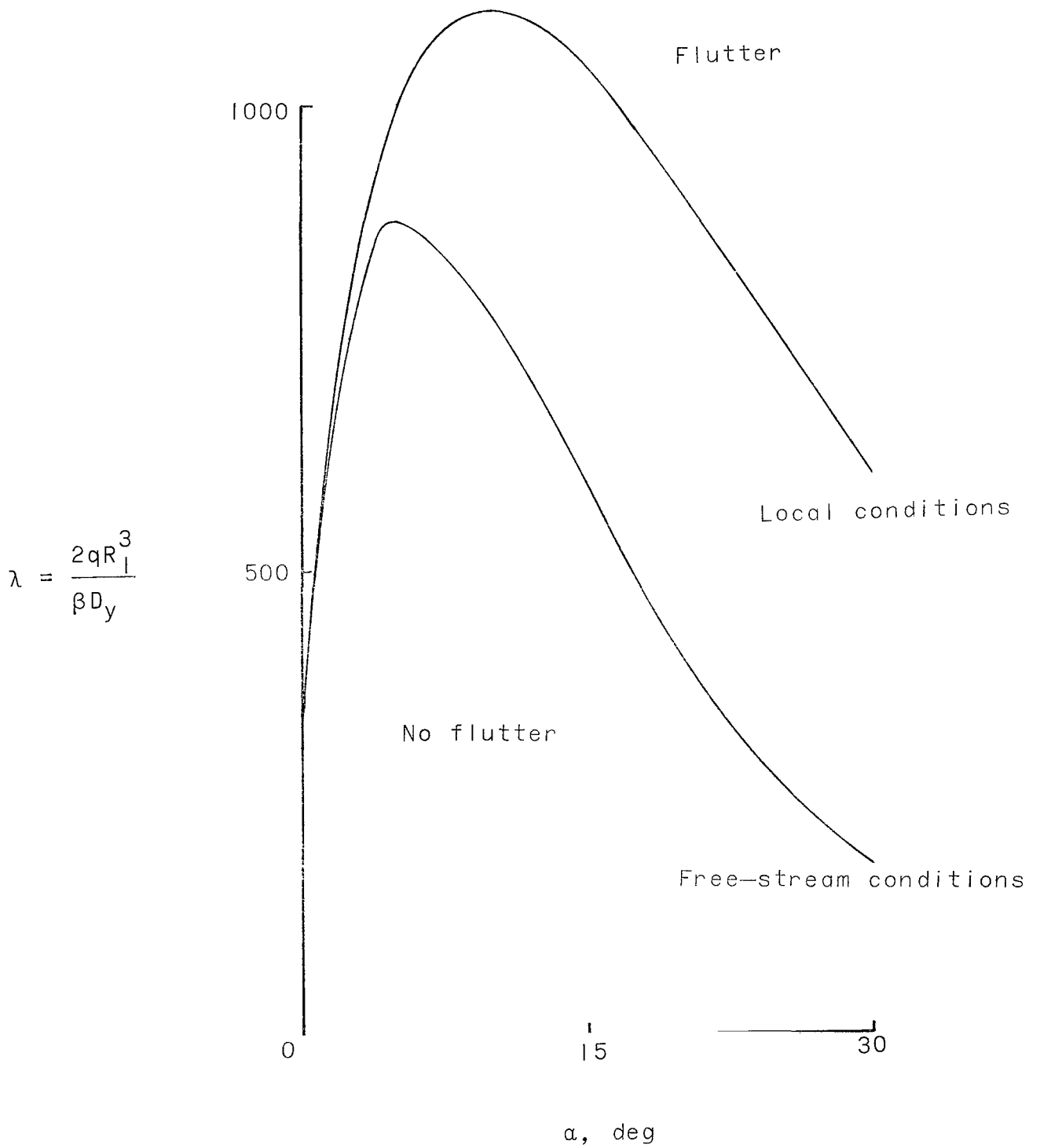
Figure 6.- Comparison of λ for flutter of conical shell with cylindrical simple support based on local and free-stream conditions. $L/R_1 = 6$; $R_1/h = 200$; $g_a = 0$; $p = P = 0$; $M_\infty = 3$.

(a) $\alpha = 15^0$.

(b) $\alpha = 30^0$.

(c) $\alpha = 45^0$.
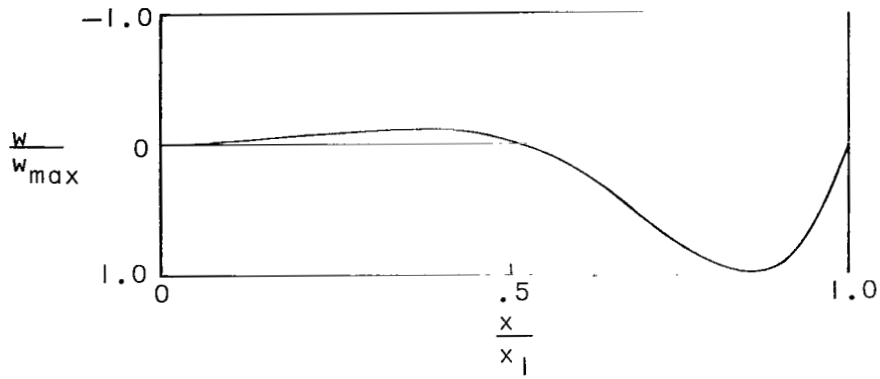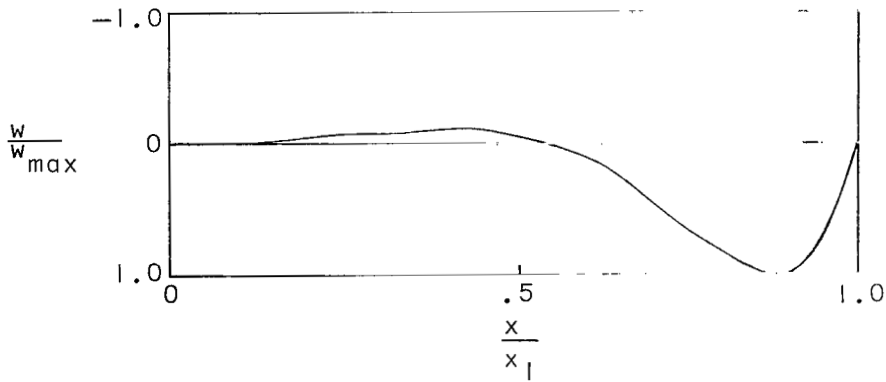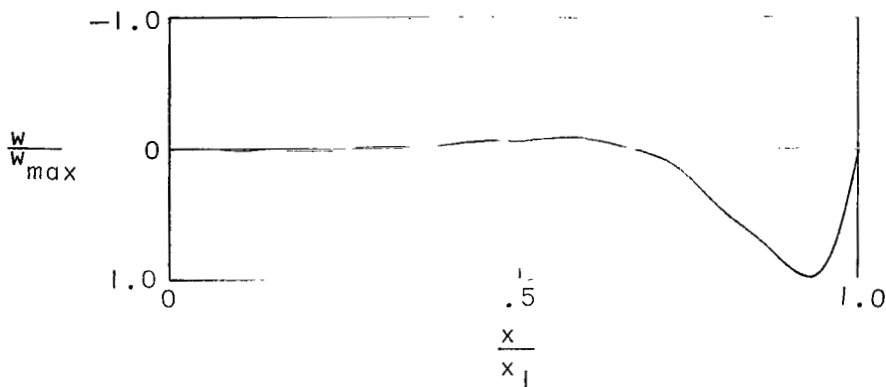
Figure 7.– Some effects of cone angle on flutter mode shape of isotropic conical shells with cylindrical simple support. $L/R_1 = 2$; $R_1/h = 200$; $g_a = 0$; $p = P = 0$.
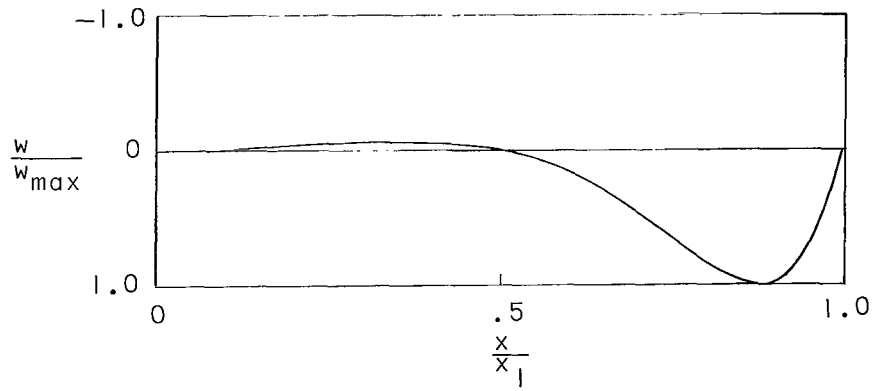
(a) $L/R_1 = 1$.
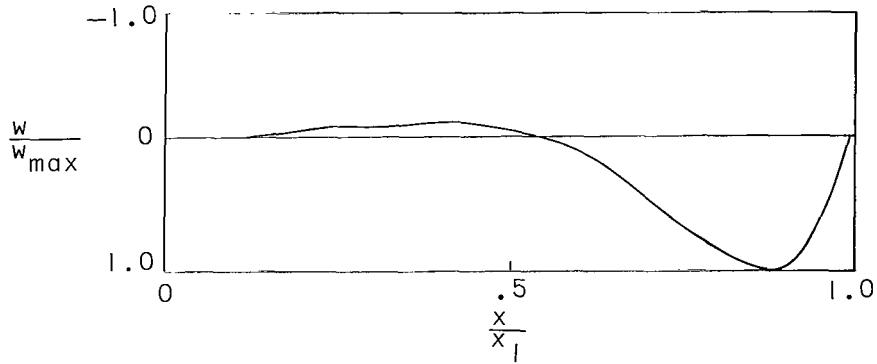
(b) $L/R_1 = 2$.
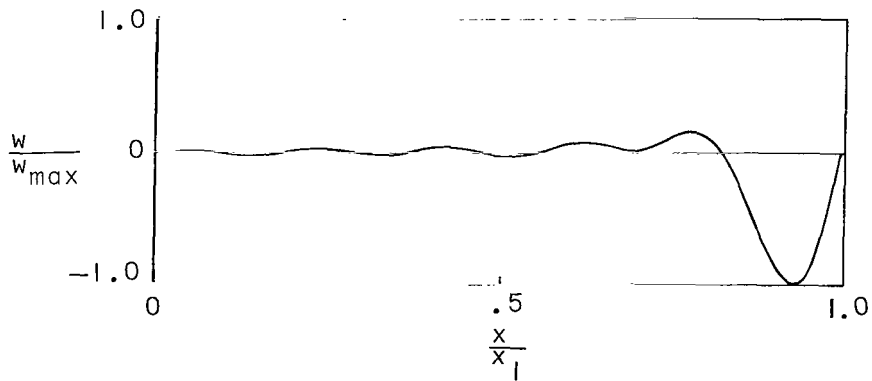
(c) $L/R_1 = 6$.

Figure 8.- Some effects of length-radius ratio on flutter mode shape of isotropic conical shells with cylindrical simple support. $R_1/h = 200$; $\alpha = 30°$; $g_a = 0$; $p = P = 0$.

$$\overline{\lambda} = \frac{2qR_1^3 / \beta D_y}{(1-\mu^2)(R_1/h)^x} \;;\; x = \tanh(.5L/R_1)$$

(a) $0^o \leqq \alpha \leqq 15^o$.

(b) $15^o \leqq \alpha \leqq 60^o$.
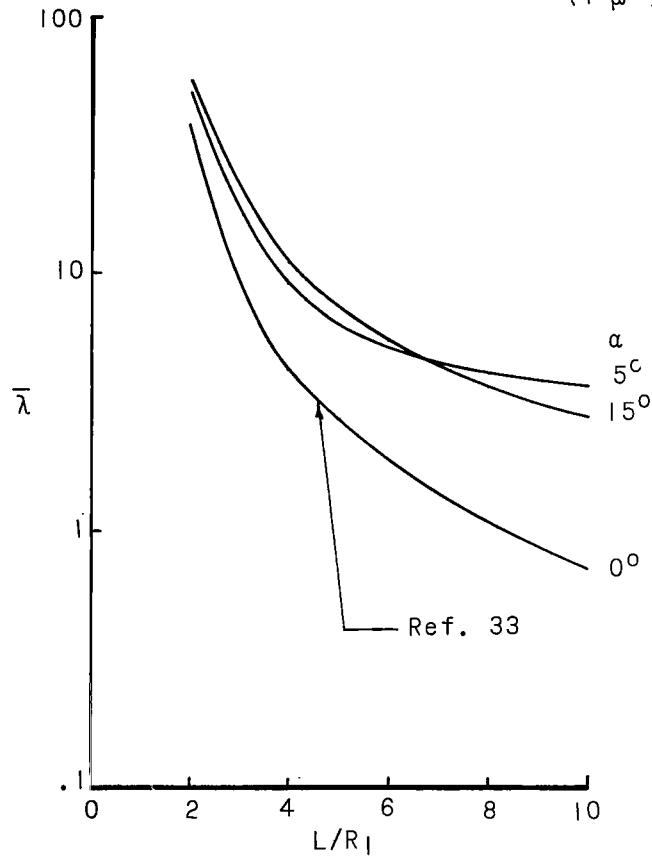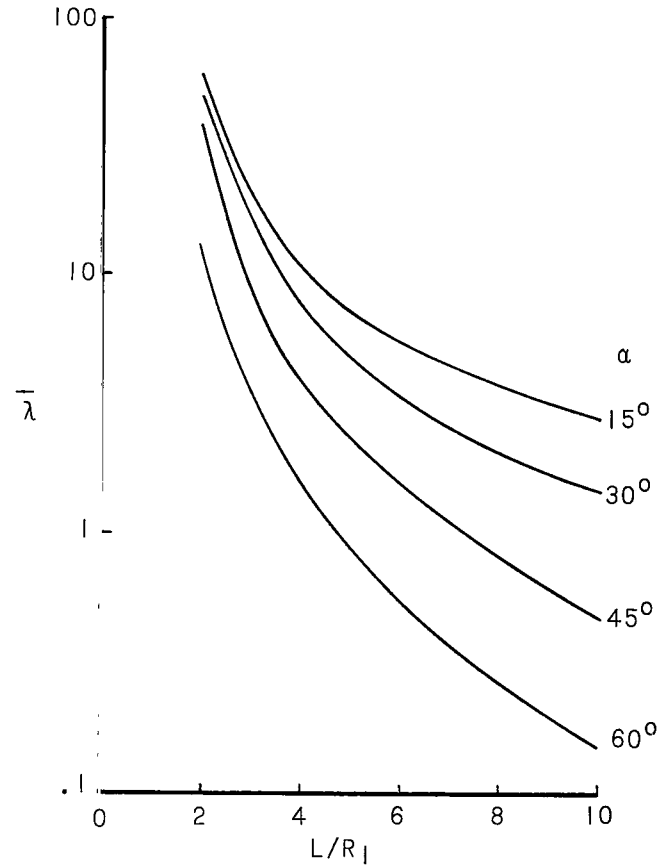
Figure 9.- Variation of $\overline{\lambda}$ with L/R_1 for isotropic conical shells with cylindrical simple support. $p = P = 0$; $g_a = 0$; $100 \leqq R_1/h \leqq 2000$.
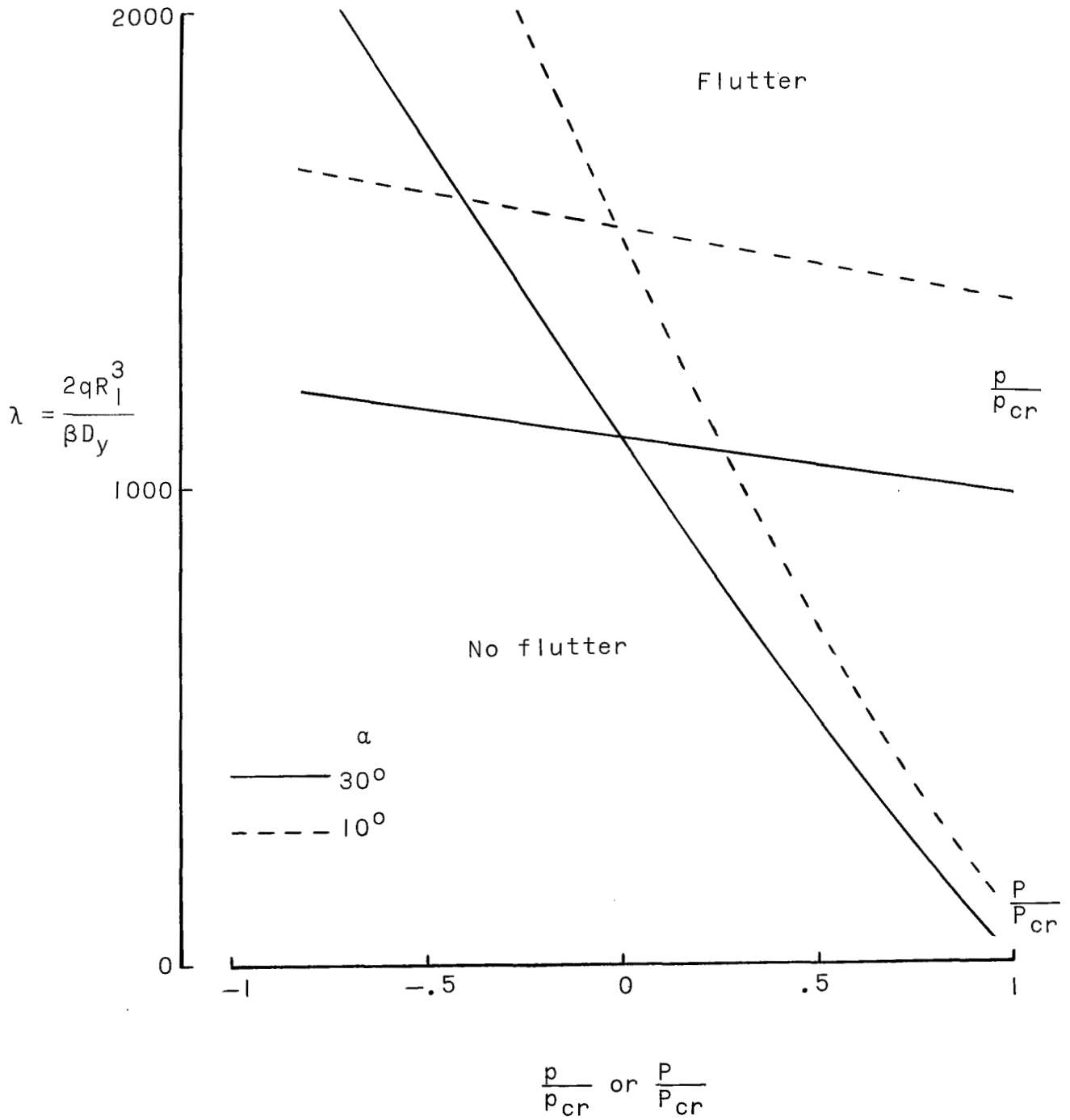
Figure 10.- Some effects of hydrostatic pressure and axial load on flutter of isotropic conical shells with cylindrical simple support. $L/R_1 = 4$; $R_1/h = 200$; $g_a = 0$.

64
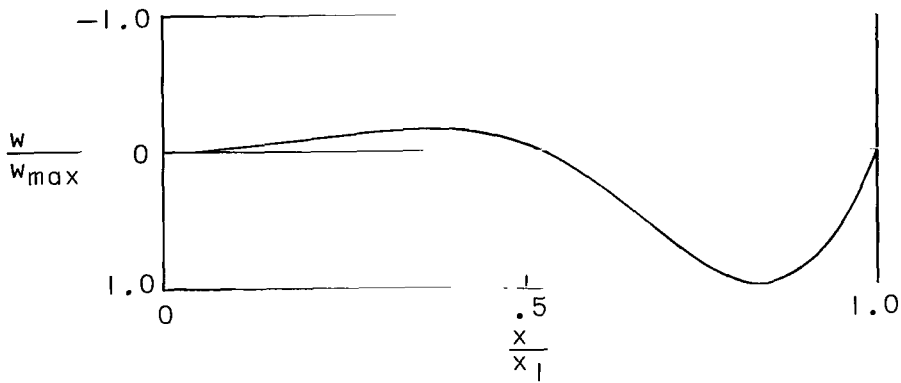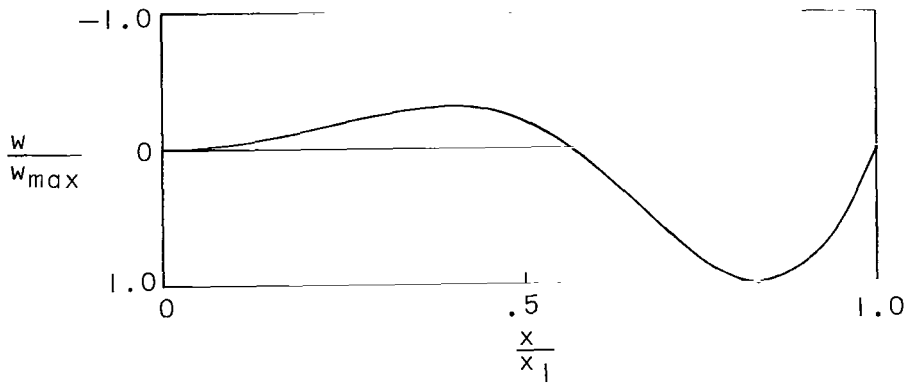
(a) $P/P_{cr} = 0.$

(b) $P/P_{cr} = 0.4.$
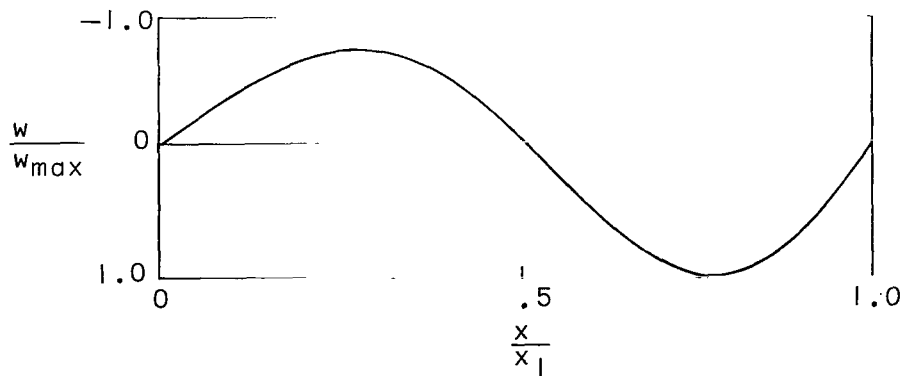
(c) $P/P_{cr} = 0.8.$

Figure 11.- Some effects of axial load on flutter mode shape of isotropic conical shells with cylindrical simple support. $L/R_1 = 4$; $R_1/h = 200$; $\alpha = 10^0$; $g_a = 0$; $p = 0.$
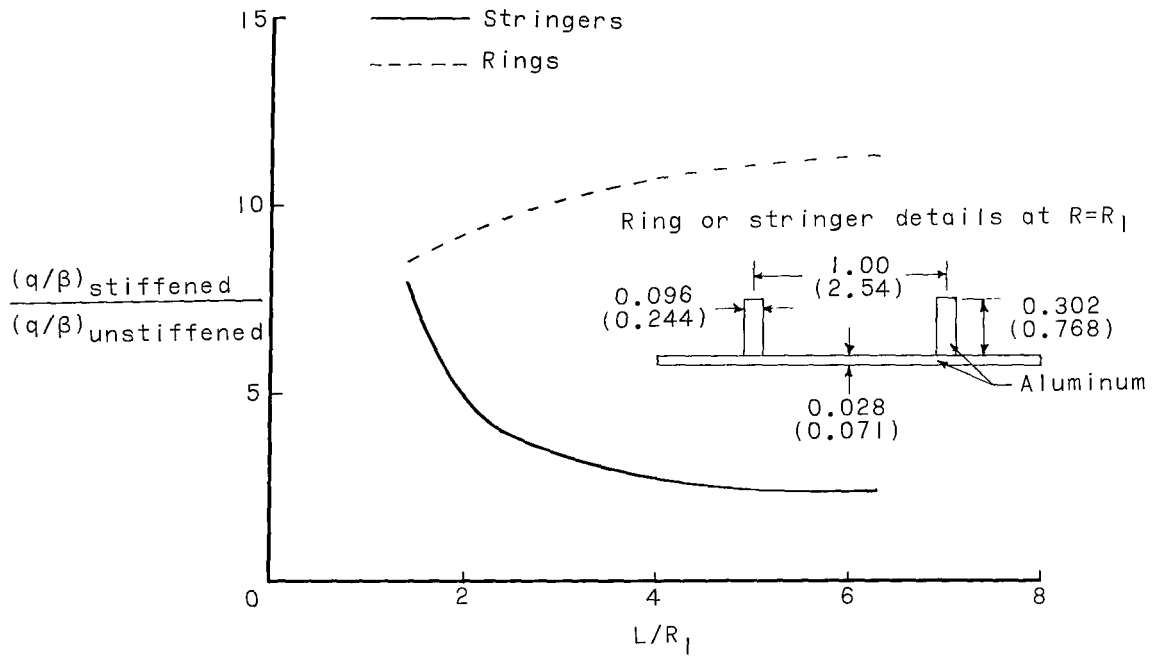
Figure 12.- Variation of effects of ring and stringer stiffening with L/R_1 for flutter of conical shells with cylindrical simple support. $R_1/h = 341$; $\alpha = 30^0$; $p = P = 0$; $g_a = 0$; dimensions are in in. (cm).
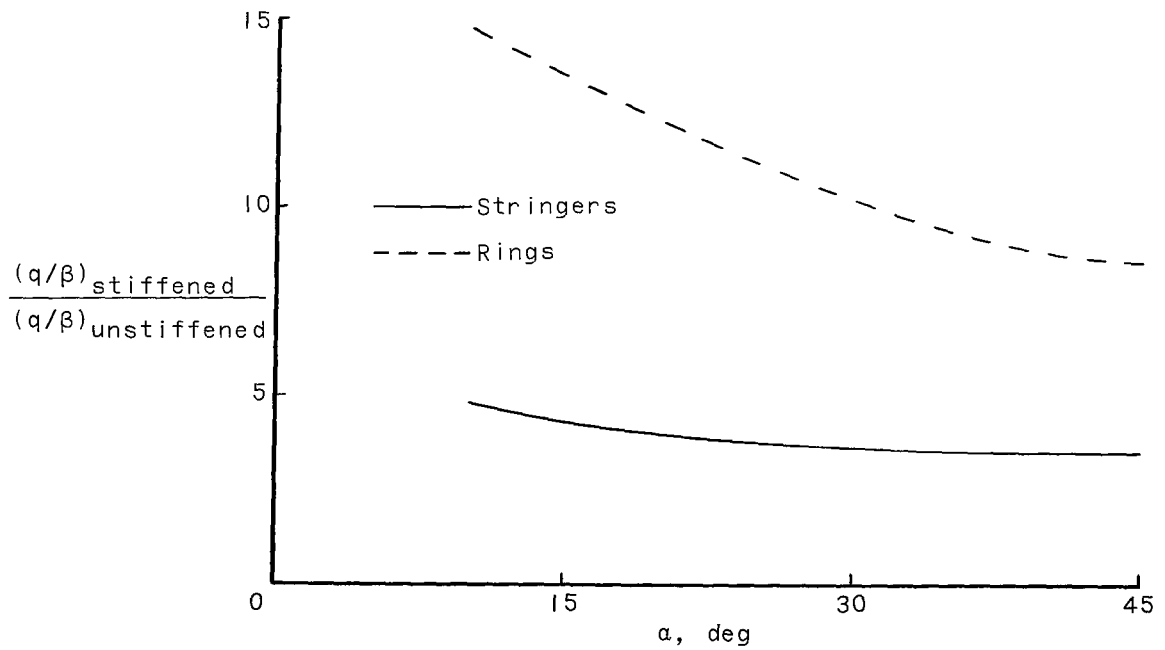
Figure 13.- Variation of effects of ring and stringer stiffening with α for flutter of conical shells with cylindrical simple support. $L/R_1 = 2.51$; $R_1/h = 341$; $p = P = 0$; $g_a = 0$; ring and stringer details are shown in fig. 12.

$$\lambda = \frac{2qR_1^3}{\beta D_y}$$
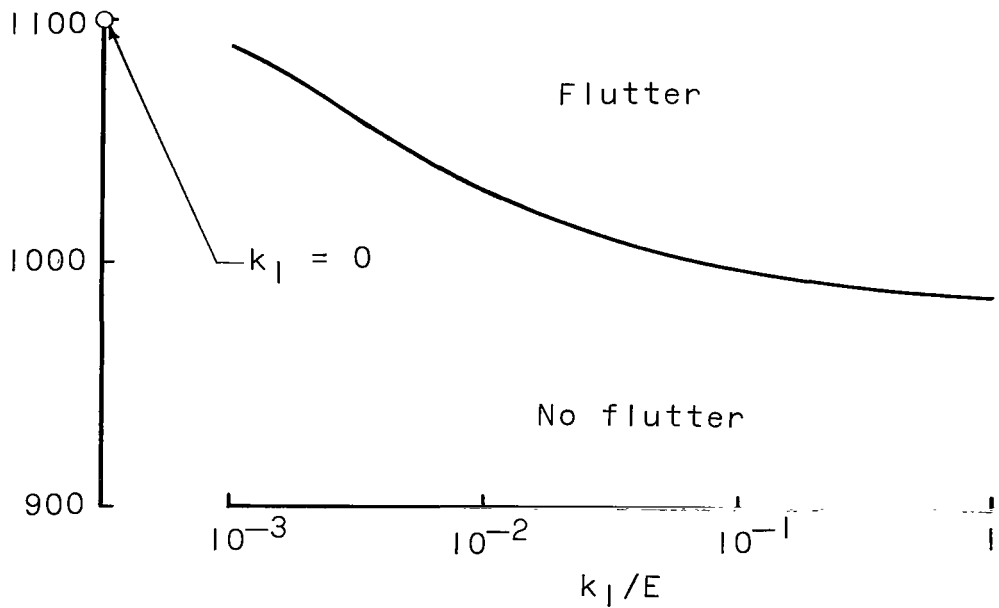
(a) Flutter parameter λ.

$$\Delta = \frac{\omega_2^2 - \omega_1^2}{\omega_r^2}$$
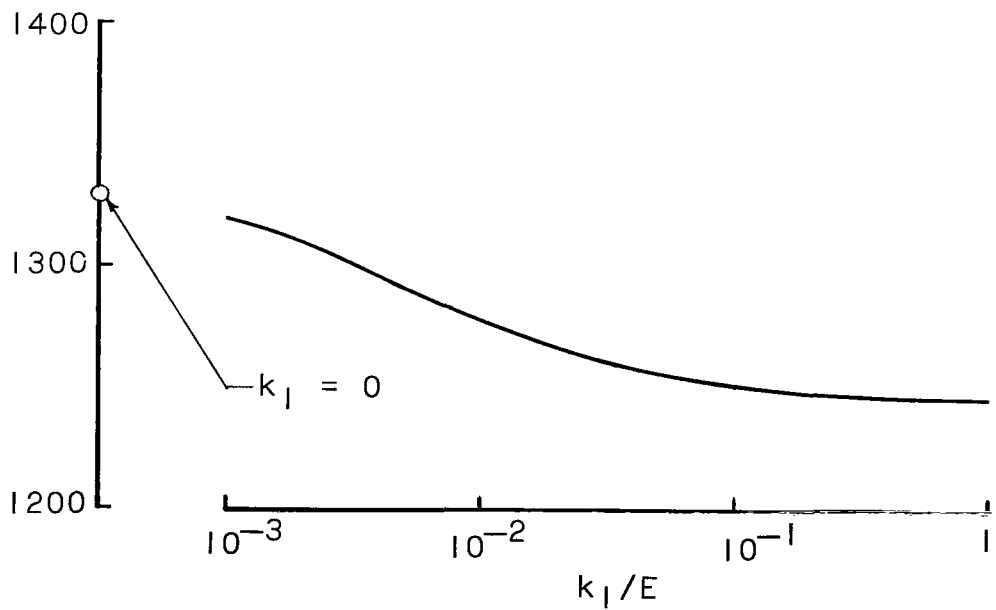
(b) Frequency spectrum parameter Δ.

Figure 14.- Some effects of axial restraint on flutter characteristics of isotropic conical shell. $L/R_1 = 4$; $R_1/h = 200$; $\alpha = 30^0$; $p = P = 0$; $g_a = 0$; $v_B = u_{HB} = M_{yB} = 0$.

Figure 15

o "Cylindrical" simple support

□ Clamped

Flutter

$$\lambda = \frac{2qR_1^3}{\beta D_y}$$

$V_B = 0$

$u_{VB} = 0$

No flutter

$$\frac{R_1 k_4}{D_y}$$
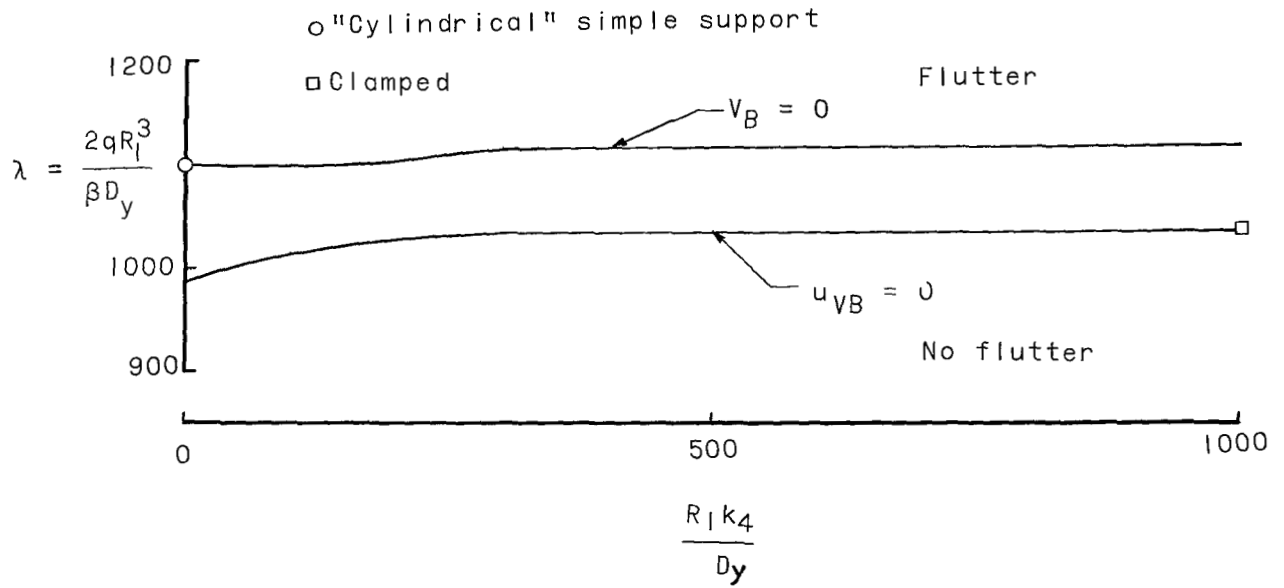
Figure 15.- Some effects of rotational restraint on flutter of isotropic conical shell with no axial restraint and complete axial constraint. $L/R_1 = 4$; $R_1/h = 200$; $\alpha = 30^0$; $p = P = 0$; $g_a = 0$; $v_B = u_{HB} = 0$.

Figure 16

Flutter

$\eta = 8$

$$\lambda = \frac{2qR_1^3}{\beta D_y}$$

$k_2/E = 1$

$k_2/E = k_3/E$

No flutter

$$\begin{array}{ll} \square\ v_B = 0 \\ \circ\ N_{y\theta B} = 0 \end{array}\Bigg\}\ u_{HB} = 0$$

$$\begin{array}{ll} \blacksquare\ v_B = 0 \\ \bullet\ N_{y\theta B} = 0 \end{array}\Bigg\}\ Q_{yB} = 0$$

k_3/E
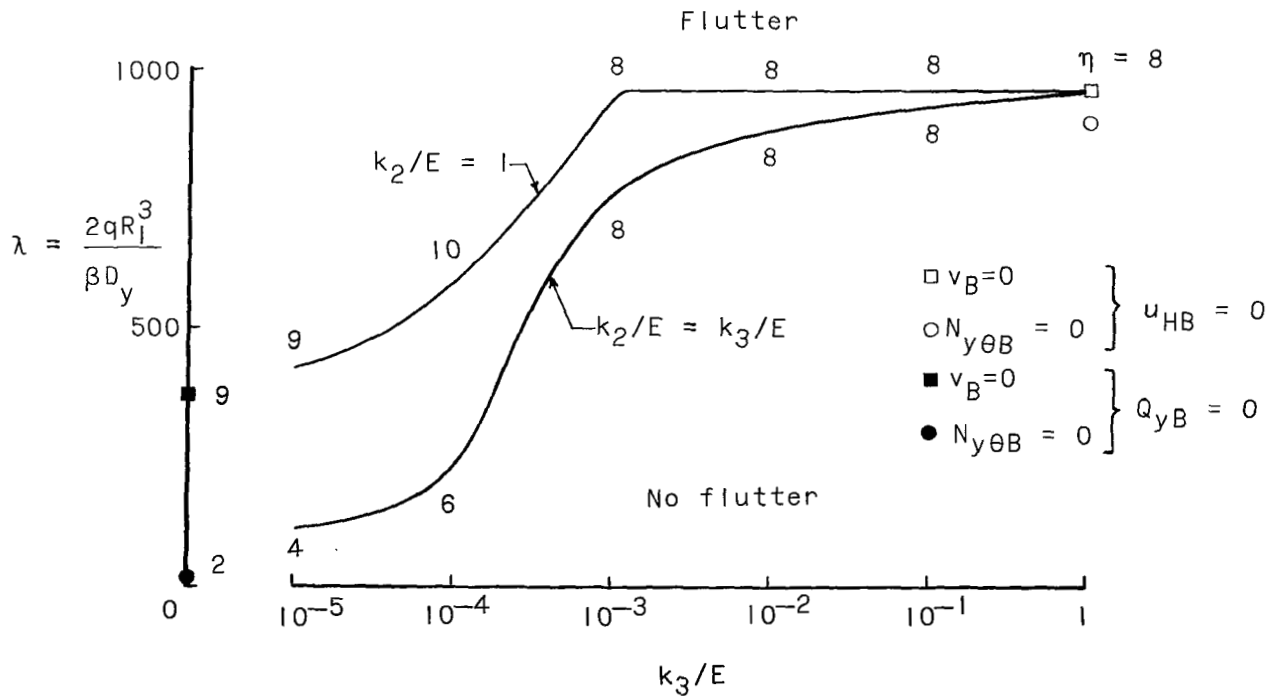
Figure 16.- Some effects of elastic circumferential (k_2) and radial (k_3) edge restraint on flutter of isotropic conical shell. $L/R_1 = 3.5$; $R_1/h = 107$; $\alpha = 20^0$; $p = P = 0$; $g_a = 0$; $V = M_{yB} = 0$.

$$C_p = \frac{R_1^3 p}{D_y}$$

(a) Cone angle.

$$C_p = \frac{R_1^3 p}{D_y}$$
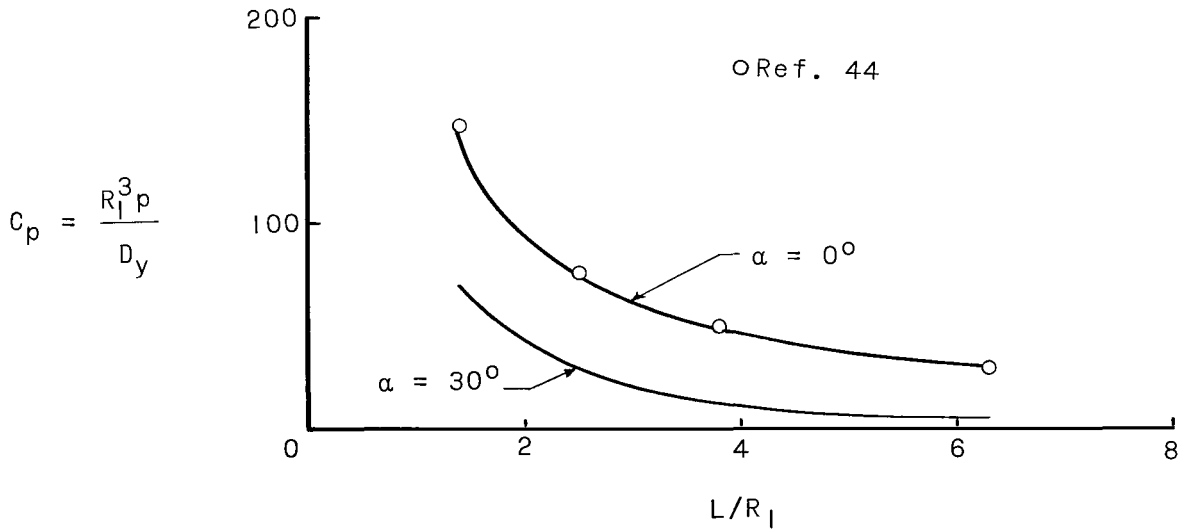
(b) Length-radius ratio.

Figure 17.- Some effects of conicity on buckling of isotropic conical shells with cylindrical simple support subjected to hydrostatic pressure. $R_1/h = 341$; $P = 0$.
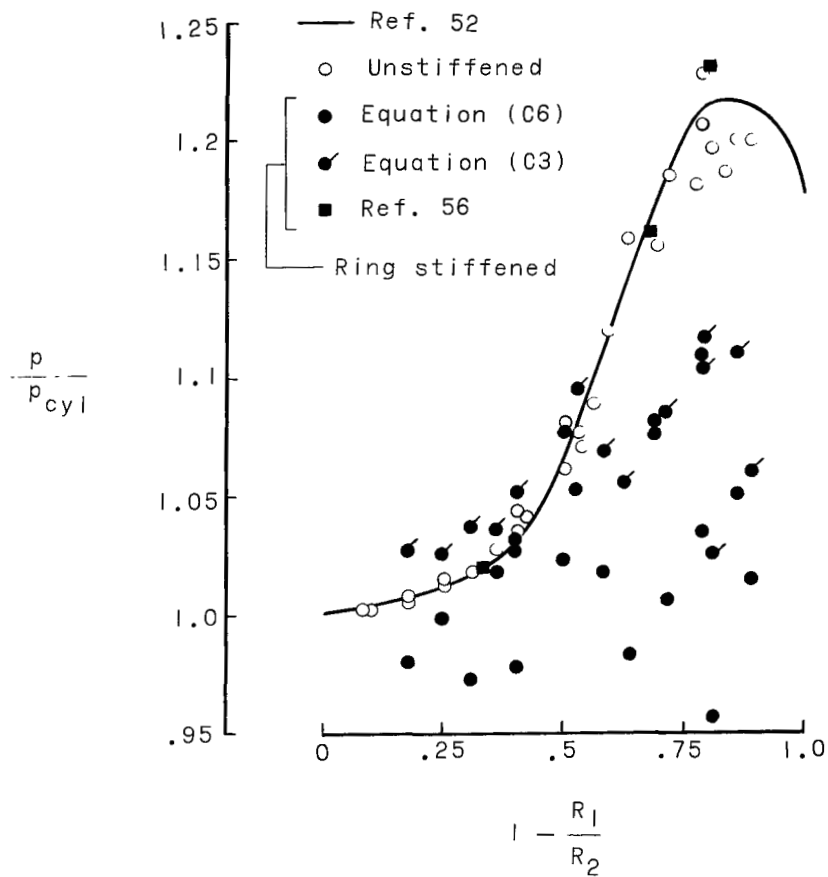
Figure 18.- Correlation of results for buckling of equivalent cylindrical shells with conical shells with cylindrical simple support subjected to hydrostatic pressure. P = 0.
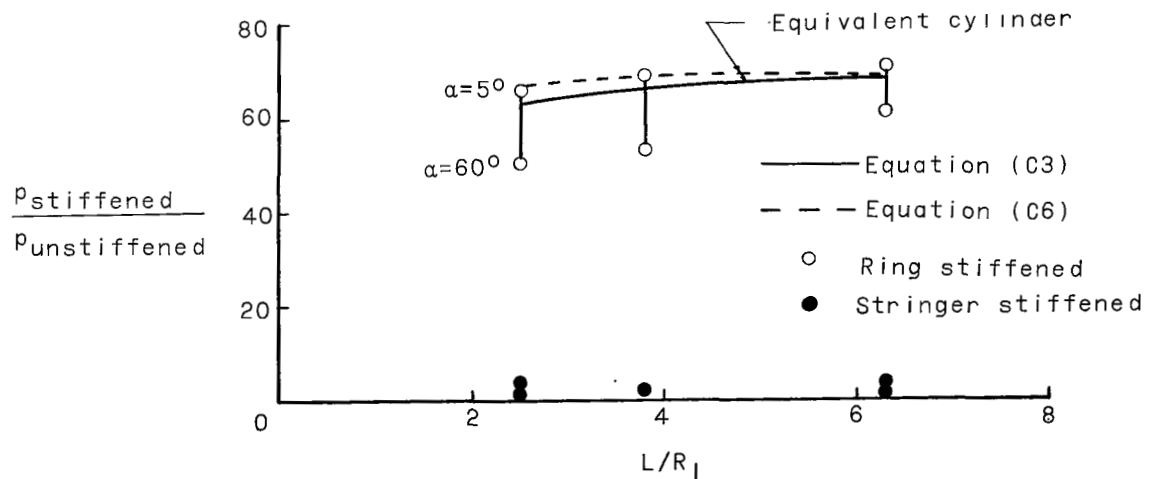
Figure 19.- Some effects of ring and stringer stiffening on buckling of conical shells with cylindrical simple support subjected to hydrostatic pressure. $R_1/h = 341$; $P = 0$; $5^0 \leqq \alpha \leqq 60^0$; ring and stringer details are shown in fig. 12.
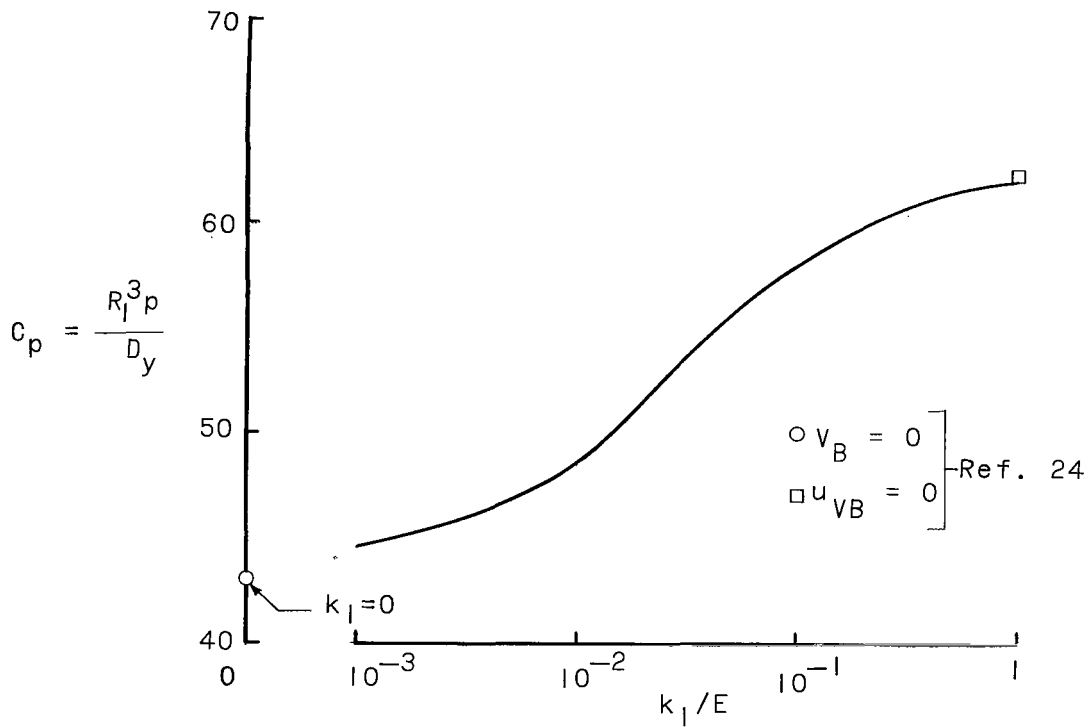
Figure 20.- Some effects of elastic axial restraint on buckling of isotropic truncated conical shell subjected to hydrostatic pressure. $L/R_1 = 2$; $R_1/h = 500$; $\alpha = 30°$; $P = 0$; $v_B = u_{HB} = M_{yB} = 0$.
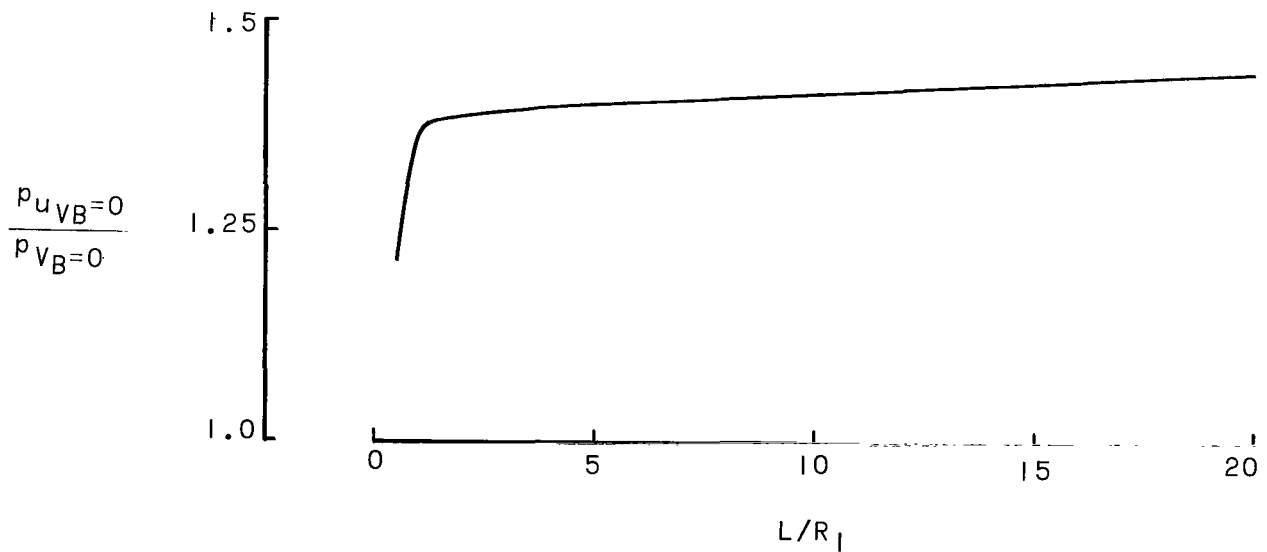
Figure 21.- Variation of effects of complete axial constraint with length-radius ratio L/R_1 for buckling of isotropic truncated conical shell subjected to hydrostatic loading. $R_1/h = 707$; $\alpha = 45°$; $P = 0$; $v_B = u_{HB} = M_{yB} = 0$.

71

$$C_p = \frac{R_1^3 p}{D_y}$$
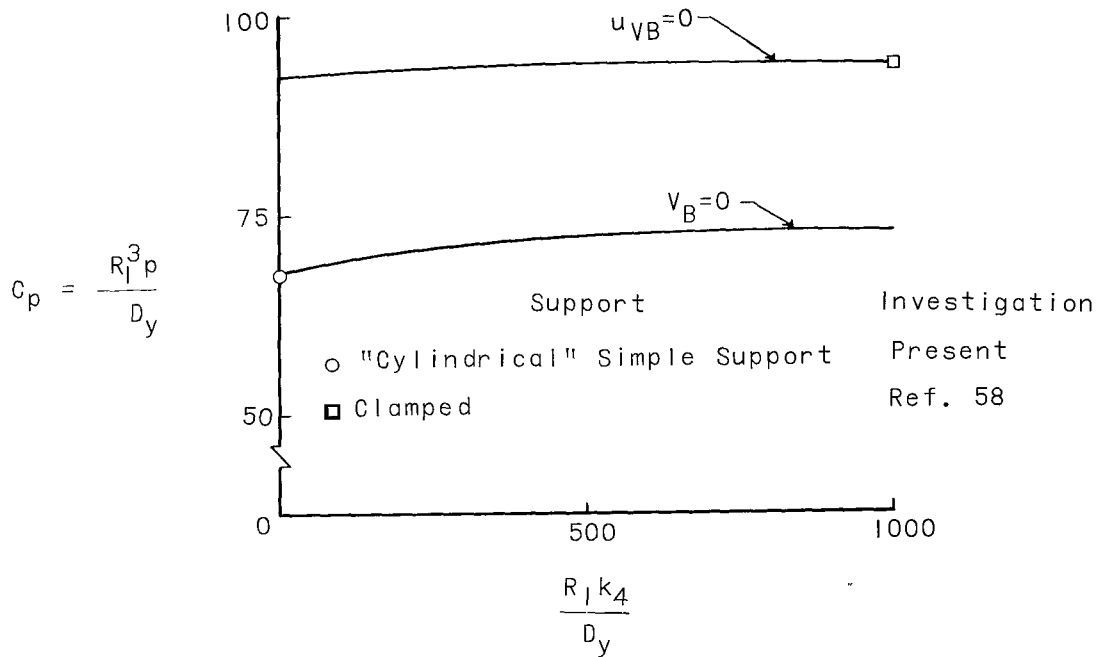
Figure 22.- Some effects of rotational restraint on buckling of isotropic truncated conical shell subjected to hydrostatic pressure. $L/R_1 = 1$; $R_1/h = 707$; $\alpha = 45^\circ$; $P = 0$; $v_B = u_{HB} = 0$.

$$C_p = \frac{R_1^3 p}{D_y}$$
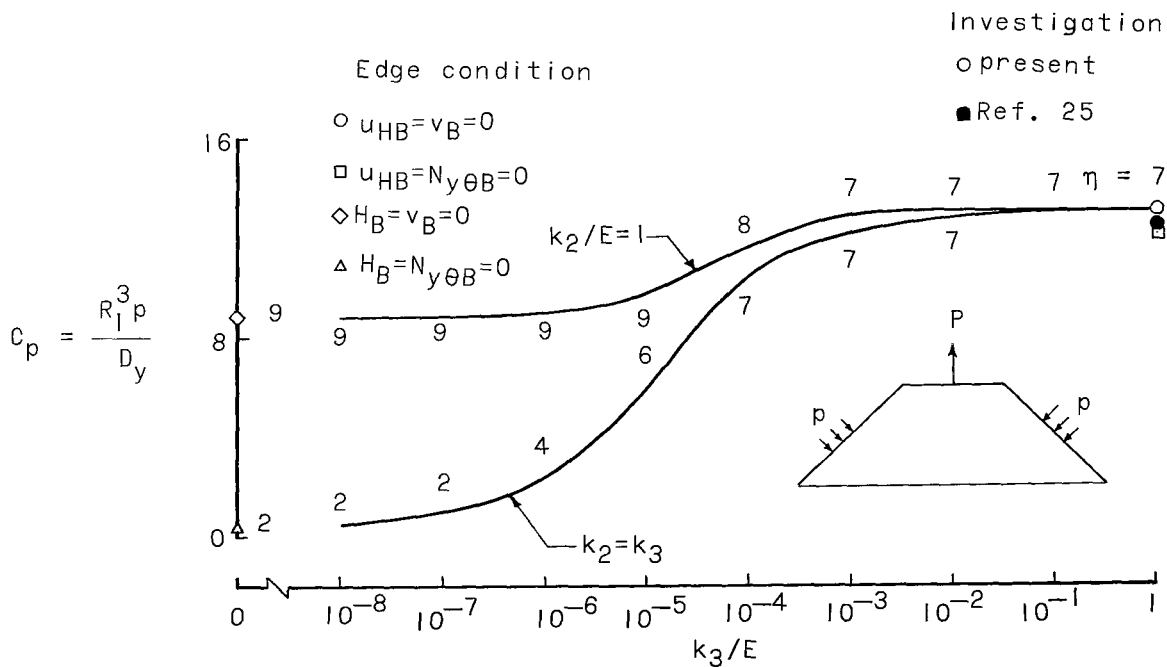
Figure 23.- Some effects of elastic circumferential (k_2) and radial (k_3) edge restraint on buckling of truncated conical sandwich shell subjected to lateral pressure. $L/R_1 = 0.72$; $\alpha = 60^\circ$; $V_B = M_{yB} = 0$; shell details are given in table II.
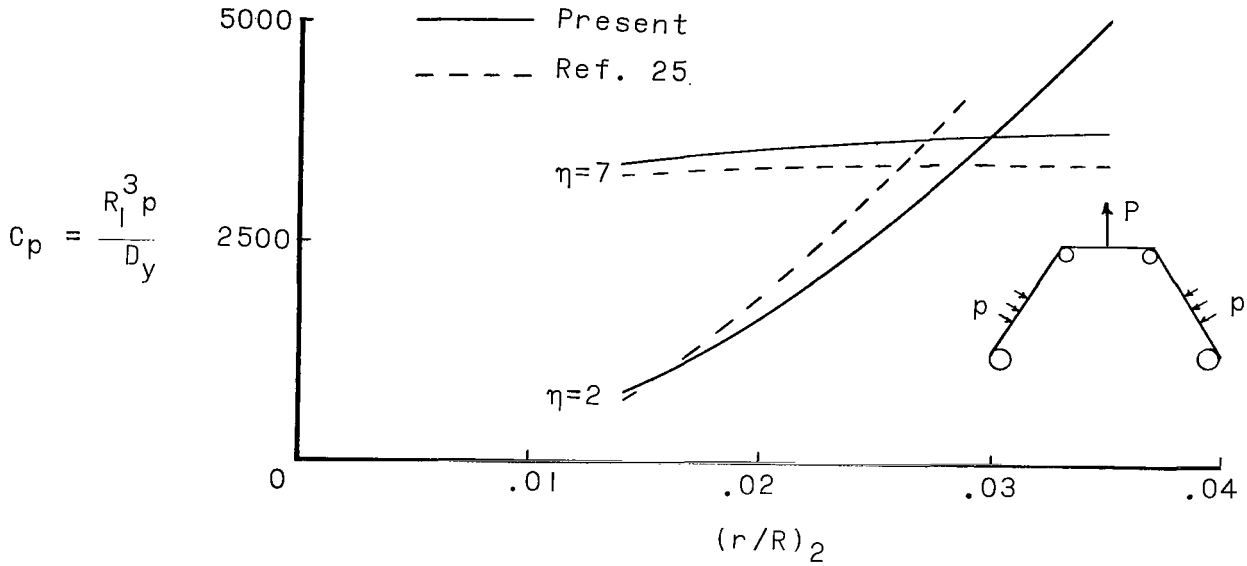
(a) Ring stiffened monocoque.
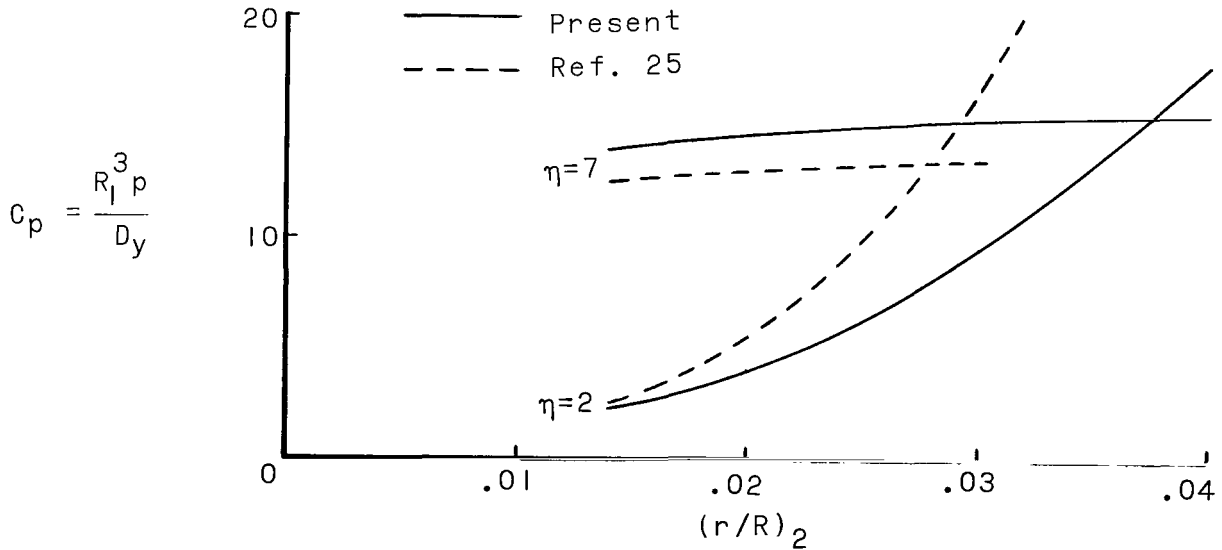
(b) Sandwich construction.

Figure 24.- Some effects of circular tubular end rings on buckling of truncated conical shells subjected to lateral pressure. $L/R_1 = 0.72$; $\alpha = 60^o$; $(r/R)_1 = 0.0312$; $R_1 = 80.2$ in. (204 cm); $\tau = 0.125$ in. (0.318 cm); shell details are given in table II.
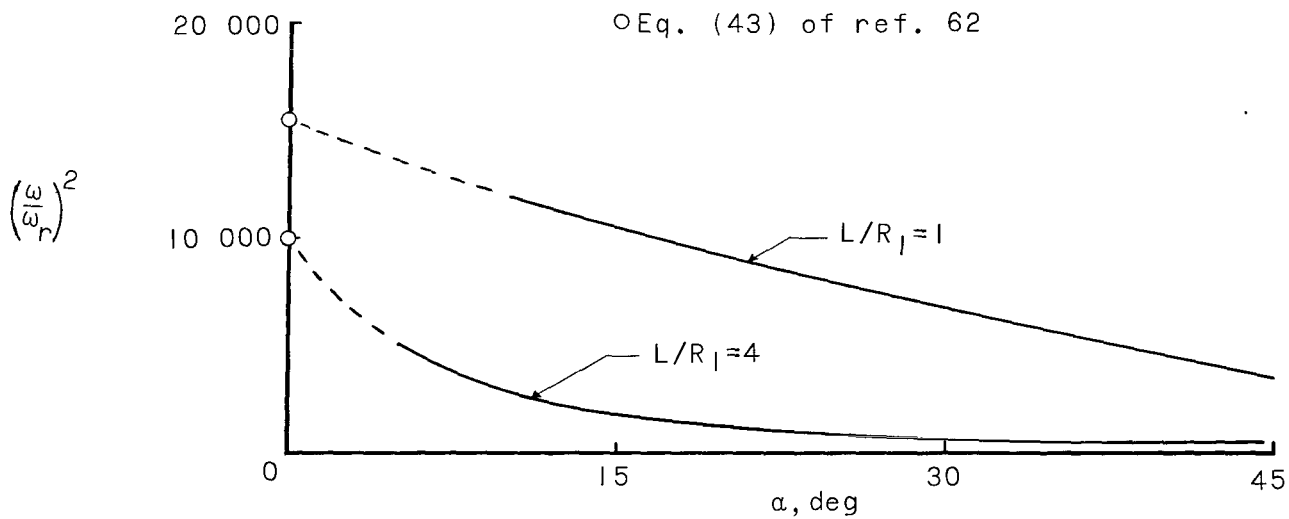
(a) Cone angle.
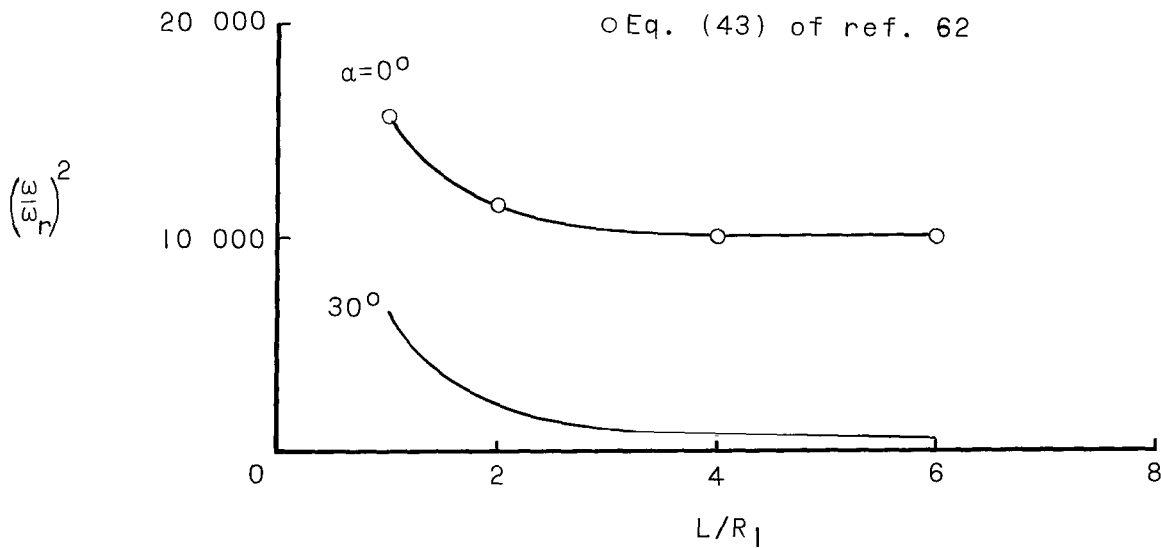
(b) Length-radius ratio.

Figure 25.- Some effects of conicity on natural frequencies of isotropic conical shells with cylindrical simple support. $R_1/h = 341$; $\eta = 10$; $p = P = 0$.

74
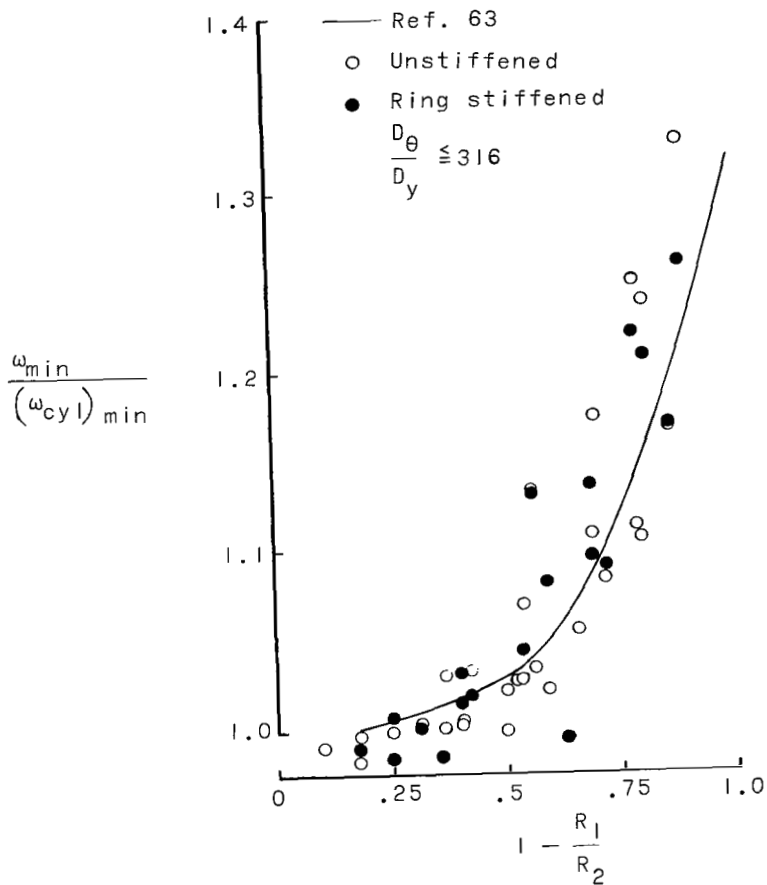
Figure 26.- Correlation of minimum frequencies of equivalent cylindrical shells with conical shells with cylindrical simple support. $p = P = 0$.

(a) Hydrostatic pressure.

(b) Axial load.
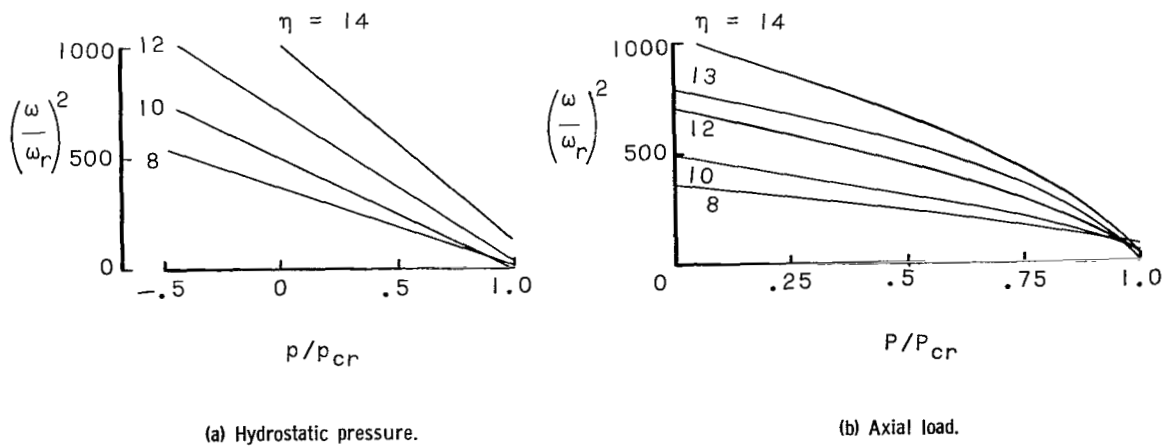
Figure 27.- Some effects of applied loads on natural frequencies of isotropic conical shell with cylindrical simple support. $L/R_1 = 4$; $R_1/h = 200$; $\alpha = 30^0$.
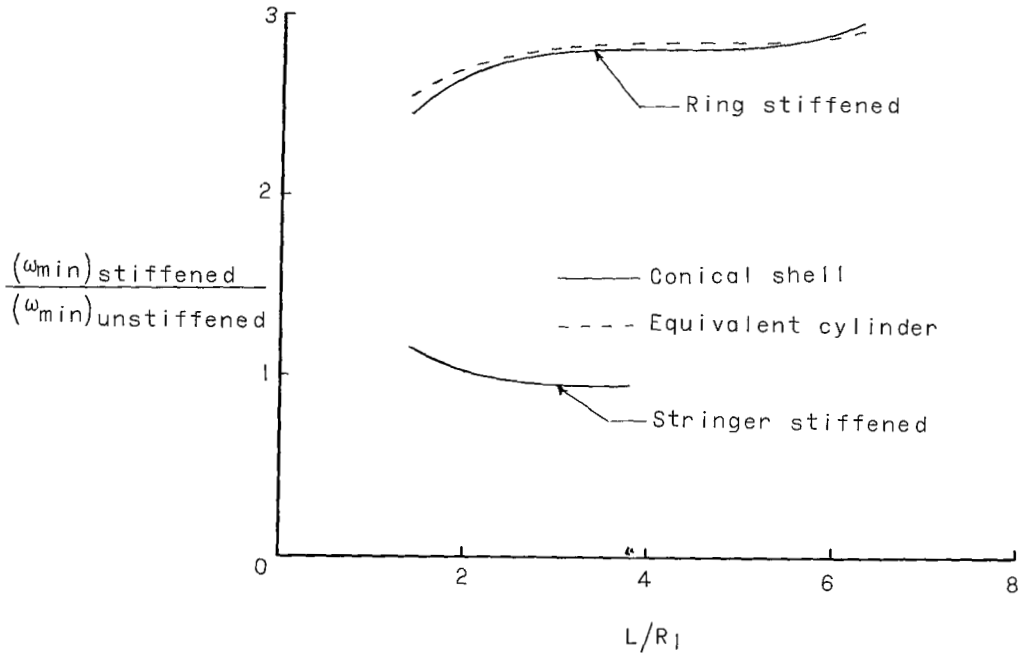
Figure 28.- Some effects of ring and stringer stiffening on minimum natural frequencies of conical shells with cylindrical simple support. $R_1/h \doteq 341$; $5^0 \leqq \alpha \leqq 60^0$; ring and stringer details are shown in fig. 12; $p = P = 0$.

(a) Effects of axial restraint with no rotational restraint.

(b) Effects of rotational restraint with no axial restraint and complete axial constraint.
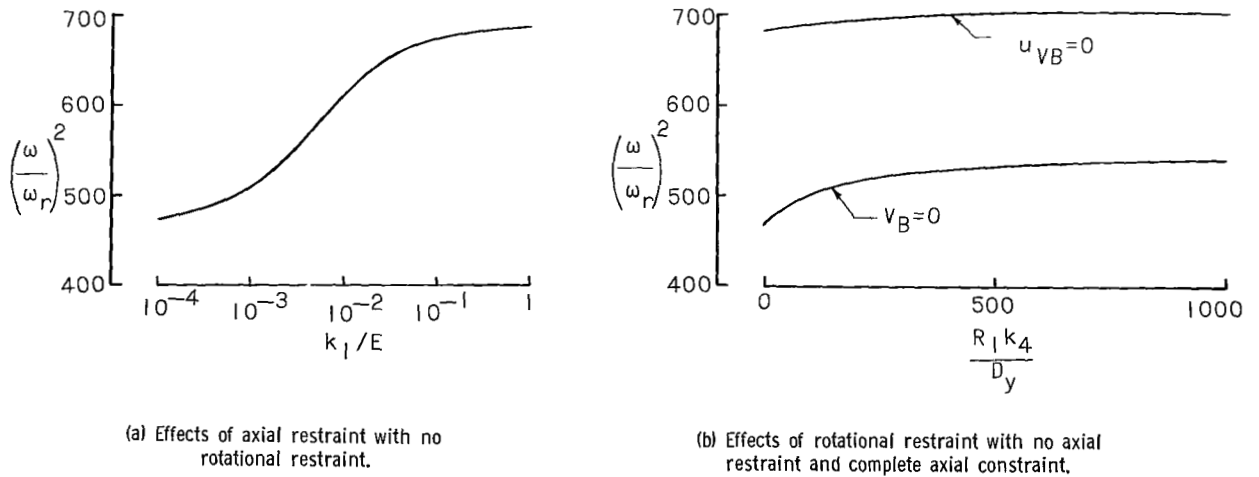
Figure 29.- Some effects of elastic axial restraint (k_1) and rotational restraint (k_4) on natural frequencies of isotropic conical shell. $L/R_1 = 4$; $R_1/h = 200$; $\alpha = 30^0$; $\eta = 10$; $v_B = u_{HB} = 0$; $p = P = 0$.

(a) $p/p_{cr} = -0.446$. (b) $p/p_{cr} = 0$. (c) $p/p_{cr} = 0.446$.
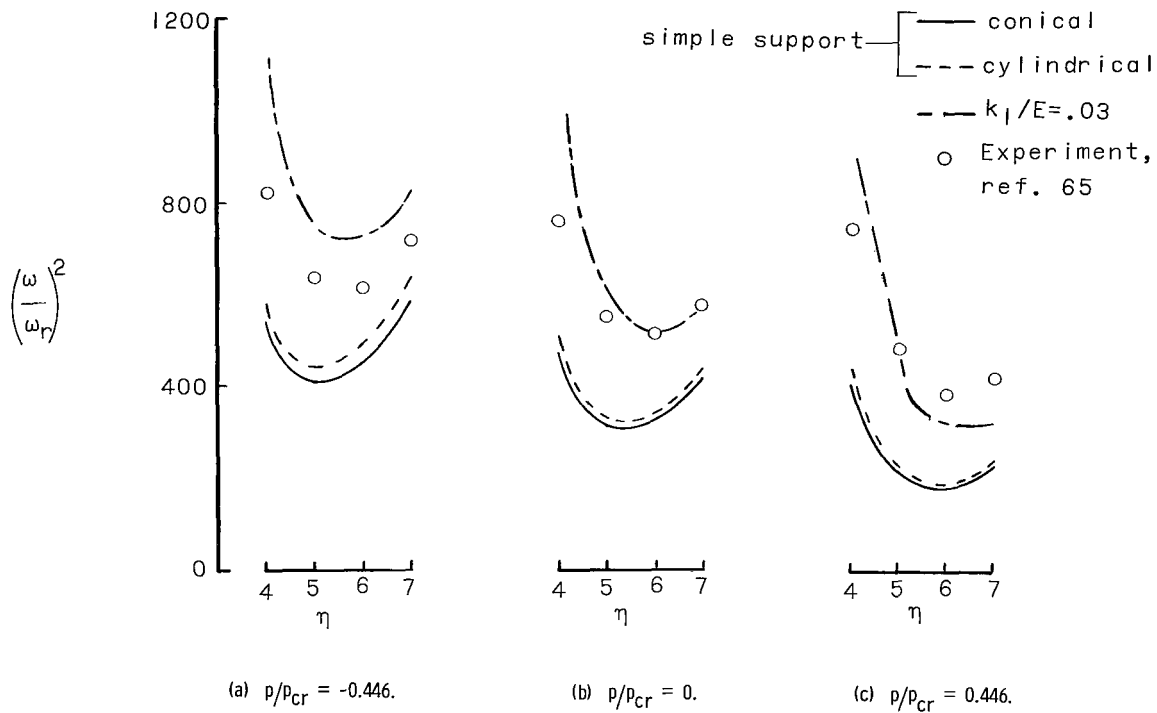
Figure 30.- Comparison of theoretical and experimental vibration results for isotropic conical shell. $L/R_1 = 3.5$; $R_1/h = 107$; $\alpha = 20^0$; $P = 0$; $v_B = M_{yB} = 0$.
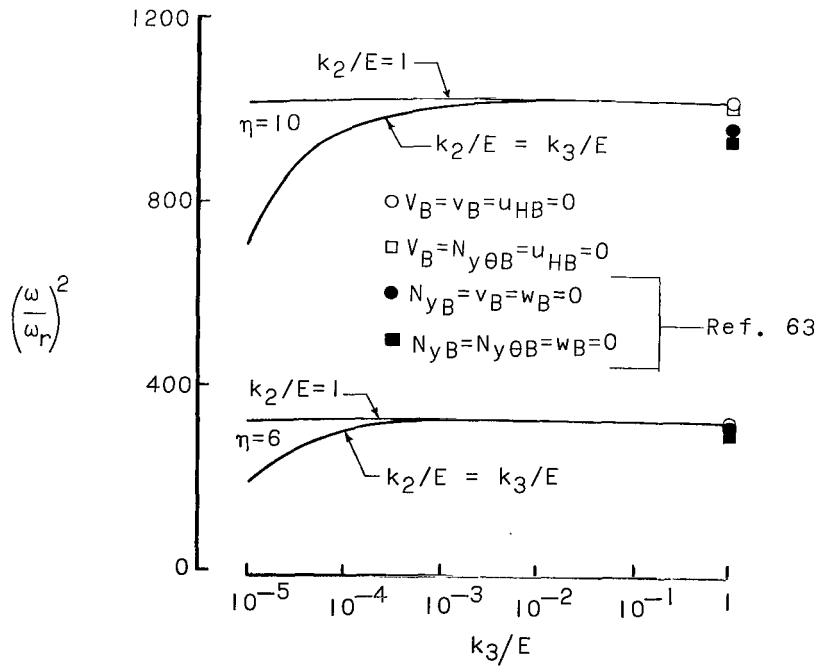
Figure 31.- Some effects of elastic circumferential (k_2) and radial (k_3) edge restraint on natural frequencies of isotropic conical shell. $L/R_1 = 3.5$; $R_1/h = 107$; $\alpha = 20^0$; $p = P = 0$; $V_B = M_{yB} = 0$.

The lengthy expressions developed in the analysis and required for complete documentation are included in a "Supplement to NASA TN D-5759."

Copies of this "Supplement to NASA TN D-5759" will be furnished upon request. Requests for the supplement should be addressed to:

NASA Scientific and Technical Information Facility
P.O. Box 33
College Park, Maryland   20740

- - - - - - - - - - - - - - - - CUT - - - - - - - - - - - - - - - - - -

Date _____

Please forward "Supplement to NASA TN D-5759" to

_____

Name of organization

Street number   _____

City and State   Zip code

Attention: Mr. _____

Title _____

FIRST CLASS MAIL

```
03U 001 57    51 30S              70195  00903
AIR FORCE WEAPONS LABORATORY /WLOL/
KIRTLAND AFB, NEW MEXICO   87117
```

ATT E. LOU BOWMAN, CHIEF,TECH. LIBRARY

"The aeronautical and space activities of the United States shall be conducted so as to contribute . . . to the expansion of human knowledge of phenomena in the atmosphere and space. The Administration shall provide for the widest practicable and appropriate dissemination of information concerning its activities and the results thereof."

— NATIONAL AERONAUTICS AND SPACE ACT OF 1958

NASA SCIENTIFIC AND TECHNICAL PUBLICATIONS

TECHNICAL REPORTS: Scientific and technical information considered important, complete, and a lasting contribution to existing knowledge.

TECHNICAL NOTES: Information less broad in scope but nevertheless of importance as a contribution to existing knowledge.

TECHNICAL MEMORANDUMS: Information receiving limited distribution because of preliminary data, security classification, or other reasons.

CONTRACTOR REPORTS: Scientific and technical information generated under a NASA contract or grant and considered an important contribution to existing knowledge.

TECHNICAL TRANSLATIONS: Information published in a foreign language considered to merit NASA distribution in English.

SPECIAL PUBLICATIONS: Information derived from or of value to NASA activities. Publications include conference proceedings, monographs, data compilations, handbooks, sourcebooks, and special bibliographies.

TECHNOLOGY UTILIZATION PUBLICATIONS: Information on technology used by NASA that may be of particular interest in commercial and other non-aerospace applications. Publications include Tech Briefs, Technology Utilization Reports and Notes, and Technology Surveys.

Details on the availability of these publications may be obtained from:

SCIENTIFIC AND TECHNICAL INFORMATION DIVISION

NATIONAL AERONAUTICS AND SPACE ADMINISTRATION
Washington, D.C. 20546